NOAA Technical Memorandum ERL PMEL-47

# CIRCULATION AND HYDROGRAPHY OF UNIMAK PASS AND THE SHELF WATERS NORTH OF THE ALASKA PENINSULA

James D. Schumacher
Paul D. Moen

Pacific Marine Environmental Laboratory
Seattle, Washington
June 1983

UNITED STATES
DEPARTMENT OF COMMERCE
Malcolm Baldrige,
Secretary

NATIONAL OCEANIC AND
ATMOSPHERIC ADMINISTRATION
John V. Byrne,
Administrator

Environmental Research
Laboratories
George H. Ludwig
Director

NOTICE

Mention of a commercial company or product does not constitute an endorsement by NOAA Environmental Research Laboratories. Use for publicity or advertising purposes of information from this publication concerning proprietary products or the tests of such products is not authorized.

CONTENTS

# CIRCULATION AND HYDROGRAPHY OF UNIMAK PASS AND THE SHELF WATERS NORTH OF THE ALASKA PENINSULA*

James D. Schumacher
Paul D. Moen

ABSTRACT. We present wind, current, bottom pressure, and hydrographic observations from Unimak Pass and the adjacent shelf. Mean flow was from the Gulf of Alaska into the Bering Sea and resulted from the Kenai Current. Shorter period fluctuations were bi-directional and coherent with divergence along the coast. Observations along the northern side of the Alaska Peninsula indicated Kenai Current water had an impact on the local salt content in the coastal domain, and together with freshwater discharge maintained a stronger horizontal density gradient in the vicinity of the 50-m isobath. Associated with this front was a moderate (1 to 6 cm/s) mean flow. Wind forcing, manifested both as coastal divergence and as a source of strong mixing, was evident at shorter periods. Results substantiated previous studies, but they also revealed subtle features including impact of freshwater discharge not associated with gaged rivers, importance of gaps in the mountains to the generation of pressure gradient winds, and the nature of processes which destroy and establish the inner front and the typically two-layered middle shelf domain structure.

## 1. INTRODUCTION

Between March 1980 and October 1981, oceanographic studies were conducted in Unimak Pass and along the shelf north of the Alaska Peninsula as part of the Outer Continental Shelf Environmental Assessment Program (OCSEAP). The goal of this report is to provide a description of the data collected and to interpret the data with respect to important shelf features noted in previous studies. We first describe the regional setting, including a review of previous oceanographic studies. We then discuss methods of observation and analysis. Results are discussed in Section 4, where they are treated separately for Unimak Pass[1] and the north Aleutian Shelf. The major features are summarized in Section 5, Summary and Conclusions.

## 2. SETTING

### 2.1 Geography

The Alaska Peninsula (Figure 1) extends about 700 km (~157°W to 165°W) from the mainland to Unimak Pass and is oriented southwestward. The northern coast contains several major embayments: Bechevin Bay and

[1] Parts of the Unimak Pass studies have appeared previously in a different format, see Schumacher et al., 1982.

* Contribution number 646 from the Pacific Marine Environmental Laboratory.

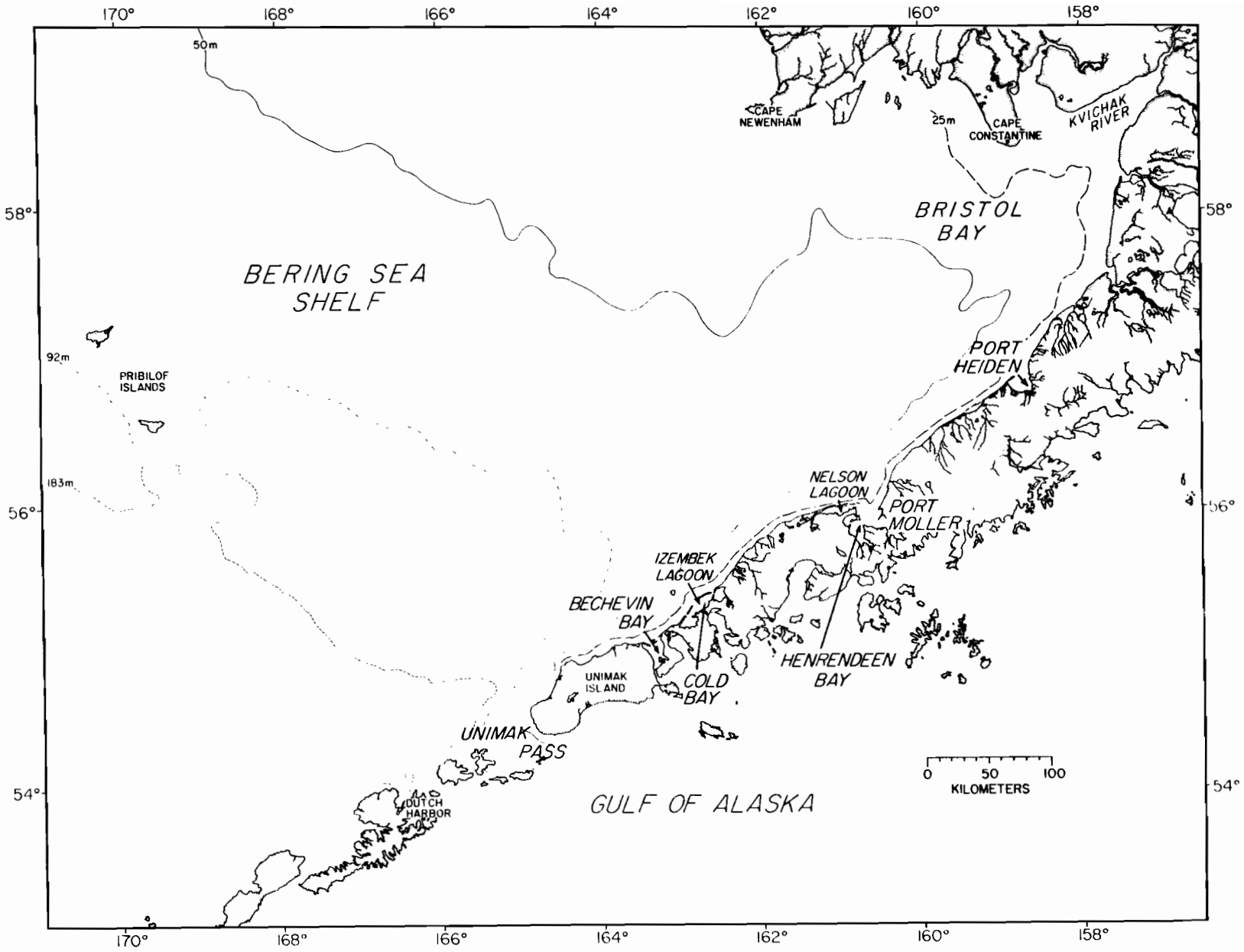


Fig. 1. Geomorphology of the southeastern Bering Sea shelf, including the present study area. (Depths are in meters.)

Isanotski Strait, which separate Unimak Island from the peninsula; Izembek/Moffet Lagoon located north of Cold Bay; the Nelson Lagoon, Herendeen Bay, Port Moller complex; and Port Heiden. These indentations in an otherwise relatively straight coastline are accompanied by passages across the peninsula which break the rugged orographic contours. Such features permit local winds to become down gradient rather than geostrophic and hence can dramatically modify local winds over length scales of up to 30 km offshore.

Unimak Pass is the eastern-most passage of significant cross section ($\sim 10^6 m^2$) between the Bering Sea and the Gulf of Alaska. Complex orographic and bathymetric contours are typical in the vicinity of Unimak Pass. At the narrowest location (Scotch Gap to Ugamak Island) which we call the Pass proper, it is 19 km wide and has an average depth of ~55 m with an along-pass axis of 285°T. The presence of the Krenitzin Islands southwest of Unimak Island and the passes between these islands and Unimak Pass proper also contribute to the complexity. On the Krenitzen Islands, there are many peaks in excess of 800 m, and elevations up to 2500 m exist on the western end of Unimak Island.

Bathymetry along the remainder of the study area is less complex, the 50-m isobath generally trends toward ~60°TN from the northern coast of Unimak Island to about 159°W, where it becomes nearly orthogonal to the coastline. The shelf shoreward of the 50-m isobath is generally 20 to 30 km wide west of Nelson Lagoon, where it becomes ~40 km in width and then is constricted to 20 km just east of Port Moller. From Port Moller to Port Heiden, the width of the coastal region gradually broadens to 40 km. Seaward of the 50-m isobath, depths increase monotonically to greater than 100 m off Unimak Island; however, the 92-m isobath becomes nearly orthogonal to the peninsula east of Cold Bay. Isobaths up to 80-m parallel the 50-m isobath and form a trench-like feature which extends into Kvichak Bay. This feature, which is most pronounced east of Port Moller, results in depths greater than 25 m to just east of Cape Constantine.

## 2.2 Physical Properties

Kinder and Schumacher (1981a) characterize this region of the shelf in terms of hydrographic properties and structure; along most of the peninsula, the relevant domains are those of the coastal and middle shelf. The coastal domain, away from the direct influence of freshwater addition, is typically well mixed and lies shoreward of the 50-m isobath. The middle-shelf domain generally is two-layered and lies seaward of the 50-m isobath. Separating these domains is a structural front (Schumacher et al., 1979), where a transition between well-mixed and two-layered vertical structure occurs. A typical width of the front is about 5 to 10 km. Geopotential contours across the front suggest baroclinic flow into Bristol Bay with surface speeds of 0.02-0.05 m/s. During winter, waters in the middle shelf are mixed to the bottom so that structural differences between domains are slight; however, fresher water remains in the coastal domain, and cross-shelf density gradients persist.

Sources of freshwater or less saline water include ice melt, local addition from rivers, and, as will be shown later, flow of Kenai Current water through Unimak Pass. Recent studies of sea ice climatology include Webster (1979), Overland and Pease (1981), and Pease, Schoenberg, and Overland (1982). The average progression (50% probability) of ice extent during the growth season (see Figure 2) (Pease, Schoenberg, and Overland, 1982) indicates that ice growth occurs in northern Bristol Bay by December and progresses to maximum extent by March with ice covering much of Bristol Bay and extending along the peninsula to about 160°W. However, during extreme ice years, e.g., winter 1975-76, ice covered most of the shelf westward to Unimak Island. Local (rather than transported) ice production occurs along the northern shore of Bristol Bay, and perhaps to a limited extent within the Port Moller system. Although there are no major rivers along the peninsula, rainfall is substantial. Brower et al. (1977) show a decrease from ~3.2 m at ~158°W to 0.8 m at 162.5°W (Cold Bay). Just north of the eastern end of the Peninsula, the Kvichak River enters Bristol Bay. Seifert and Kane (1977) indicate that this river has a basin area of 16,800 $km^2$ and an average annual flow of $1.84 \times 10^5$ $m^3/s$. Hydrographs indicate that mean daily discharge can vary by a factor of three between wet and dry years and that the greatest monthly discharge occurs in October (1,700 $m^3/s$), with the minimum in April (~283 $m^3/s$). However, a clear freeze cycle is not detectable, so that during winter, discharge does not cease.

## 2.3 Circulation and tides

Since there are abundant fisheries (including Alaskan King crab, halibut, and salmon) along the Alaska Peninsula, much of the early (pre-1975) oceanography was in support of these resources. Although only a few, short-term (~4 days) current observations were made in the past (Reed, 1971), there exists the supposition that waters of the Gulf of Alaska enter the Bering Sea through Unimak Pass; general inflow vectors appear on large-scale circulation schemes (e.g., Hughes, Coachman, and Aagaard, 1974; Takenouti and Ohtani, 1974; and Favorite, Dodimead, and Nasu, 1976). This belief is based on mariner's reports as given in *The Coast Pilot,* drift bottle studies (Thompson and Van Cleve, 1936; Favorite and Fisk, 1971), and on hydrographic data. The inflow of water through Unimak Pass has also been inferred in studies of lateral water mass interactions on the southeastern Bering Sea shelf (Coachman and Charnell, 1977; Coachman and Charnell, 1979).

Circulation along the peninsula is less well known. Kinder and Schumacher (1981b) present limited current meter data which suggest flow along the 50-m isobath into Bristol Bay. Schumacher and Pearson (1980) present drift card and radar-tracked drogue data which support the inference of inflow in the vicinity of the 50-m isobath.

Tides constitute more than 90% of the horizontal kinetic energy (Kinder and Schumacher, 1981a) and are important to mixing and, through interaction with bathymetry and/or relative sea level changes versus mean depth, to the generation of residual flow. Pearson, Mofjeld, and Tripp (1981a) described the tides over the Bering Sea shelf. The tide enters

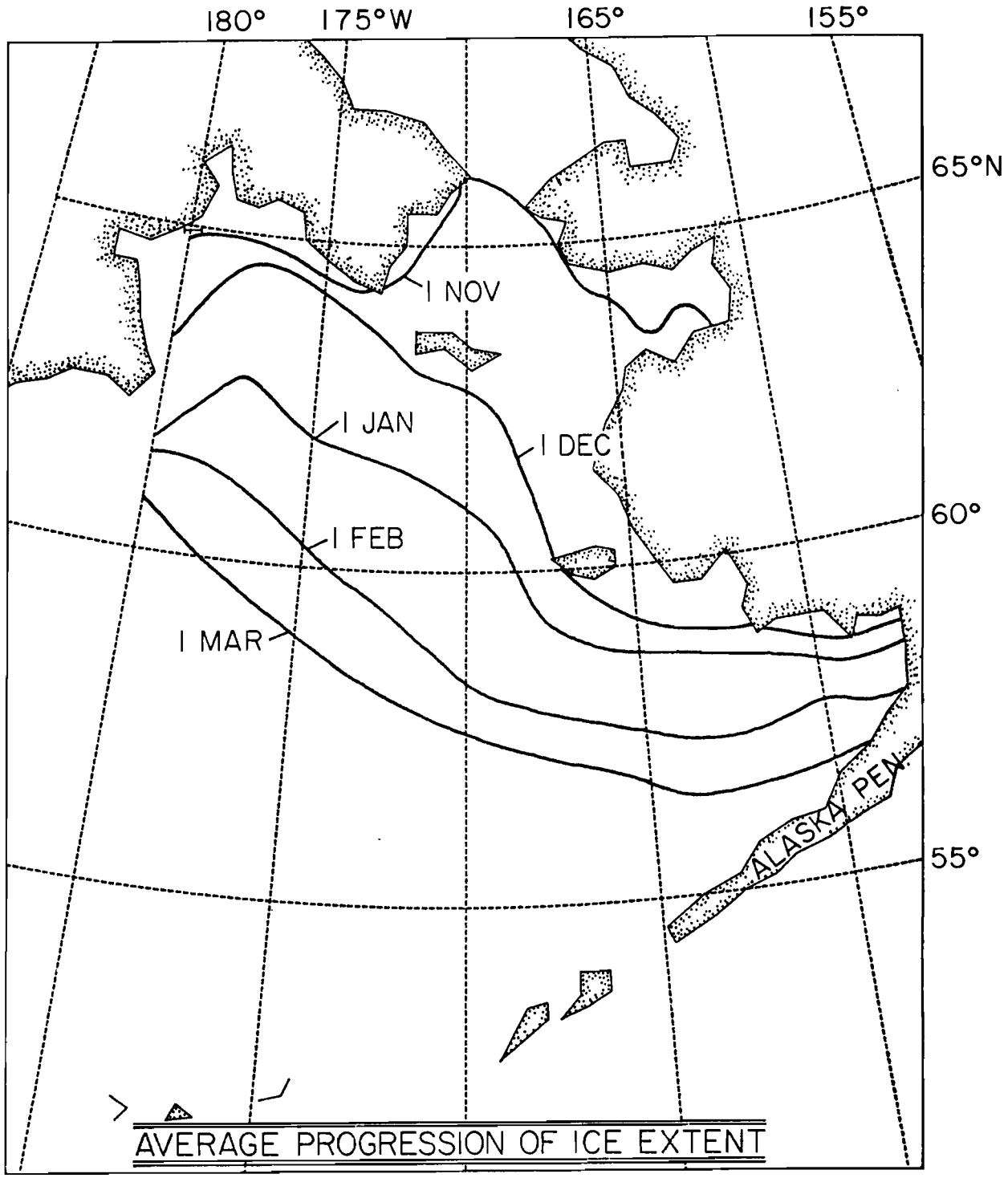


Fig. 2. Average progression (50% probability) of ice extent during the growth season, based on 1972-1979 ice extents (from Pease et al., 1982).

the Bering Sea through the central and western Aleutian Island passes and progresses as a free wave to the shelf. Largest tidal amplitudes are found over the southeastern shelf region, especially along the Alaska Peninsula and interior Bristol Bay. Each semidiurnal tide propagates as a Kelvin wave along the Alaska Peninsula but appears to be converted on reflection in interior Bristol Bay to a Sverdrup wave. In general, tidal ellipses are oriented along isobaths and are nearly rectilinear.

### 2.4 Climatology

A major influence of the general atmospheric circulation on the area is the region of low pressure, normally located in the vicinity of the Aleutian chain, referred to as the Aleutian Low. On monthly mean pressure charts (e.g., Brower et al., 1977) this region appears as a low-pressure cell normally oriented with the major axis in an east-west direction. This is a statistical low, indicating only that pressures are generally lower along the major axis as a result of the passage of low-pressure centers or storms. Storms are most frequent in this area and are more intense than in adjacent regions. The most frequent trajectory of these storms is along the Aleutian Islands and into the Gulf of Alaska in winter, and along the same general path in the west but curving northward into the Bering Sea in summer (Overland, 1981). The monthly frequency of low-pressure centers in the southern Bering Sea is slightly higher in winter (generally four to five) than in summer (three to four), with winter storms being more intense. Climatology of the southern Bering Sea can be characterized by a progression of storms rather than fixed weather types (Overland, 1981), and the presence of mountain passes will further complicate local wind characteristics.

## 3. METHODS

### 3.1 Current and Bottom Pressure

Most of our measurements were made using RCM-4 Aanderaa recording current meters on taut-wire moorings. Typical instrument placement was 20 m below the surface and 10 m above the bottom. Where water depths were less than 35 m, a single RCM-4 was located at 10 m above the bottom. The subsurface flotation was usually at 18-m depth, and exerted about 1000-lb (1 lb = 4.45N) buoyancy. Sampling interval was 30 minutes. Aanderaa RCM-4 current meters record speed by summing the number of rotor turns for, in our case, 15- or 30-min intervals. Direction is recorded at the time of sampling by measuring compass and vane orientation. Therefore, speed recorded at time $t_n$ is integrated over $\Delta t = t_n - t_{n-1}$, while direction is instantaneous at time $t_n$. Speed at $t_n$ and $t_{n-1}$ were averaged before converting to east and north components of velocity at time $t_n$. These components were then low-pass filtered (filter half-amplitude response was at a period of 2.9 hr) and a second-order polynomial was used to interpolate the observations to whole hours. We estimate that directions were accurate to ±5° and speeds to ±1 cm/s, exclusive of rotor pumping, mooring motion, or fouling. A summary of meter location and depth and observation period is given in Appendix A. Note that on most of the Transport Processes (TP) moorings, one of the RCM-4's was fitted with a transmissometer.

It is well known that mechanical current meters such as the RCM-4 may give erroneous speeds because of effects from either mooring motion or high-frequency water motion (e.g., Quadfasel and Schott, 1979, give several references). Pearson et al.(1981b) have examined the performances of moorings like ours on the Alaskan shelves, and they found speed differences at tidal frequencies of ≦10% when windy and calm seasons were compared; however, during storms erroneous speeds do occur. Extrapolating their results to lower frequencies, we believe that the effects of mooring motion and rotor pumping were minor and that errors were probably limited to a few percent increase of the speeds of low-frequency flows (which were usually strongest during windy periods).

At some locations along the Alaska Penninsula, Neil Brown acoustical current meters (ACM) were used because biological fouling was a problem (Schumacher and Pearson, 1980). The ACM's emit continuous high-frequency acoustic signals which are phase advanced or phase delayed as they travel with or against the current. The relative phase is converted to a voltage directly proportional to the water velocity. Currents are measured along two right-angled, horizontal paths. At a pre-determined interval, in this case one minute, the component velocities are averaged and recorded. Ten-minute segments of the original one-minute-sample interval data were averaged.

In order to characterize the bottom pressure field and to estimate sea level changes, Aanderaa TG-2 or TG-3 pressure gauges were deployed on all of the moorings. These instruments were located in a cage welded to the anchor to eliminate any possible noise due to mooring motion. Sampling intervals varied between 15 and 30 minutes.

Data from the current meters and pressure gauges are processed in a similar manner. The original series are converted to engineering units, and the time base is checked by comparing field logs to the number of records. Excessive values are removed by determining the standard deviation ($\sigma$) of consecutive one-thousand-record segments and eliminating values greater than six $\sigma$ from the segment mean. A tidal analysis is then performed on the edited data set to check consistency of tidal amplitudes and phases.

Two sets of time series are produced from edited current and pressure observations using a Lanczos filter (cf. Charnell and Krancus, 1976). The first set is filtered so that over 99% of the amplitude was passed at periods greater than 5 hr, 50% at 2.9 hr, and less than 0.5% at 2.0 hr. These sets are used to determine tidal constituents and spectral estimates. The second set is filtered to remove most of the tidal energy; the filter passed 99% of the amplitude at periods greater than 55 hr, 50% at 35 hr, and less than 0.5% at periods less than 25 hr. These sets are resampled at 6-hr intervals for use in examining subtidal current and pressure.

## 3.2 Hydrographic Data

Conductivity and temperature versus depth (CTD) data were obtained from three cruises conducted by NOAA's Pacific Marine Environmental

Laboratory and one "ship-of-opportunity" cruise (Appendix A). The CTD systems sampled five times per second during the down-cast (lowering rate of 30 m/min). Nansen bottle samples were taken at most stations to provide temperature and salinity calibration. Data from monotonically increasing depth were "despiked" to eliminate excessive values and were averaged over 1-m intervals to produce temperature and salinity values from which density and geopotential anomaly were computed.

### 3.3 Wind Observations

Because orography can affect large-scale geostrophic winds (Livingstone and Royer, 1980), a meteorological station was established near Lagoon Point and was maintained throughout the current meter observation period. The wind sensor was located about 7 m above ground level. The ensuing parameters are recorded like the Aanderaa RCM-4 and are processed similarly. We also have surface-wind time series for the mooring period which were computed by Fleet Numerical Weather Central from 6-hr synoptic surface-pressure maps, using a 3°-grid mesh and interpolated at 57°N, 163.5°W. The surface winds were estimated by rotating computed geostrophic wind by 15° to the left and reducing it in magnitude by 30% (Bakun, 1973). Climatological data from Brower et al. (1977) were also used.

## 4. RESULTS

### 4.1. The Unimak Pass Experiment

Three current meter/pressure gauge moorings (Figure 3) were deployed in Unimak Pass and on both adjacent shelves to describe currents and evaluate forcing mechanisms. Each mooring consisted of two Aanderaa RCM-4 current meters separated by ∿1 m and located 20 m above the bottom and an Aanderaa TG-3 pressure gauge. Such redundancy of current meters increases the probability of recovering at least one data set per mooring. (Of our six meters, one meter did fail).

From 11 March 1980 to 15 August 1980, the atmospheric pressure gradient across Unimak Pass was determined using the National Meteorological Center's twice-daily sea level pressure analyses for the Northern Hemisphere. Each map was quality checked for station accuracy and pressure analysis, and then a pressure gradient vector was determined for 54°N, 165°W and recorded in terms of direction from true north and magnitude in mb 1° at latitude. Wind time series over the mooring period were computed by Fleet Numerical Weather Central from 6-hr synoptic surface pressure maps, using a 3°-grid mesh and interpolated at 54°N, 163°W.

#### 4.1.1. Introduction

Straits or passes which connect large bodies of water are a common geographical feature throughout the world and water transported through the straits can have a profound impact on oceanographic characteristics

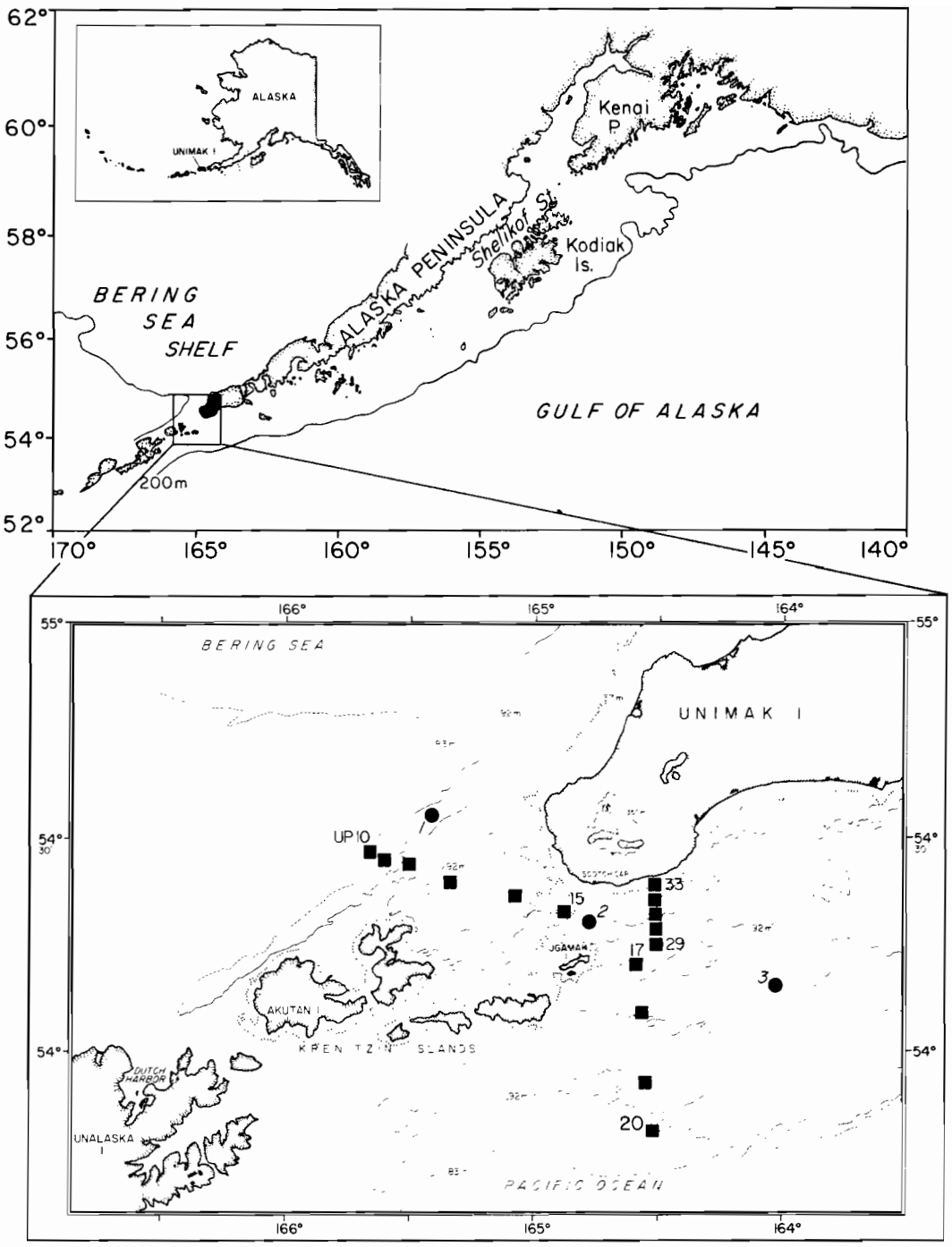


Fig. 3. Geographic setting showing (a) the Gulf of Alaska and Bering Sea shelves and (b) a detailed view of the Unimak Pass study area with some orographic features and the location of current meter and pressure gage moorings (dots) and CTD stations (squares). Depth contours (given in meters) were constructed from the 20 (dotted line), 50, and 100 fathom isobaths.

in the surrounding bodies of water. In his review of currents in a strait, Defant (1961) discusses the oceanography of several well-known examples and notes that the dynamic cause of currents in these straits lies in the density difference between the adjacent bodies of water. While mean flow generally may be driven by such differences, shorter period fluctuations (two to ten days) are driven by barotropic sea level differences along the strait. These, in turn, can be produced by large-scale meteorological forcing which results in sea level changes at the coast. Examples of passages where such forcing was observed include the English Channel (Bowden, 1956), the Bering Strait (Coachman and Aagaard, 1981), and the Strait of Belle Isle (Garrett and Toulany, 1981; Garrett and Petrie, 1981).

We present results from current, bottom pressure, and hydrographic data which support the supposition of inflow to the Bering Sea; however, the waters are from the shelf of the Gulf of Alaska and not from the Alaska Stream. Further, both driving mechanisms noted above are operative: the mean flow was related to a baroclinic coastal current along the southern side of the Alaska Peninsula, and fluctuations were related to an along-pass bottom pressure difference generated by sea level changes mainly over the Gulf of Alaska shelf.

### 4.1.2 Low Frequency and Mean Current

The 35-hr-filtered current meter data are shown as scatter diagrams and progressive vector diagrams (PVD's) in Figure 4. The scatter diagrams depict the distribution of the 6-hourly current vectors, and thus provide a visualization of variance about axes, while PVD's emphasize the time-dependent nature of the low-frequency flow. In the Bering Sea (UP1), about 50% of the vectors were in the northwest quadrant with a mean speed of about 15 cm/s. There were, however, pulses toward the south with magnitudes of 15 to 20 cm/s. Currents at UP2 tended to parallel the isobaths in the pass, and about 75% of the observations indicated flow from the Gulf of Alaska shelf into the Bering Sea. Maximum pulses (60 to 75 cm/s) prevailed over tidal current reversals. On the Gulf shelf (UP3), flow was highly variable in direction with a slight westward tendency. The strongest flows were 15 to 30 cm/s toward the southeast. The PVD's (Figure 4B) show similar flow features; however, the 5-day time ticks suggest that two distinct levels of current magnitude occurred during the observation period: the strongest flow existed during approximately the first 70 days, while flow was markedly less during the last half of the current records.

In Figure 5, we present plots of the 35-hr-filtered currents and bottom pressure for each of the moorings, the UP3-UP1 bottom pressure difference ($\Delta P$), the atmospheric pressure gradient, and the geostrophic (Bakun) winds. The currents are resolved along the axis of greatest variance (defined by the principal eigenvector of the covariance matrix for the orthogonal velocity component computed for the entire record), which also corresponds to flow through the pass. The atmospheric pressure gradient is resolved along an axis of 165°T approximately normal to the Gulf of Alaska coastline. The winds are resolved along 255°, parallel to the Alaska Peninsula.

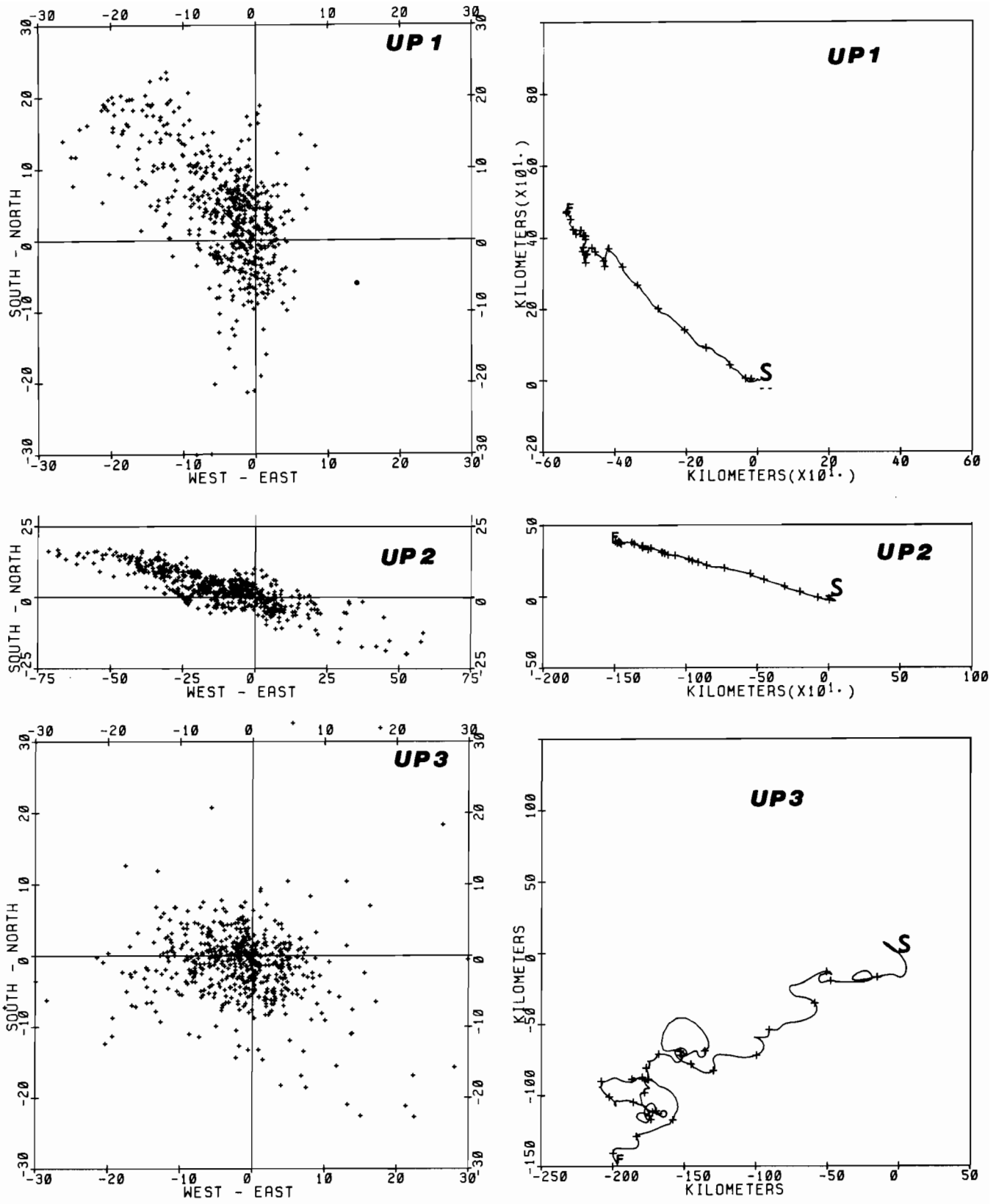


Fig. 4. Results from 35 hour filtered current data presented as scatter plots and progressive vector diagrams (S represents the start of the record, and the crosses are at 5-day intervals.) Note the different speed and length scales.

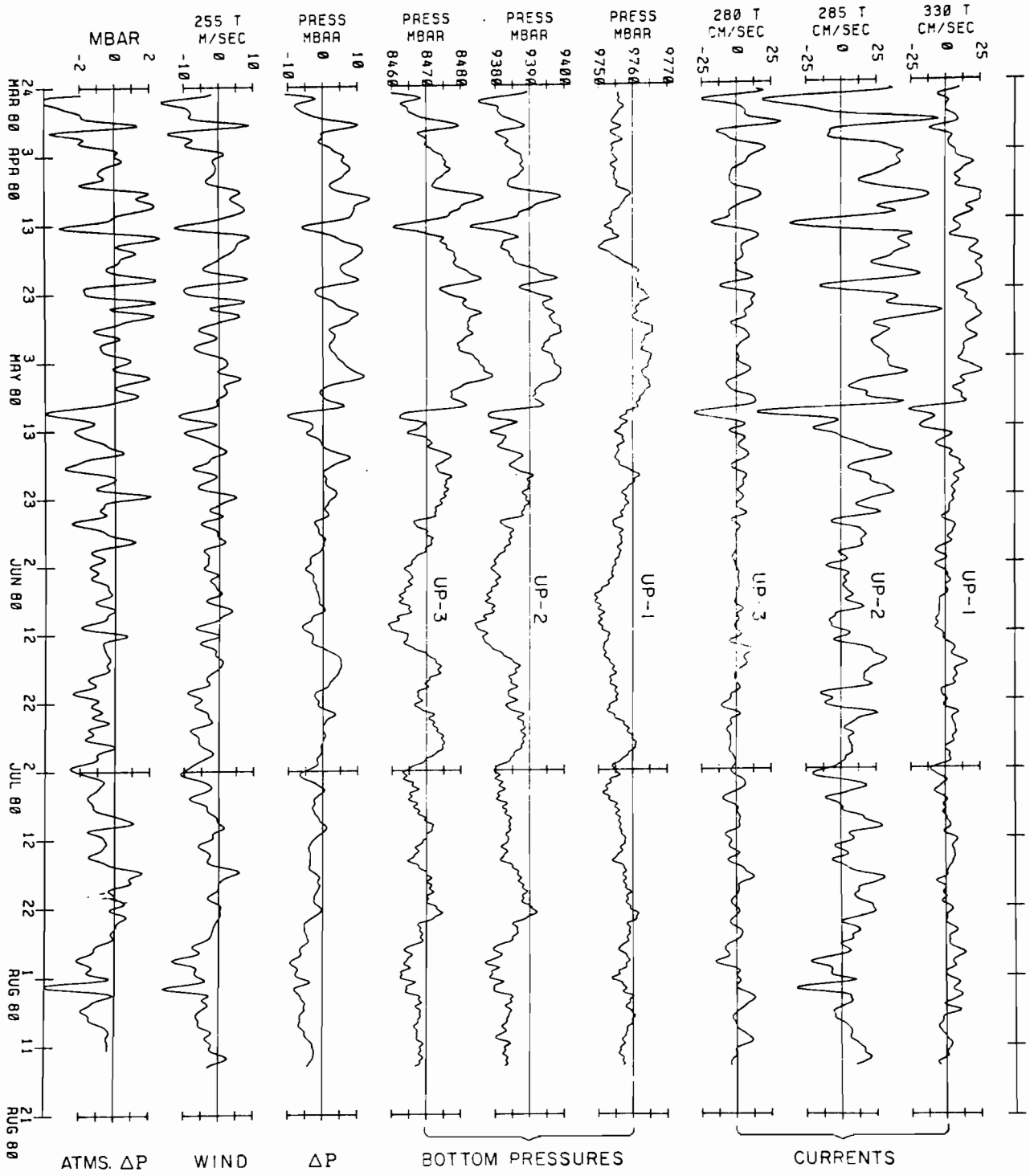


Fig. 5. Current vector time-series (35 hour filtered data) of current, bottom pressure, bottom pressure difference between UP3 and UP1 (Δ1P), alongshore geostrophic wind, and atmospheric pressure gradient (ATMSΔP in mbar/°lat).

A characteristic common to all the time series was the transition from a period of large fluctuations to one of lesser variance which occurred about halfway through the records. Analysis of the atmospheric pressure gradient series showed that while the direction of the principal axis remained constant toward 336°T (i.e., higher pressure over the Gulf of Alaska), magnitude increased during the second half by a factor of two and variance decreased. A dramatic change also occurred in winds with along-shore magnitude increasing from -1.7 m/s in the first period to -3.5 m/s in the later period. This suggests a four-fold increase in wind stress and enhanced coastal divergence along the Gulf side of the Alaska Peninsula. These results are consistent with the establishment of high pressure over the north Pacific Ocean which is a summer climatological feature (Brower, et al., 1977). Thus, that component of current which is a local response to meteorological forcing will also undergo a seasonal change.

A seasonal signal exhibiting less energy during summer was evident in current and wind time series from both the northwest (Schumacher and Reed, 1980) and northeast Gulf of Alaska (Lagerloef, Muench, and Schumacher, 1981) and from the southeastern Bering Sea (Kinder and Schumacher, 1981a). As will be discussed later, an important aspect of flow through Unimak Pass is a non-locally generated coastal current which has a seasonal signal linked to freshwater discharge (Royer, 1981). Although our records are too short to unequivocally define the amplitude and phase of a seasonal signal in flow through the pass, we clearly have observed a marked change between first and second halves of the records. The impact of this difference on mean current is given in Table 1. The first half of the records (26 March to 3 June) is called spring and the second half (4 June to 12 August) summer because the derived winds during this time were very similar to climatological mean winds and hence reflect a seasonal signal.

Within Unimak Pass, vector mean speed decreased by a factor of three between first and second halves, while direction remained nearly constant. The error estimate is a measure of statistical significance for the vector mean; the values in TABLE 3 are twice the RMS error estimate and thus are analogous to a 95% confidence interval. Using this measure, mean flow in the pass was always significant while on the shelves adjacent to the pass there was significant mean flow only during spring.

### 4.1.3 Time Series Relations:

We consider the correlations given in Table 2 in the context of a simple conceptual model of low-frequency currents as follows: 1) currents in Unimak Pass are driven by the difference in pressure between the two sides of the pass, 2) the pressure difference is produced by sea level changes, which can occur along the coast on both sides of the pass, and 3) currents observed on the adjacent shelves represent a barotropic response to pressure gradients rather than an Ekman-layer response. All of the observed currents were collected at least 47 m below the surface. As noted by Winant (1980), conventional estimates of the thickness of the Ekman layer are about 40 m, and Royer, Hansen, and Pashinski (1979)

TABLE 1: CURRENT AND WIND DURING FIRST (SPRING) AND SECOND (SUMMER) HALVES OF THE OBSERVATIONS

| Record | Observation Period | Vector Mean Speed (cm/s: °T) | Error Estimate[1] (cm/s) | Variance ($cm^2/s^2$) |
|---|---|---|---|---|
| UP1 | spring | 9.8 : 306 | ± 6.6 | 14.1 |
| | summer | 2.2 : 334 | ± 2.2 | 8.9 |
| UP2 | spring | 19.3 : 285 | ± 9.2 | 37.4 |
| | summer | 6.0 : 282 | ± 4.6 | 13.1 |
| UP3 | spring | 3.2 : 240 | ± 2.4 | 41.0 |
| | summer | 1.0 : 198 | ± 1.2 | 12.4 |
| Geostrophic Wind | spring | $2.3 \times 10^2$ : 030 | ± 2.6 | $18.1 \times 10^4$ |
| | summer | $3.8 \times 10^2$ : 048 | ± 1.6 | $11.6 \times 10^4$ |

[1] Estimate of Error = $2\sigma/(\ell/\tau)^{\frac{1}{2}}$, where $\sigma$ is the standard deviation along the vector mean speed axis, $\ell$ is the record length and $\tau$ is the integral time scale or area under the auto-correlation function (Allen and Kundu, 1978).

suggested that the stratified Ekman-layer depth in the northern Gulf of Alaska is probably less than 35 m.

The linear relation between pressure difference and current at UP2 accounted for 76% of the current variance (85% in spring and 50% in summer). When alongshore winds increased, bottom pressure at UP3 decreased; however reponse at UP1 was not significantly correlated with alongshore wind. Further, the variance in the bottom pressure record from UP1 was only one-third of that estimated in the record at UP3. Thus, changes in the bottom pressure difference were primarily a result of forcing on the Gulf shelf with a large fraction, 42% (50% in spring and 25% in summer) accounted for by the relation with alongshore wind. To address the question why there was more energy in current and bottom pressure records from the Gulf shelf than from the Bering Sea at meteorological frequencies we use climatological data (Brower, et al., 1977) and principal storm track data from March through August 1980 (*Mariner's Weather Log*, 1981). We divided data from a 10°-by-10° region (50° to 60°N: 150° to 170°W) into a Bering Sea area north of 55° and a Gulf of Alaska area south of that latitude. There were seven principal storm tracks located in the Gulf and three in the Bering Sea. During our observations in 1980, there were eleven principal and eight secondary storm tracks south of the Peninsula, while over the Bering Sea there were only six principal and three secondary storm tracks. In general, we expect to find greater meteorologically induced activity over the Gulf shelf.

TABLE 2. CORRELATION MATRIX

| | CURRENT | | | BOTTOM PRESSURE | | | WIND | | BOTTOM PRESSURE DIFFERENCE | ATMOSPHERIC PRESSURE |
|---|---|---|---|---|---|---|---|---|---|---|
| | UP1 | UP2 | UP3 | UP1 | UP2 | UP3 | ALONG-SHORE | CROSS-SHELF | ($\Delta$P) | GRADIENT |
| UP1 | 1.0 | .67 | .34 | .47(4) | .69 | .47(4) | .40(1) | .44(4) | .69(1) | .47(2) |
| UP2 | -- | 1.0 | .70(1) | * | .69 | .79 | .77(1) | .24(5) | .87 | .76(2) |
| UP3 | -- | -- | 1.0 | * | .38 | .41 | .57(1) | .24(6) | .50(1) | .55(1) |
| UP1 | -- | -- | -- | 1.0 | .78(1) | .66(1) | * | .25(5) | * | * |
| UP2 | -- | -- | -- | -- | 1.0 | .93 | .46(1) | .35(5) | .65 | .54(1) |
| UP3 | -- | -- | -- | -- | -- | 1.0 | .54(1) | .38(6) | .50(1) | .58(2) |
| ALONG SHORE | -- | -- | -- | -- | -- | -- | 1.0 | * | -.65(-1) | .58(2) |
| CROSS SHELF | -- | -- | -- | -- | -- | -- | -- | 1.0 | .32(6) | .29(2) |
| BOTTOM PRESSURE DIFF. | -- | -- | -- | -- | -- | -- | -- | -- | 1.0 | .60(2) |

* indicates that the correlation coefficient was not significant at the 95% level.
Note: rows lag columns, and numbers in ( ) are multiples of 6 hrs.

It appeared that cross-shelf wind also contributed to the pressure difference, with significant correlation to bottom pressure on both shelves. The strength of these relations only accounts for ~6% (12% in spring, not significant in summer) and 14% (28% in spring, not significant in summer) of the variance at UP1 and UP3 respectively. Hayes (1979) noted the importance of cross-shelf wind to pressure gradient and estimated correlation coefficients of similar magnitude over the northeast Gulf of Alaska shelf. Chao and Pietrafesa (1980) noted that a larger contribution from cross-shelf wind-forcing usually results in a phase lag of sea level fluctuation response. The results in TABLE 2 are consistent with their results. In general, our conceptual model of interaction between wind, bottom pressure, and current in Unimak Pass accounts for much of the observed current fluctuations.

In order to examine relations between pressure difference and both current and geostrophic wind in Unimak Pass as a function of frequency, we present coherence-squared estimates in Figures 6 and 7. Current in the pass was coherent at all frequencies with the pressure difference series during both spring and summer with the largest coherence-squared (~0.70 to 0.96) at periods of about 3 to 10 days. During both record segments, coherence decreased at the longest period resolved (~23 days). In order to present coherence results as a single, phase-independent measure, we use the following technique. At each frequency where coherence-squared was significant at the 95% level, the product of the dependent variable (*i.e.*, current) variance times the coherence-squared was determined. Summing this product over all frequencies and dividing by the total record variance, we determined that 89% and 66% of the current fluctuations were accounted for by fluctuations in the pressure difference series during spring and summer, respectively.

Coherence-squared estimates between the pressure difference and geostrophic wind components (Figure 7) were greatest during spring: 70% and 26% of the fluctuations in bottom pressure difference were accounted for by relations with alongshore and cross-shelf winds, respectively. During summer, the percent of variance explained was only 9% and 7%, respectively. If the variance at periods longer than 10 days was neglected (the series were not coherent at these periods), then the values were 43% and 33%. It appears that at periods longer than ~10 days, the bottom pressure field was responding to forcing other than wind-induced pressure gradients; it is most likely that changes of density were the cause. Reed and Schumacher (1981) noted that as early as June insolation is important to monthly mean sea level anomalies at Dutch Harbor.

The current time series indicated that flow was generally from the Gulf of Alaska to the Bering Sea shelf and both mean and fluctuating currents were significantly greater during spring. Relations between the various series suggest that large-scale atmospheric pressure fields, hence geostrophic winds, were responsible for the 3- to 10-day fluctuations. The mode of interaction was mainly perturbation in sea level along the Gulf of Alaska coast. The longer period wind stress was alongshore (northeastward) which would generate a barotropic component of current alongshore (towards the northeast), rather than the observed negative alongshore or westward mean flow through the Pass. So, we now

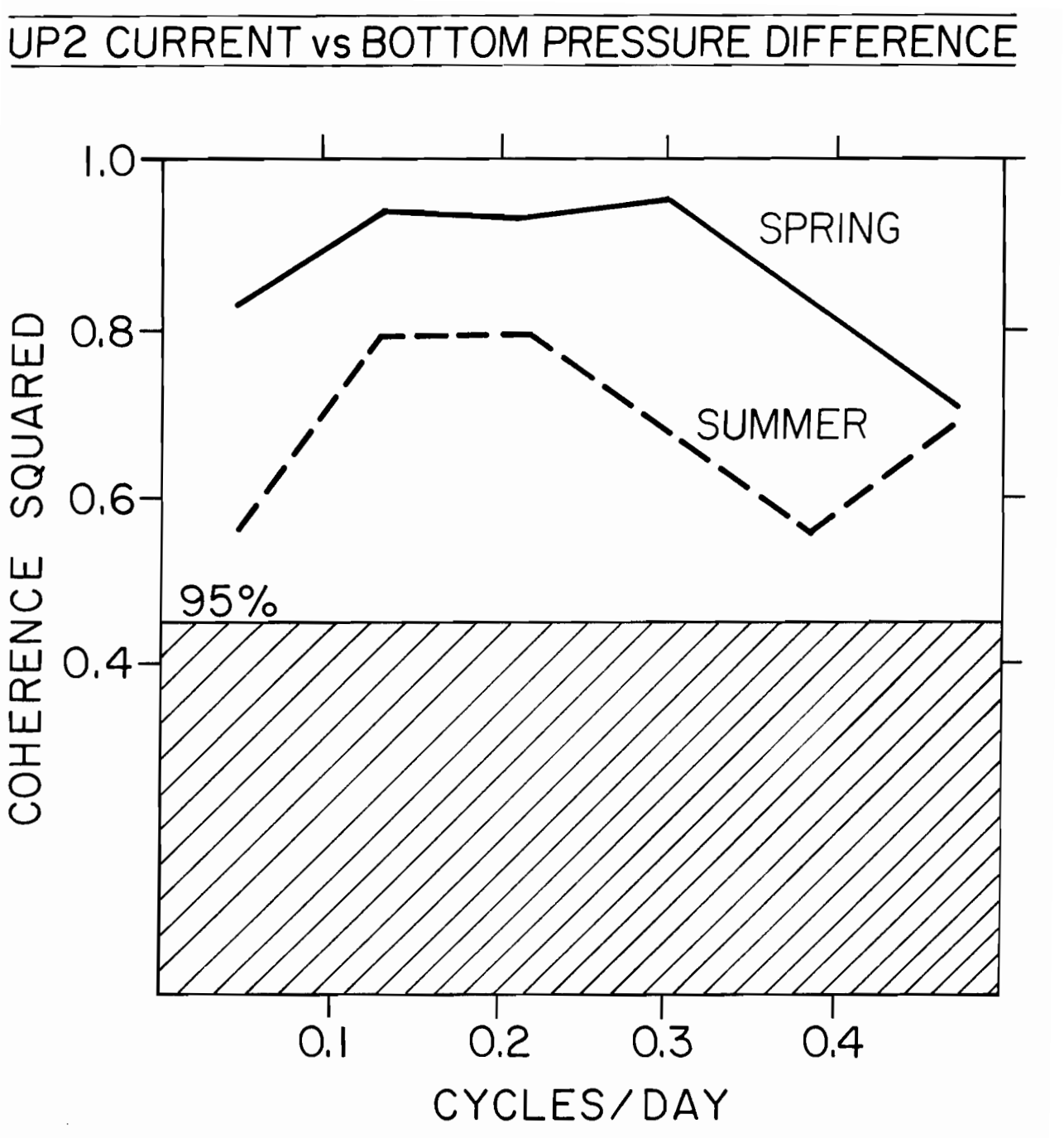


Fig. 6. Coherence between current in Unimak Pass (UP2) and bottom pressure difference along the pass for spring (solid line) and summer (dashed line) record segments.

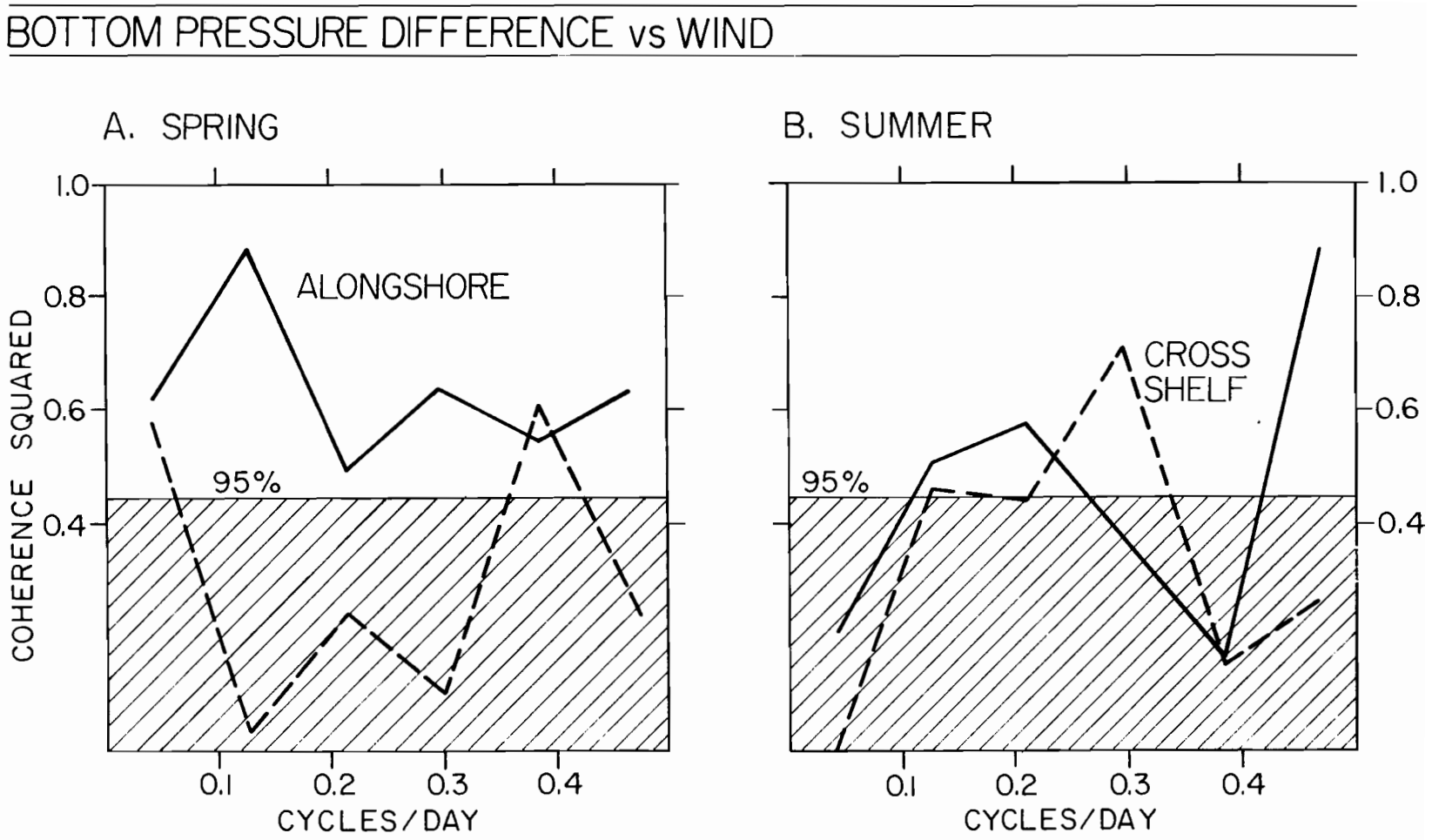


Fig. 7. Coherence between bottom pressure difference and geostrophic wind components during (a) spring and (b) summer record segments. The coherence with alongshore wind component is shown as a solid line and with the cross-shelf component as a dashed line.

examine hydrographic data to describe property distributions and to elucidate the role of mass distribution in generating long-term mean flow through Unimak Pass.

### 4.1.4 Property Distributions

Vertical sections of temperature, salinity, and sigma-t for 4 to 5 September 1980 are shown in Figures 8A, B, and C, respectively. Across the bottom of each panel the magnitude of the surface minus the bottom value of each parameter is also shown. Over the Gulf of Alaska shelf (stations 17 to 20) thermal stratification exceeded 4.0°C, and the upper 50 m were considerably warmer there than over the Bering Sea shelf (stations 14 to 10). Although tides, and thus tidal mixing, are more energetic within Unimak Pass proper (station 15), thermal stratification in the pass (∿2.5C) was greater than thermal stratification (∿0.9 to 1.5°C) observed in Bering shelf waters. A similar distribution existed in salt content; $\Delta S$ values were greatest over the Gulf shelf, persisted within the pass, and were least west of the pass proper. We note a region of low salinity (≦31.75 gm/kg) existed within ∿25 km of Unimak Island. The impact of temperature and salinity upon density is shown in the bottom panel of Figure 8. As expected, the distribution of density bears a marked resemblance to salinity. When water temperatures are less than 10°C, the equation of state for seawater dictates that variations of salinity contribute more than those of temperature to changes in density (Gebhart and Mollendorf, 1977).

A second hydrographic section through Unimak Pass was occupied on 17 February 1981, and we present the vertical section of salinity with the $\Delta T$ and $\Delta\sigma_t$ values across the bottom (Figure 9) for comparison to conditions observed in September 1980. Surface temperatures (not shown) were ∿3.5 to 4.0°C and increased less than 1.0°C with depth, so there was little structure in the thermal field. Isohalines again indicated regions of low salinity (≦31.75 gm/kg); however, the only substantial stratification ($\Delta\sigma_t \geqq 0.5$) existed over the Bering Sea shelf. As was observed in September 1980, the strongest vertical and horizontal salinity gradients were found over the Bering Sea shelf. A five-station hydrographic section normal to Unimak Island was occupied on 13 May and again 2 June 1981. Both sections showed low-salinity water (≦31.75 gm/kg) within ∿20 km of Unimak Island (cf., Figure 10) and little thermal structure.

The most extensive spatial coverage was attained on a cruise conducted between 2 and 3 September 1981. Hydrographic data are presented as the areal extent of waters with salinity less than 31.75 gm/kg in the upper 50 m (or to the bottom, Figure 11A) and as dynamic topography (0/50 db) in Figure 11B. West of the pass proper, the bulk of less saline water was in a band within ∿10 km of the coast, while south of Unimak Island the band extended ∿20 km offshore and less saline waters existed in a thin layer at least 60 km offshore. The dynamic topography (0/50 db) reflects the narrowing trend of the low-salinity band, with relief increasing from 0.008 dyn m between stations 32 and 29 south of Unimak Island to 0.025 dyn m between stations 48 and 51 northwest of the island. The steep relief between stations 51 and 52 resulted from the

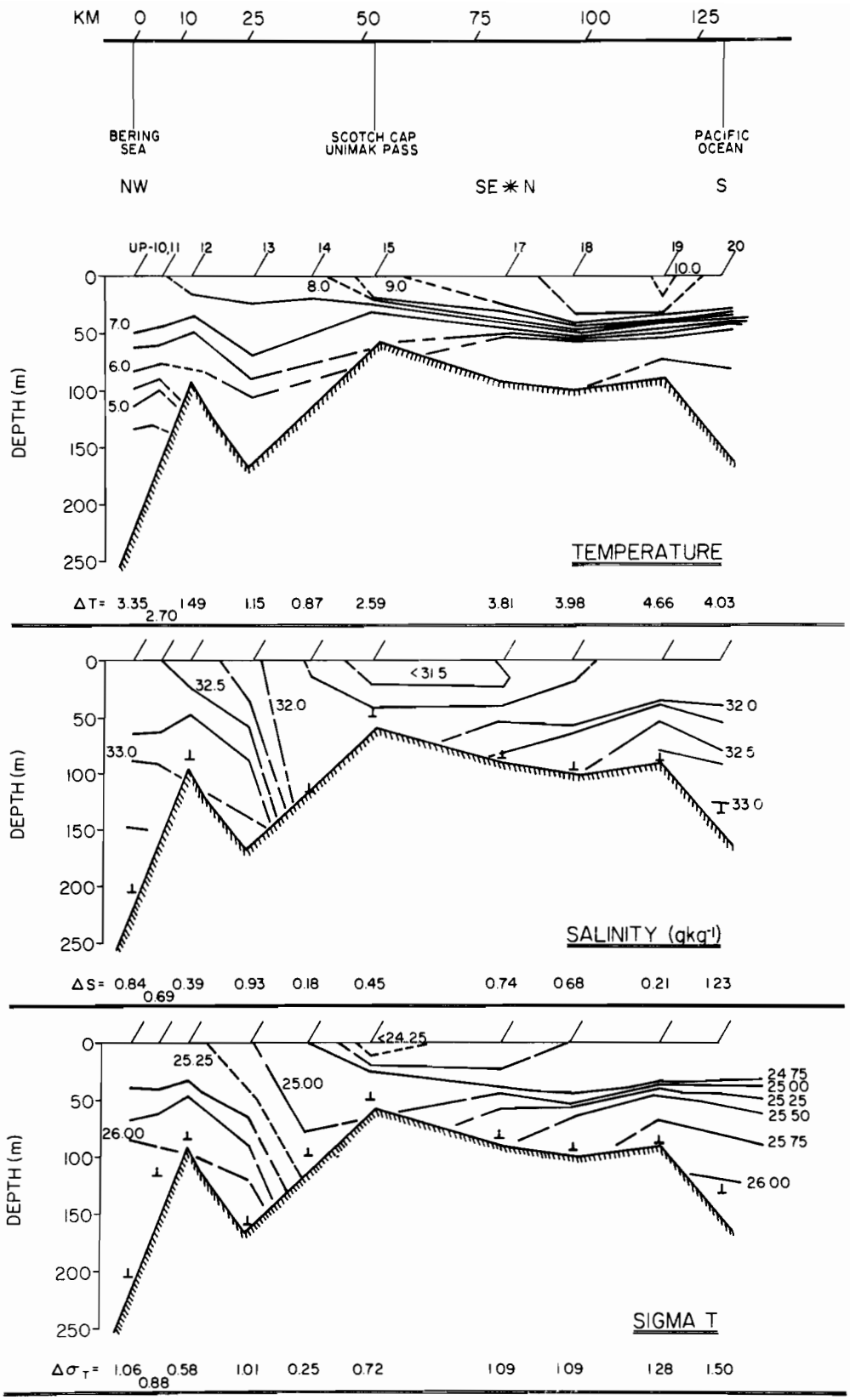


Fig. 8. Hydrographic data from September 1980 presented as (a) temperature (°C), (b) salinity, and (c) sigma-t sections. The Δ values are the magnitude of surface minus bottom 1 m averaged values. See Figure 1 for stations locations.

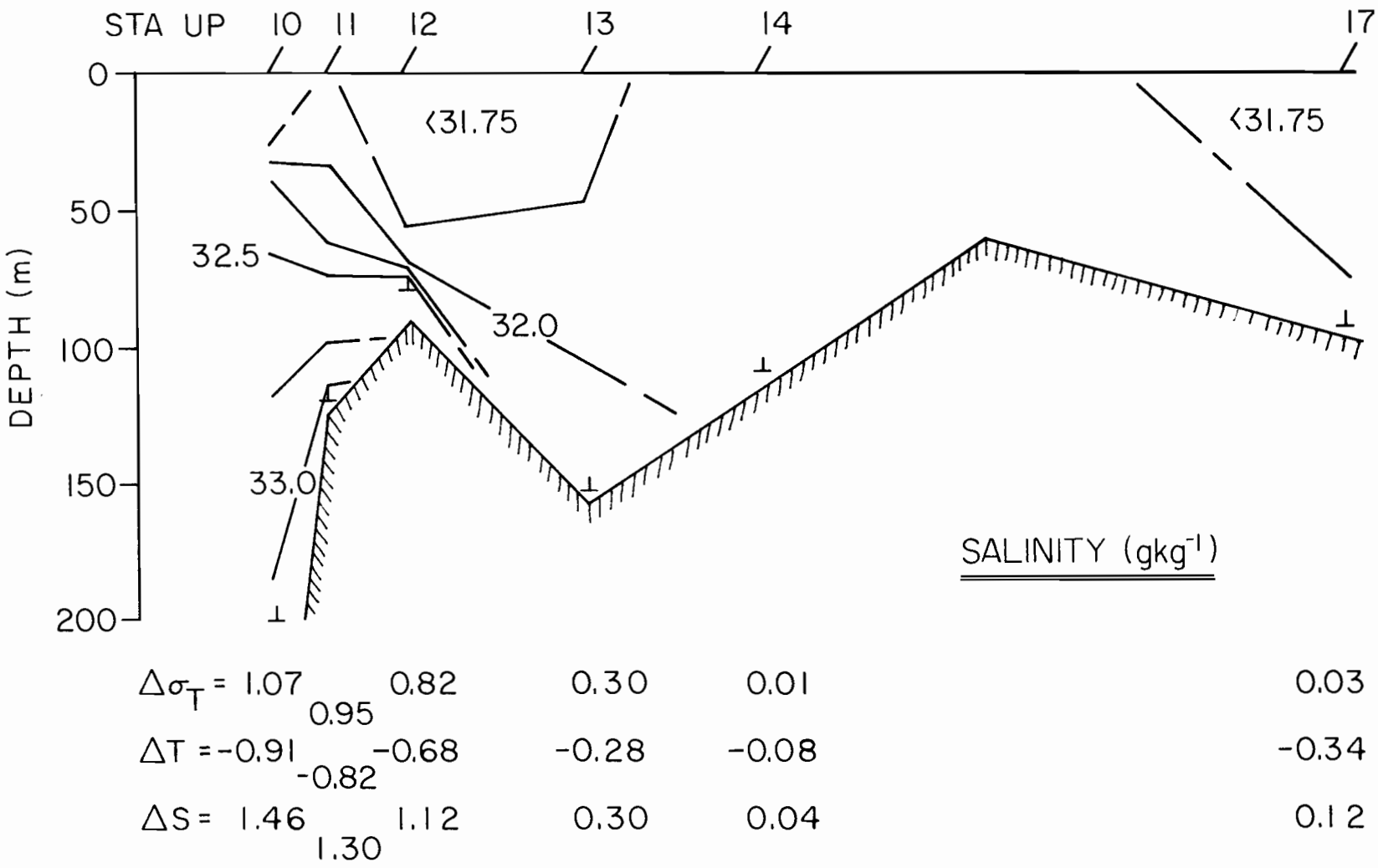


Fig. 9. Hydrographic data collected during February 1981 along the same section as in Figure 6. The Δ values are the magnitude of surface minus bottom 1 m averaged values.

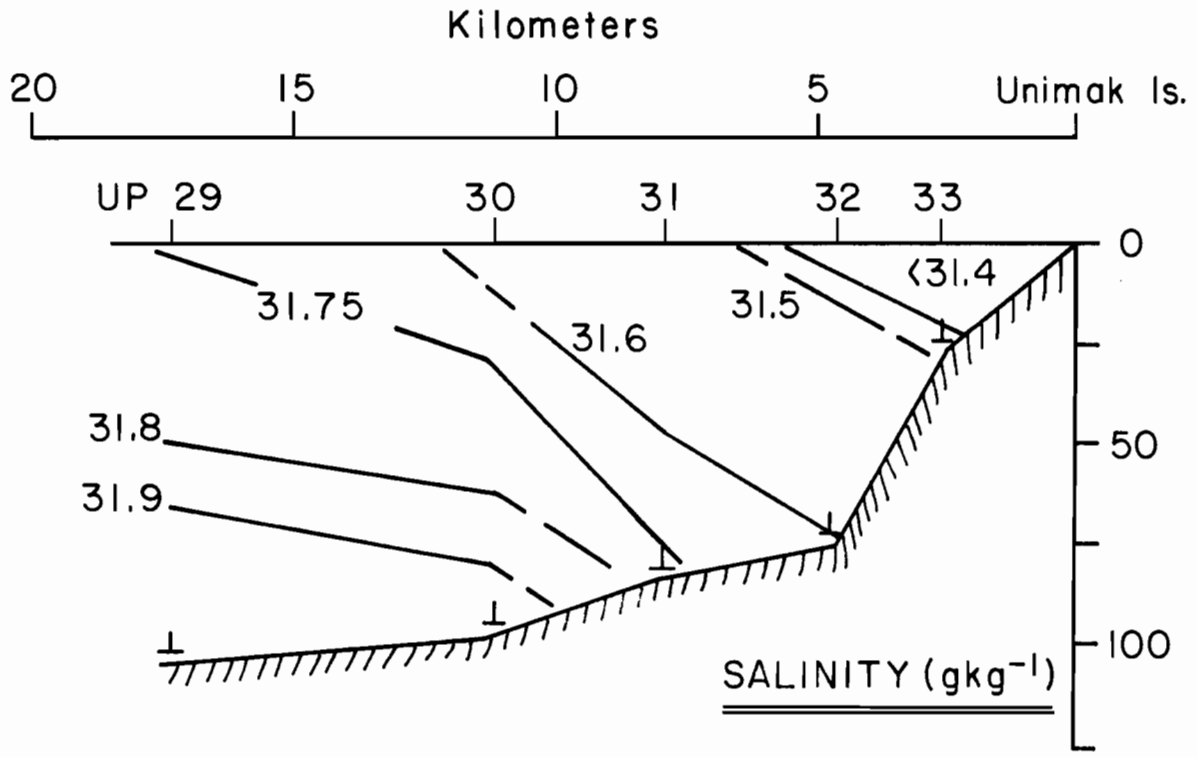


| | | | | | |
|---|---|---|---|---|---|
| $\Delta\sigma_T$ = | 0.23 | 0.35 | 0.18 | 0.36 | 0.09 |
| $\Delta T$ = | 0.80 | 0.70 | 0.30 | 0.91 | 0.33 |
| $\Delta S$ = | 0.21 | 0.34 | 0.21 | 0.33 | 0.14 |

Fig. 10. Hydrographic data for May 1981 from stations normal to Unimak Island. The Δ values are the magnitude of surface minus bottom 1 m averaged values.

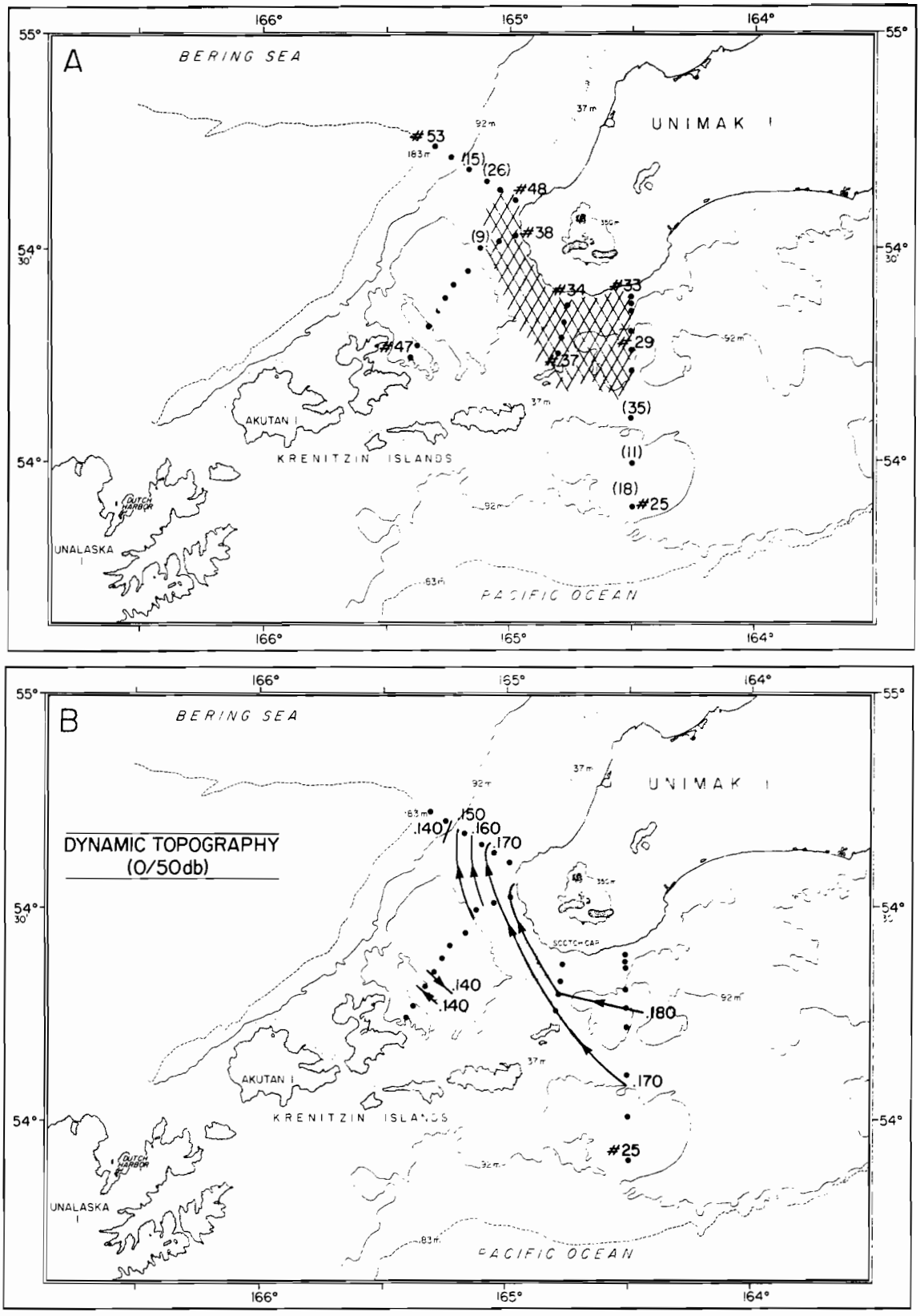


Fig. 11. Hydrographic data for September 1981 presented as (a) areal extent of waters with salinity ≧31.75 gm/kg in the upper 50 m (or bottom) where the numbers in parentheses are depths of the low-salinity band for $z>50$ m and (b) dynamic topography (0/50 d) with a 0.01 dyn m contour interval. CTD station numbers are indicated by the number sign.

presence of saline water (>32.50 gm/kg) over the Bering Sea shelf. These waters also resulted in lower relief west of station 40. The suggested curvature of geopotential contours indicates that relative vorticity generated either by changes in depth or a horizontal velocity gradient in the pass proper may be important to flow dynamics west of the pass.

### 4.1.5 Baroclinic geostrophic currents

A persistent feature of the mass distribution in the five data sets was the presence of low-salinity water along the coast of Unimak Island. Other hydrographic surveys (Kinder et al., 1978; Wright, 1981) have also shown less saline waters exist off Unimak Island and south of the Alaska Peninsula. We estimate the impact of the observed mass distribution on the velocity field by assuming a geostrophic balance. While this method neglects such factors as wind stress, bottom friction, and barotropic pressure gradients, over the Bering Sea shelf (Kinder and Schumacher, 1981a) and along the Gulf of Alaska coast (Royer, Hansen, and Pashinski, 1979; Schumacher and Reed, 1980), good agreement was shown between baroclinic geostrophic flow and both Eulerian and Lagrangian current observations.

In Table 3, we present baroclinic currents of the surface relative to 50 db for each set of station pairs where the dynamic relief was ≧0.01 dyn m. The inferred flow from the first three station pairs in September 1980 and the first four pairs in September 1981 together with set 11/12 suggests moderate flow (7 to 22 cm/s) through Unimak Pass.

TABLE 3. Dynamic Relief and Baroclinic Speed

| Observation Date | [-Station Pair | 0/50 db Dynamic Relief (dyn m) | Speed (cm/s) | Direction (°T)-] |
|---|---|---|---|---|
| 4 - 5 Sept. 1980 | 12/13 | 0.014 | 9 | NE |
| | 13/14 | 0.015 | 10 | NNE |
| | 14/15 | 0.011 | 7 | NE |
| | 18/19 | 0.012 | 5 | W |
| 17 Feb. 1981 | 11/12 | 0.011 | 13 | NE |
| 13 May 1981 | 32/29 | 0.011 | 12 | W |
| 2 June 1981 | 32/29 | 0.010 | 7 | W |
| 2 - 3 Sept. 1981 | 36/37 | 0.010 | 17 | W |
| | 38/39 | 0.012 | 20 | N |
| | 39/40 | 0.013 | 22 | N |
| | 49/50 | 0.012 | 19 | NE |
| | 50/51 | 0.014 | 33 | NE |
| | 51/52 | 0.020 | 30 | NE |
| | 27/26 | 0.010 | 7 | W |

This is consistent with our current observations and compares favorably with dynamic topographies presented by Coachman and Charnell (1977) from March 1976 CTD data collected north and west of the pass. Relief across the remaining station pairs suggests a weaker westward-flowing current (5 to 12 cm/s) along the Gulf side of the Alaska Peninsula and a stronger current (19 to 33 cm/s) northwest of the pass.

Since 1975, 61 CTD stations were occupied within about 50 km of Unimak Pass proper. Separating these data into two sets, Gulf side (N=29) and Bering Sea side (N=32) of the pass, we can strengthen our hypothesis that water east of the pass is generally less dense (due to lower salinity) than water west of the pass. We note that only data sets with casts on both sides during a given cruise were used in order to avoid aliasing the results. East of the pass, the mean dynamic height (0/50 db) and standard deviation was 0.162±0.016 dyn m and 0.136±0.016 dyn m west of the pass. Thus, including CTD data from all seasons, we find that water along the Gulf side of Unimak Island is generally about 3 dyn cm greater in height (over 50 db) than waters west of Unimak Pass.

### 4.1.6 Discussion

The results presented thus far have defined the behavior of the current in Unimak Pass and the forcing for such flow: water is generally transported from the Gulf of Alaska onto the Bering Sea shelf. While subtidal flow with periods of 3 to 10 days was shown to be driven mainly by a wind-induced pressure difference along the pass, longer period flow (on the order of months) appeared to be driven by a coastal current existing along the Alaska Peninsula. Two important questions evolve from our results: what is the source of the coastal current, and what is the impact of transport through Unimak Pass?

A recent study (Schumacher and Reed, 1980) has described and defined the Kenai Current, a strong coastal current which flows westward along the Gulf of Alaska coast from about 145°W to the southwest end of Shelikof Strait (~156°N). Royer (1981) has indicated that this feature is a component of the more extensive Alaska Coastal Current, which is the consequence of the accumulation of runoff beginning along the British Columbia coast. He estimates transport in the northeast Gulf of Alaska to be $0.12\pm0.05 \times 10^6$ $m^3/s$, and Reed, Schumacher, and Wright (1981) show that the dynamic relief (0/90 db) is typically ~4 dyn cm in this portion of the Alaskan Coastal current. To the west, along the Kenai Peninsula, there is an increase in dynamic relief (4 to 20 dyn cm) and transport ($0.10$ to $1.2 \times 10^6 m^3/s$), both varying with season. The behavior of the Kenai Current west of Shelikof Strait is not well known, however, Wright (1981) indicates relatively low-salinity water exists along the Alaska Peninsula as far west as Unimak Pass. Further, it is unlikely that the freshwater signal near Unimak Pass was of local origin, since rainfall undergoes a four-fold reduction (323 to 84 cm) from ~158°W (Chignik) westward to 162.5°W (Cold Bay) (Brower et al. 1977), and there are no gauged rivers. Current records from ~156°W and 158°W (Muench and Schumacher, 1980) indicate a substantial mean flow (~15 cm/s) westward along the coast. These results, together with the hydrographic data presented above indicate that some fraction of the Kenai Current continues along the peninsula and flows through Unimak Pass.

Using CTD data collected south of Unimak Island between stations 33 and 29 in May, June, and September 1981, we estimate that baroclinic transport (computed to the greatest common depth) was ∿6, 5, and 7 x $10^4$ $m^3/s$ respectively with maximum surface speeds of 12, 8, and 5 cm/s and dynamic relief (0/60 db) of ∿2 dyn cm. For all estimates, the largest fraction of the transport (>40%) occurred between the two most seaward stations. Thus, total alongshore transport may be substantially greater; during September 1981 transport between stations 33 and 26 (see Figure 9A) was ∿24 x $10^4 m^3/s$. Transport too far offshore to flow through the pass was also indicated in August 1980 data (see set 18/19 in Table 3). CTD data collected on a line normal to the Peninsula about 150 km east of Unimak Pass (at ∿159°W) indicated alongshore transport of about ∿24 × $10^4 m^3/s$ in conjunction with a band of low-salinity water of similar cross-shelf extent to that observed south of Unimak Island. Transport estimates between stations 38/42 and 48/52 (see figure 9A) were about 12 and 16 x $10^4 m^3/s$ respectively. The hydrographic data suggest a baroclinic current south of the Peninsula with a large fraction flowing westward through Unimak Pass and continuing along the northwest coast of Unimak Island. Caution is necessary in estimating transport through Unimak Pass from a single current record. Assuming that the measured mean flow was representative of most of the cross section (there were no reversals in baroclinic speed and vertical shear was moderate), we estimate ∿6 to 20 × $10^4 m^3/s$ were transported through Unimak Pass, which is consistent with the baroclinic estimates.

The dearth of CTD data precludes establishment of a seasonal signal near Unimak Pass; however, off the Kenai Peninsula, baroclinic transport varied by an order of magnitude, with a maximum observed in October (Schumacher and Reed, 1980). Using an annual-curve fitting technique on six years of data, Royer (1981) suggested a maximum occurred in December. If continuity exists along the current, then maximum baroclinic transport through Unimak Pass should occur sometime during the first three months of the year. This is consistent with the observed current in Unimak Pass and the increase in sea level anomaly observed during December and January at Dutch Harbor (Reed and Schumacher, 1981). While baroclinic spin-up may account for increased speeds for one to two months, wind-induced coastal convergence was of equal magnitude along the Kenai Peninsula; during January through March 1978, vector mean speed was ∿25 cm/s at a depth of 75 m in Shelikof Strait. Although there is uncertainty regarding phase and amplitude due to limited data, the nature of forcing suggests that changes in mean flow through Unimak Pass appear related to seasonal behavior of the Kenai Current and not to local forcing.

We now consider the impact that transport through Unimak Pass has on water mass properties and on the water budget of the Bering Sea shelf. The CTD data presented above indicate a region of enhanced horizontal salinity gradient about 50 to 75 km west of Unimak Pass proper (Figure 6, vicinity of station 13; Figure 9, vicinity of stations 40/41 and 51/52). This feature can be compared to the so-called middle front which exists over the southeastern Bering Sea shelf (Coachman and Charnell, 1979; Coachman et al., 1980; Kinder and Schumacher, 1981b) and has a profound influence on that region's productivity and nutrient fluxes (Iverson et al., 1979; Coachman and Walsh, 1981). In these papers, the middle front, as determined from CTD data collected about 100 km northwest of Unimak

Island, was characterized in terms of a vertical salinity gradient, $\Delta S/\Delta z$, and the horizontal gradient of the mean salinity, $\Delta \bar{S}/\Delta x$. Hydrographic data collected during 1980 and 1981 west of Unimak Pass indicated the following gradients existed: $\Delta \bar{S}/\Delta Z \sim 9 \times 10^{-5}$ g/kg/cm, and $\Delta S/\Delta x \sim 45 \times 10^{-3}$ g/kg/km with a slight enhancement in the bottom 50 m. Thus, the vertical gradient was about fifty times stronger, while the horizontal gradient of mean salinity was about five hundred times greater than that observed over the shelf to the northwest. The data indicate that the two fronts may be different dynamically, and it is not known if they are contiguous; however, transport of less saline water from south of the Alaska Peninsula results in a strong salinity front west of Unimak Pass proper. Hattori and Goering (1981) note the contribution of water flowing through Unimak Pass to the fertility of the region. Although these authors identify the water as being Alaskan Stream water, their temperature and salinity data suggest that the water was from the coastal current. Upwelling along the Gulf side of Unimak Island, induced during summer by the mean alongshore (northeastward) wind-stress, may have provided the relatively high concentrations of nitrate and ammonium that they observed. Further, the less saline waters may contribute substantially to the baroclinic coastal flow observed along the Bering Sea side of the Alaska Peninsula (Kinder and Schumacher, 1981b).

Recently, mean annual water transport through Bering Strait (from the Bering Sea into the Arctic Ocean) was reevaluated to be $0.8 \pm 0.2 \times 10^6 m^3/s$ (Coachman and Aagaard, 1981). The apparent source of most of this transport was flow along the Siberian coast (Coachman, Aagaard, and Tripp, 1975; Kinder and Coachman, 1978). We note that our estimates of transport through Unimak Pass are five to ten times greater than the gauged freshwater addition along the Alaska coast of the Bering Sea and may account for up to one-fourth the mean annual transport northward through Bering Strait.

## 4.2 Hydrography and Circulation Adjacent to the Alaska Peninsula

In order to characterize currents and hydrography over the shelf north of the Alaska Peninsula, ten moorings (Figure 12) were deployed between August 1980 and May 1981 and a 72-station CTD grid was designed (Figure 13). The ensuing observations permit a description of currents and inferences to be made regarding the 50-m front.

### 4.2.1. Long-period time dependence of hydrographic features

In this section, we present CTD data by cruise, where we selected a set of casts for the most synoptic period (about six days). These data are presented as area distributions, and both spatial and between-cruise changes are discussed.

Temperature: In August 1980, surface temperatures (Figure 14A) varied along the peninsula from ~11.5°C in inner Bristol Bay to <8.0°C north of Unimak Island. Across the shelf, the strongest difference (~2.0°C) was in the vicinity of 50-m isobath. This difference decreased and became perpendicular to the peninsula off Port Heiden as it followed the 50-m

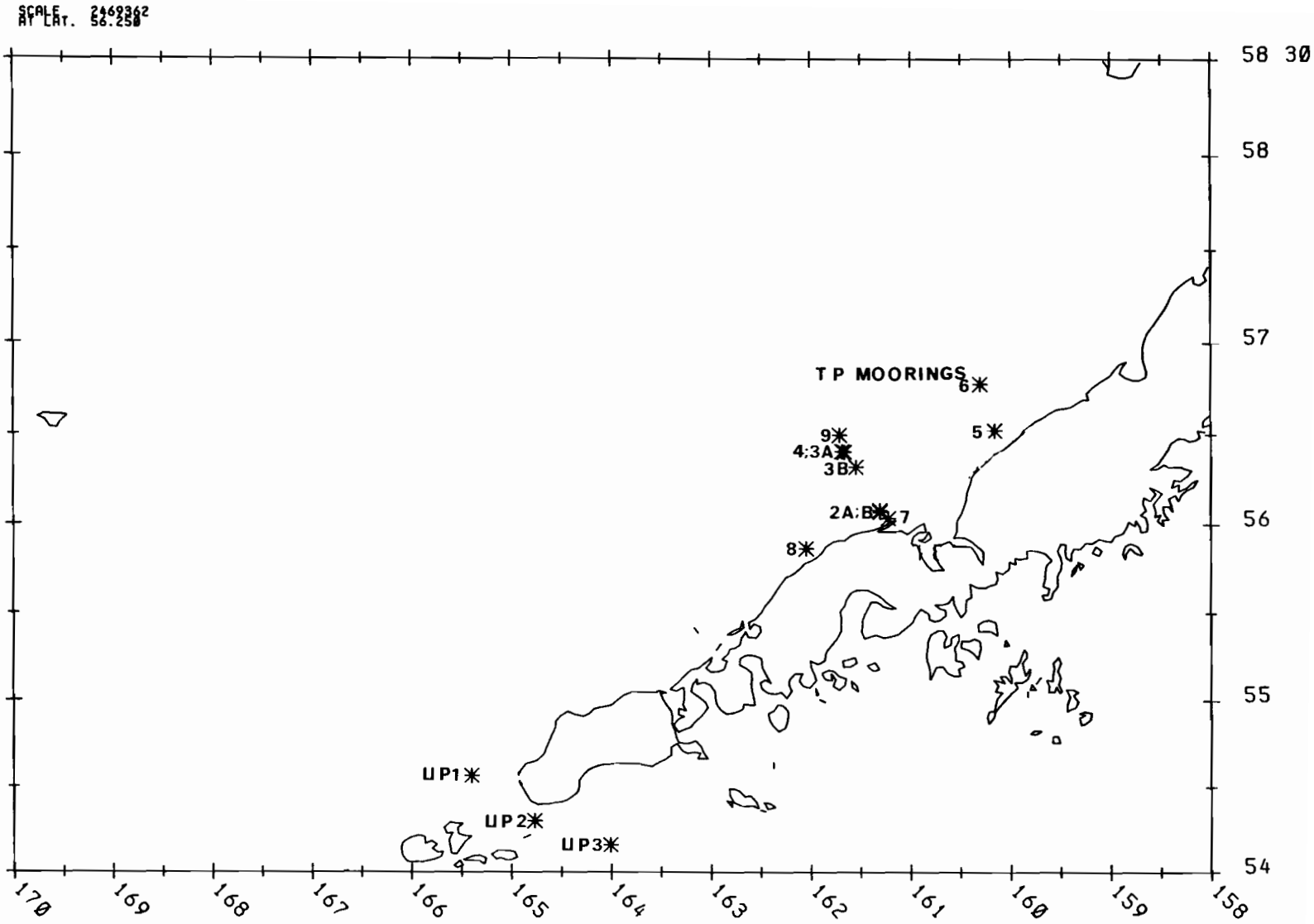


Fig. 12. Location of current meter moorings.

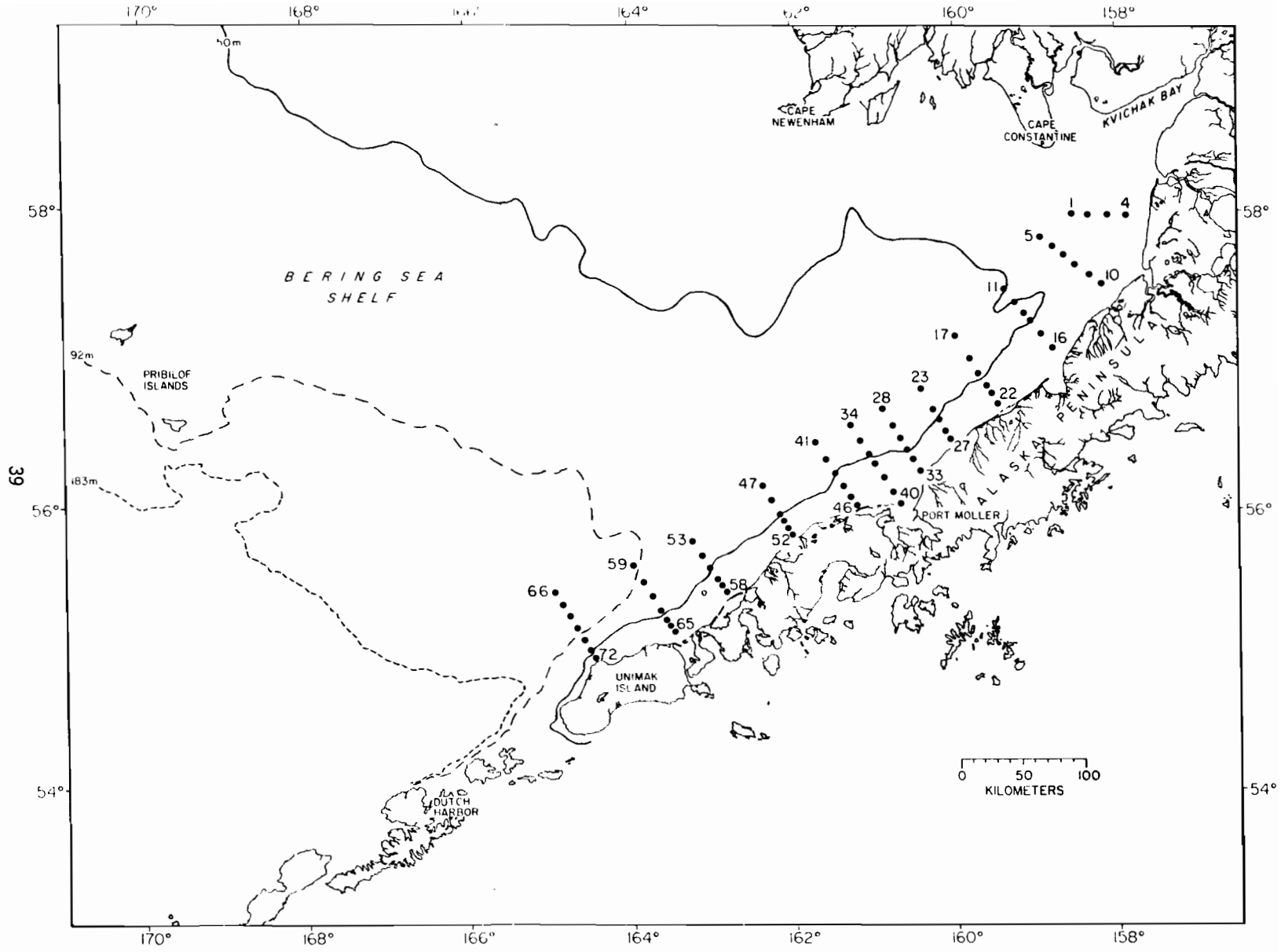


Fig. 13. Location of CTD stations (NA 1 to 72) for the north Aleutian shelf study.

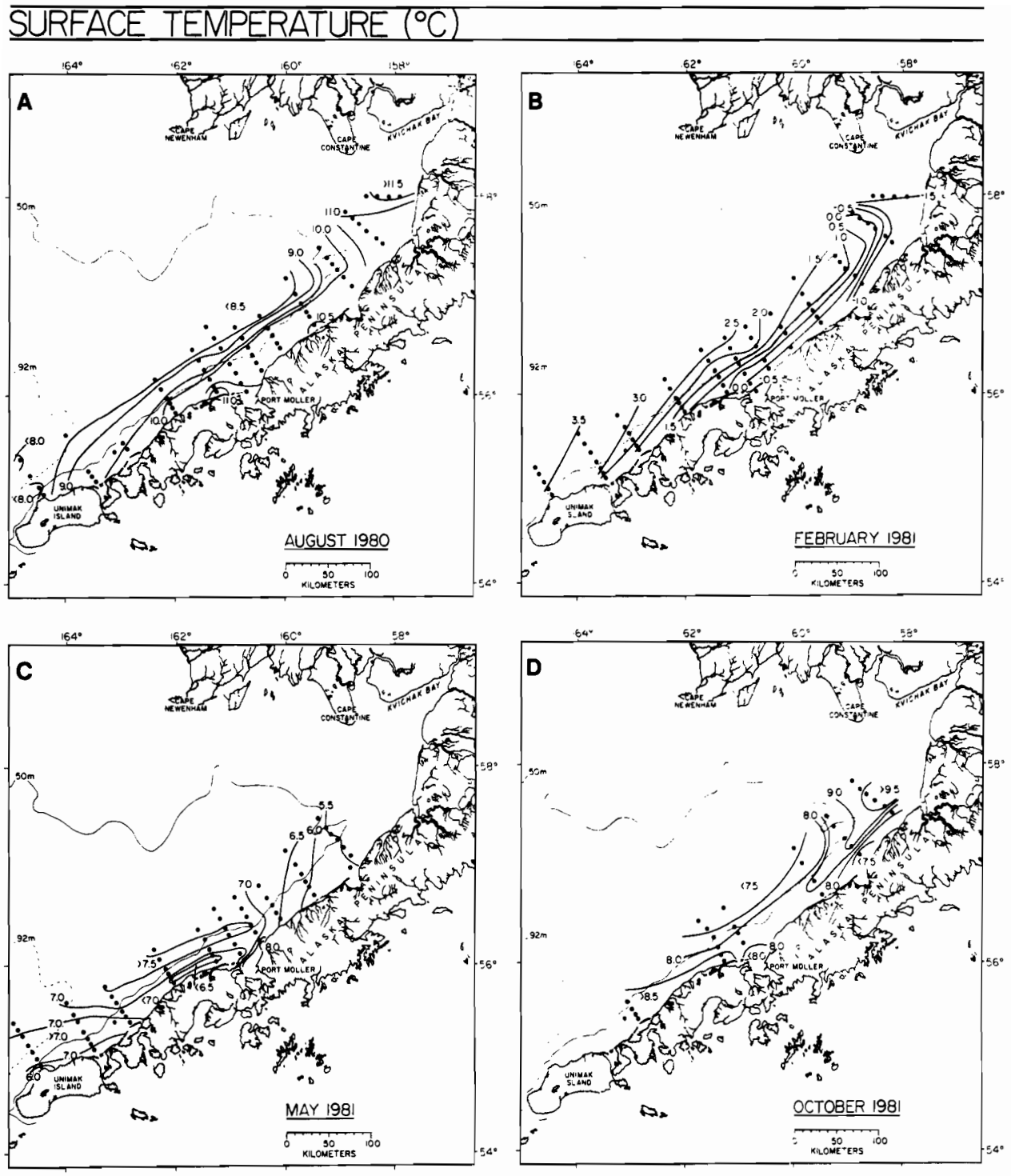


Fig. 14. Surface temperature (°C) contours.

isobath toward the northwest. West of Port Moller, the cross-shelf temperature difference decreased to <1.0°C north of Unimak Island.

By February 1981, surface temperatures (Figure 14B) were close to the freezing point in inner Bristol Bay and the 0°C contour extended westward to Port Heiden. Temperatures <0.5°C were also observed in Port Moller. Isotherms and the cross-shelf temperature difference (∿2.5°C) followed a pattern similar to that observed in August, paralleling the trend of the 50-m isobath and decreasing west of Port Moller. Off Unimak Island, maximum surface temperatures (>3.5°C) were observed over the corner of the outer-shelf domain, and the cross-shelf temperature difference was again minimal (<1.0°C).

In May, surface temperatures (Figure 14C) increased from ∿5.5°C off Port Heiden to ∿8°C near Port Moller. West of Port Moller, surface temperatures were rather constant (with an average value of 7.0°C) and displayed a tendency to be aligned with the 50-m isobath, although the cross-shelf gradient was weak and had a banded structure. This distribution suggested the establishment of nominal middle-shelf characteristics, i.e., two-layered as a result of insolation.

Surface temperatures (Figure 14D) were generally warmer by October. However, since waters over the middle-shelf domain were 1 to 2°C cooler than those inshore, the peak in thermal stratification had apparently passed, and cooling had begun. Surface temperatures in the coastal domain were greatest in regions where stratification from freshwater addition was observed. Although surface cooling had affected contours, there was a tendency for isotherms to parallel the 50-m isobath as noted before.

Bottom temperatures (nominally, 5m above the bottom) during August 1980 (Figure 15A) varied from >11.5°C in inner Bristol Bay to <6.0°C off Port Moller, with a minimum (∿3.7°C at NA59) in the corner of the outer-shelf domain north of Unimak Island. Shoreward of the 50-m isobath and between Port Moller and Port Heiden, bottom temperatures were ∿10°C, and they decreased to <8°C west of Port Moller. A strong (>3°C) difference existed from Port Heiden westward along the peninsula with a divergence of this trend off Port Moller. In general, the region of highest bottom-temperature difference paralleled the 50-m isobath. Comparison with surface temperatures indicated that the coastal domain was well mixed thermally, and both the middle-shelf and outer-shelf domains were stratified.

Near-freezing temperatures (<1.5°C) were observed on the bottom in inner Bristol Bay in February 1981 (Figure 15B), and temperatures <0°C were present westward to Port Heiden and in Port Moller. An ∿2.5°C difference was located normal to the peninsula off Port Heiden. A similar difference paralleled the 50-m isobath to the vicinity of Port Moller. West of this area bottom temperatures increased to >4.0°C off Unimak Island. In general, there was negligible thermal stratification except over the outer-shelf domain where bottom temperatures were ∿0.5°C greater than surface values.

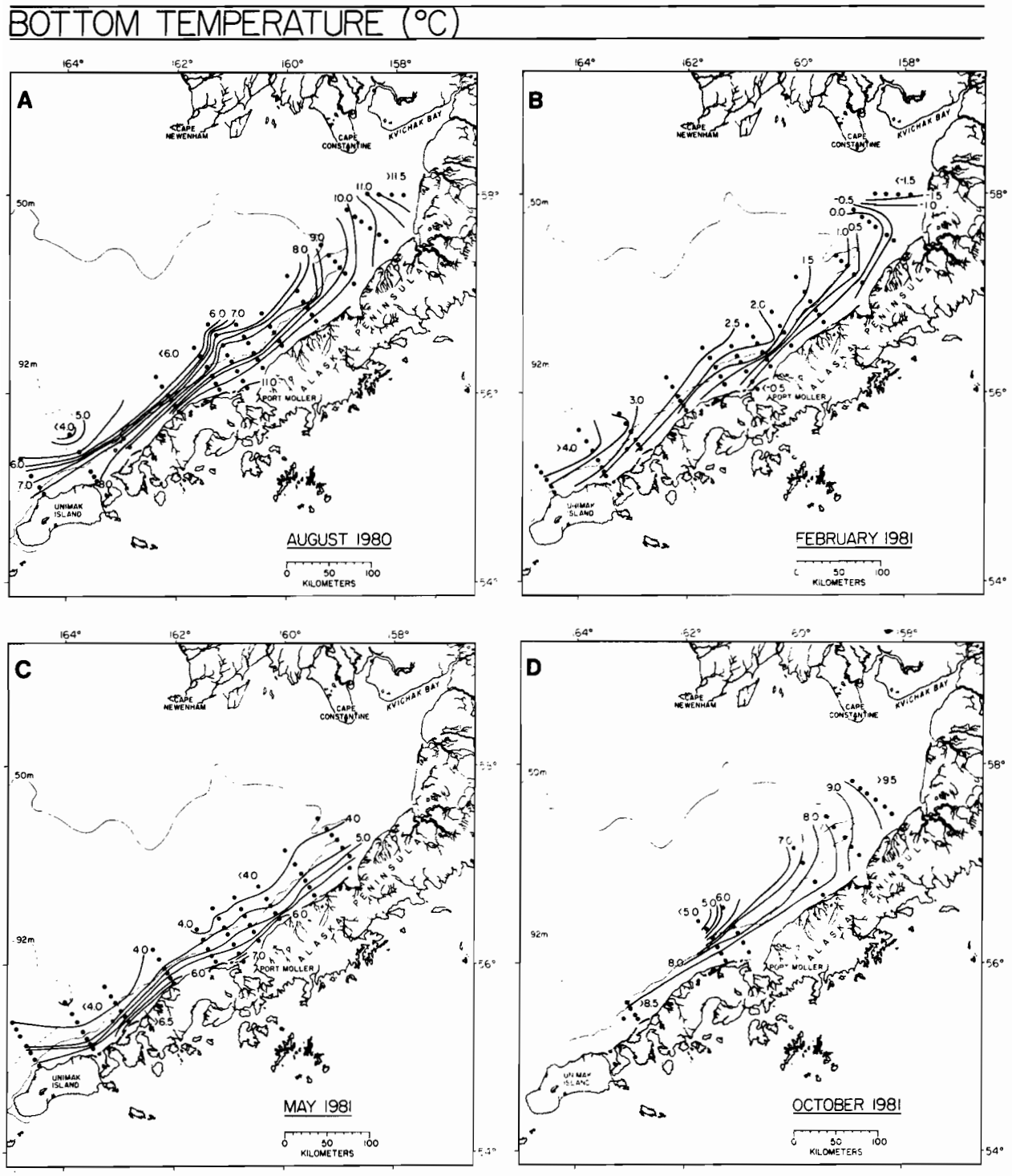


Fig. 15. Bottom temperature (°C) contours.

In May, bottom temperatures (Figure 15C) varied from <4°C seaward of the 50-m isobath to >7°C in Port Moller, and isotherms paralleled the entire peninsula. Between Port Heiden and Izembek Lagoon, and within ∿20km of the coast, thermal stratification was generally slight (<1°C), but seaward of the 50-m isobath, thermal stratification was generally >3°C along the entire peninsula.

Bottom temperatures during October (Figure 15D) had warmed since May by at least 1°C over the middle shelf, and values greater than 9.5°C were present in inner Bristol Bay. Isotherms again paralleled bathymetry and indicated a cross-shelf gradient of ∿3.5°C. Comparison with surface temperatures indicated isothermal water in Bristol Bay extending westward to near Port Heiden. Coastal waters west of Port Heiden indicated cooling, with surface temperatures as much as 2°C cooler than bottom waters. Middle-shelf waters were stratified with surface-to-bottom temperature differences ≥2°C.

Salinity: In August, surface salinities (Figure 16A) ranged from <24.5 g/kg in inner Bristol Bay to >32 g/kg over the outer-shelf domain north of Unimak Island. A strong (≧5 g/kg) difference existed normal to the peninsula (between the 50- and 25-m isobaths) in inner Bristol Bay. In the coastal domain between Port Heiden and Unimak Island, salinities increased by about 1 g/kg. Salinities over the middle shelf were ≥31.5 g/kg and relatively constant.

By February 1981, the impact of Kvichak River runoff had diminished in inner Bristol Bay, and surface salinities (Figure 16B) were ∿31 g/kg. There was a remnant of the difference normal to the peninsula, but its magnitude was only ∿0.5 g/kg. Salinities over the middle shelf were >32 g/kg, while values in Port Moller were <30.5 g/kg. This cross-shelf difference diminished to less than 0.5 g/kg off Unimak Island. The region of coastal water west of Port Moller with salinity <31.5 g/kg was substantially greater than in August.

In May, surface salinities (Figure 16C) were more uniform throughout the study area; values were <31 g/kg in Port Heiden and Port Moller with values >31.75 g/kg over the middle shelf domain between these ports. The cross-shelf difference varied from ∿1 g/kg off Port Moller to <0.5 g/kg north of Unimak Island where an intrusion of more saline water (>31.8 g/kg) was observed over the outer-shelf domain.

By October, surface salinities (Figure 16D) showed that the cross-shelf difference between Ports Heiden and Moller had increased to >2 g/kg and >1.25 g/kg respectively off the two ports. These data suggest substantial addition of freshwater along the peninsula as far west as Port Moller; however, farther west, surface salinities were greater in October than in May.

In August, bottom salinities (Figure 17A) along the peninsula varied from <29 g/kg in inner Bristol Bay to >32.5 g/kg over the outer shelf north of Unimak Island. An alongshore gradient was concentrated between inner Bristol Bay and Port Heiden where it was normal to the peninsula. The cross-shelf difference was generally weak (<0.5 g/kg). Comparison with surface values showed the greatest stratification in inner Bristol

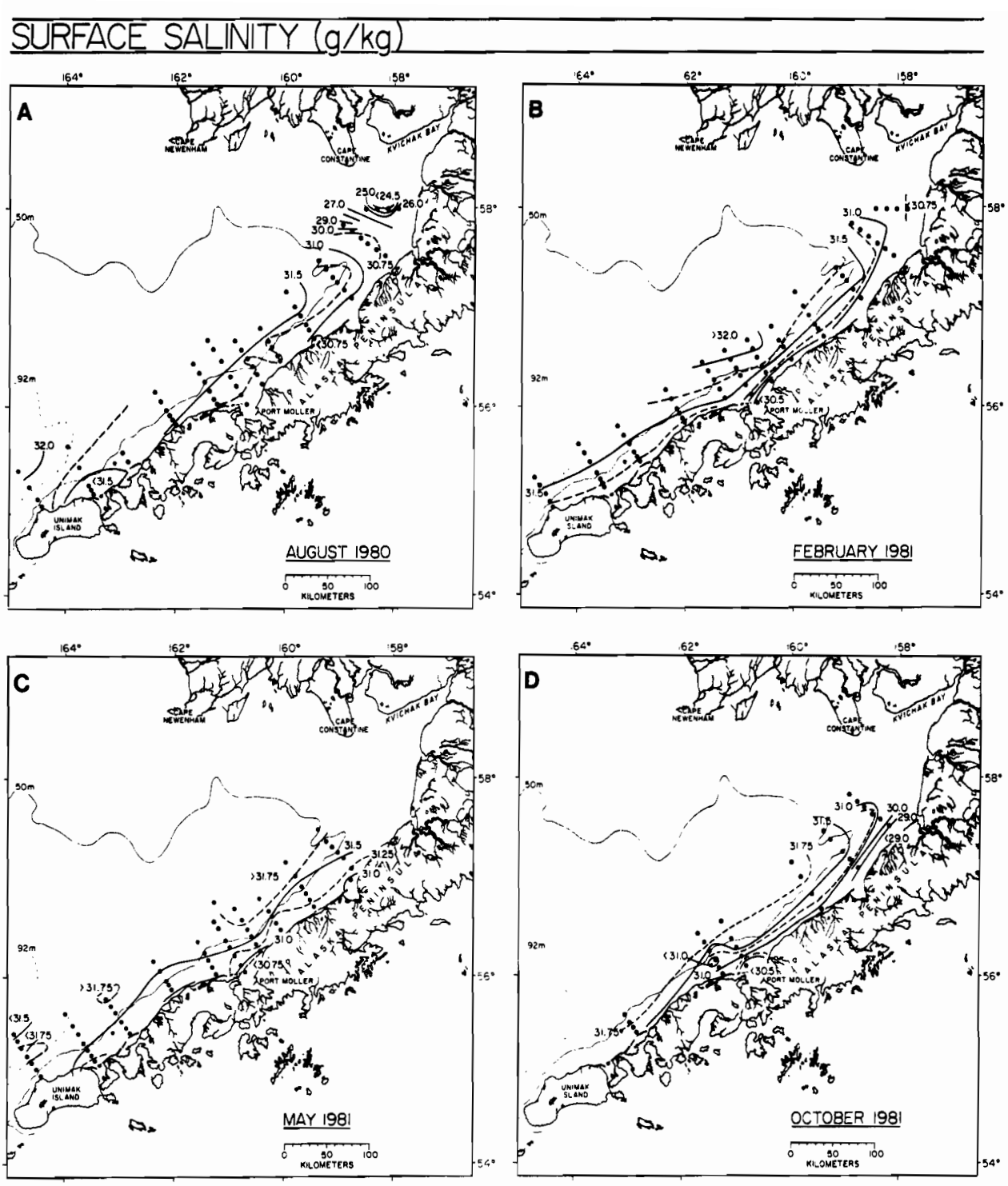


Fig. 16. Surface salinity (g $kg^{-1}$)contours.

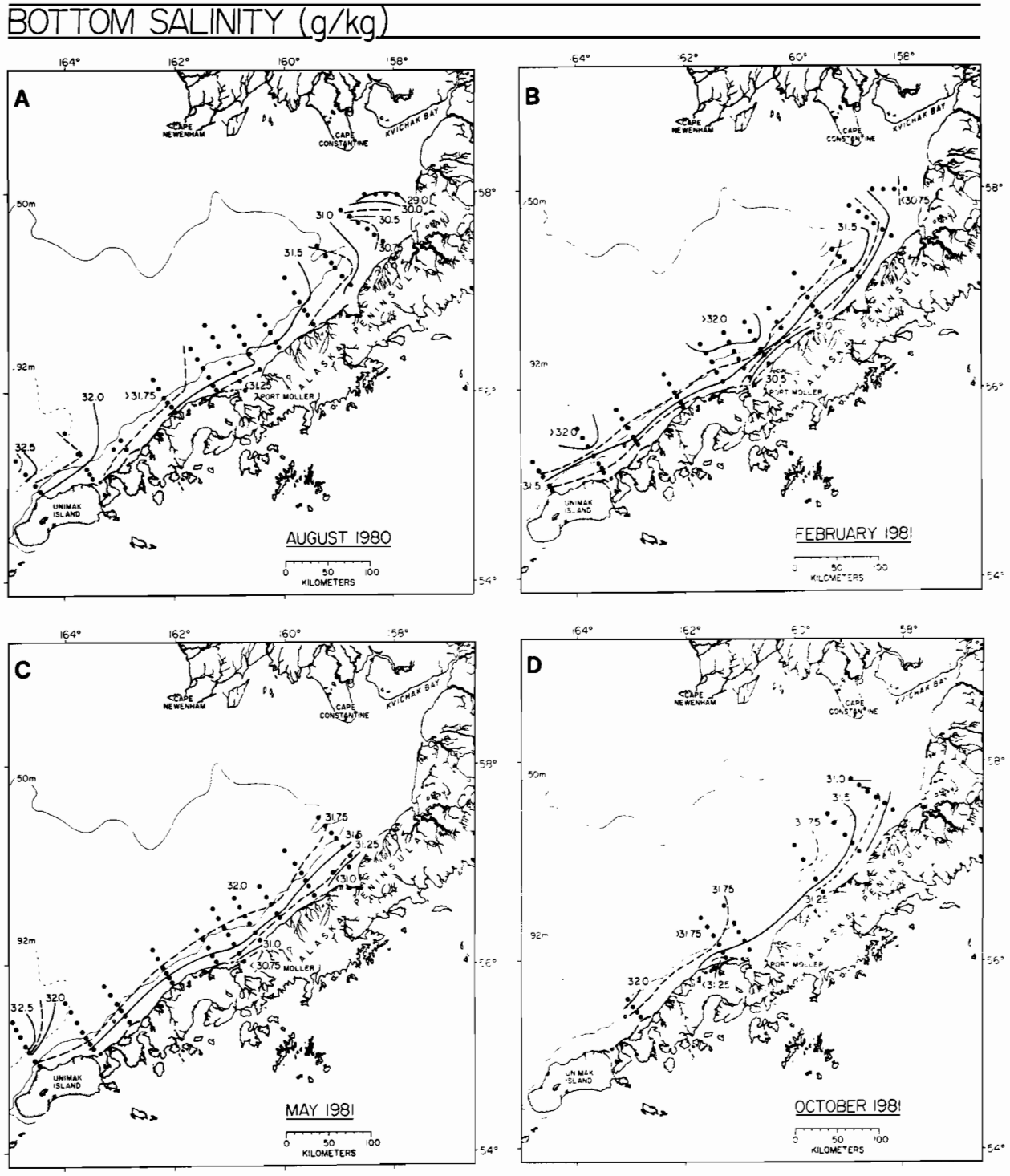


FIg. 17. Bottom salinity (g $kg^{-1}$) contours.

Bay with values of ∿5 g/kg. Over most of the coastal and middle-shelf domains stratification was weak (<0.2 g/kg), but over the outer-shelf region moderate stratification (0.5 to 1.0 g/kg) was observed.

By February, bottom salinities (Figure 17B) indicated that the along-shelf gradient had diminshed with values ranging from <30.75 g/kg in inner Bristol Bay to >32. g/kg off Unimak Island. However, the cross-shelf difference was stronger (∿1.5 g $kg^{-1}$) and more closely aligned with the bathymetric trend. Although waters over the outer shelf were less saline than observed on any other cruise, they were more saline in the middle shelf off Port Moller. As was observed in surface salinity, the area encompassed by the 31.5 g/kg isohaline was extensive (particularly west of Port Moller). Throughout most of the coastal and middle-shelf domains, stratification was weak (∿0.25 g $kg^{-1}$), whereas moderate values obtained over the outer-shelf domain.

In May, bottom salinities (Figure 17C) showed that coastal and outer-shelf domain waters were generally more saline than in February, while middle-shelf waters were less saline. Given the station coverage, the alongshore gradient did not exist, and cross-shelf differences then were weaker than in February, but still followed the bathymetric trend. Shoreward of the 50-m isobath, stratification was generally <0.25 g/kg, with slightly greater values over the middle shelf. As was noted for the previous data sets, stratification was moderate over the outer-shelf domain.

Bottom salinities in October (Figure 17D) indicated a slightly stronger alongshore gradient, ranging from <31 g/kg in Bristol Bay to >32 g/kg off Izembek Lagoon, however, the cross-shelf difference was weaker than in May. The strong cross-shelf differences in surface salinity along the coast between Ports Heiden and Moller diminished along the bottom, this resulting in a band of stratification (∿0.5 g/kg) along the coast east of Port Heiden which graded off to <0.1 g/kg over the middle shelf east of Port Moller. West of there, stratification was 0.25 to 0.7 g/kg except for the stations less than 50 m deep off Izembek Lagoon.

We present surface-to-bottom mean salinity, $\bar{s}$, (Figure 18A to D) to further elucidate the impact of the various sources of freshwater or less saline water. The lowest $\bar{s}$ (<27.75 g/kg) was observed in August and reflected the direct influence of the Kvichak River. Comparison with $\bar{s}$ from the three other cruises suggested that Kvichak River water had a controlling influence on salinity as far west as station line NA5 to 10, or ∿100 km east of Port Heiden. By February, the mean salinity had increased by ∿3 g/kg in this region, while the values from October were similar to those in August.

Values of $\bar{s}$ from the middle-shelf domain showed much less variability, minimum values were observed in August (>31.5 g/kg) with maximums in February (up to 32.1 g/kg) while values in May and October were intermediate (∿31.75 g/kg). Mean salinity over the outer-shelf domain north of Unimak Island showed similar magnitude of variability, but phasing was different: maximums occurred in August and minimums in February.

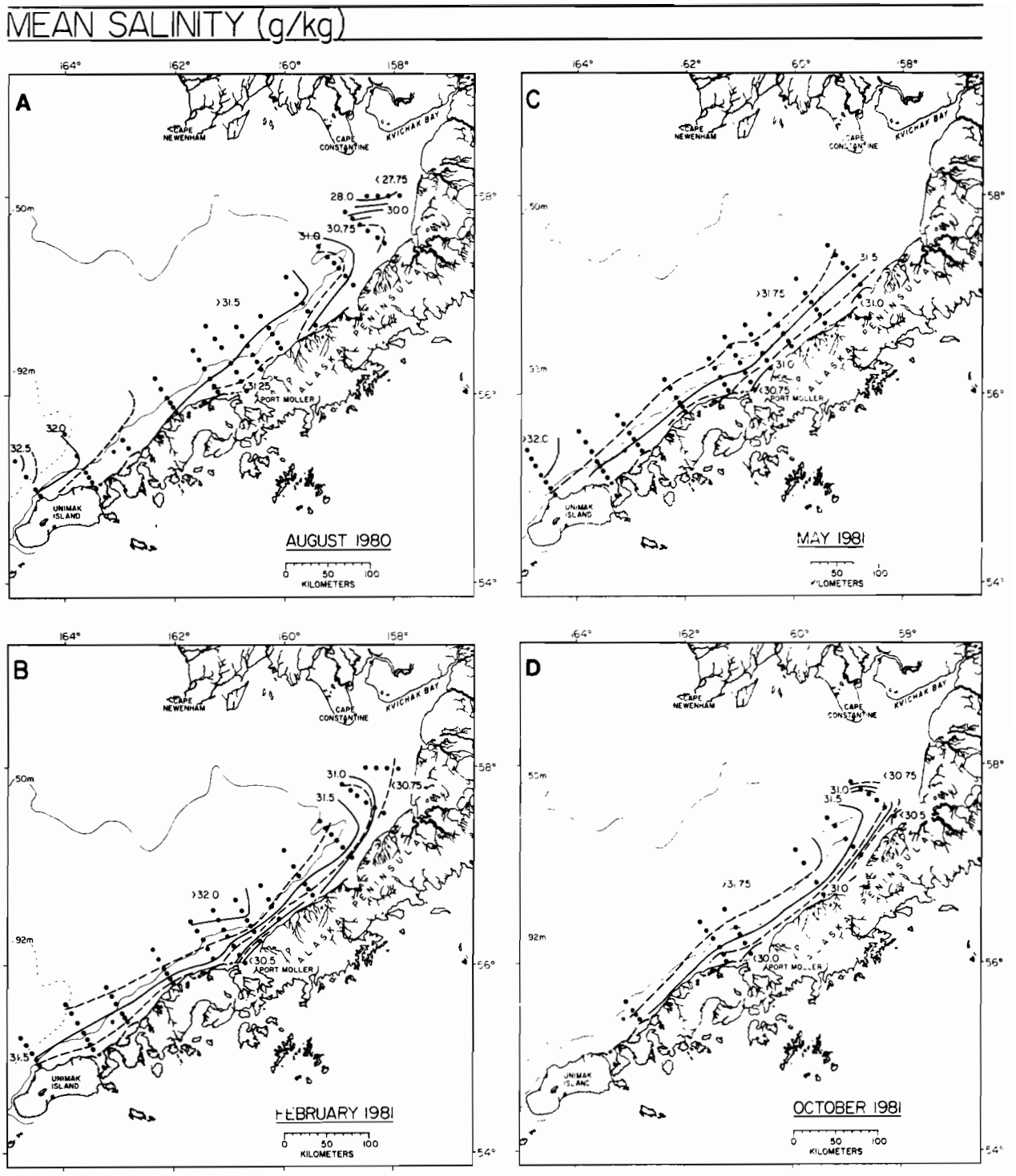


Fig. 18. Mean salinity (g $kg^{-1}$) contours.

In the coastal domain between Port Moller and Unimak Island, the range of $\bar{s}$ was again moderate (~0.5 g/kg); however, there was a substantial change in the area encompassed by the 31.5 g/kg mean isohaline. This area was most saline in August and only slightly less so in October, with the lowest values observed in February. These increased slightly by May. The Kenai Current had a baroclinic maxima in October followed by a barotropic maxima between January and April (Schumacher and Reed, 1980). Some manifestations of these maxima were observed in Unimak Pass and persisted into May (Schumacher, Pearson, and Overland, 1982). We suggest that less saline water from the Kenai Current was the cause for the observed reduction of mean salinity west of Port Moller, particularly in February. Within Port Moller, the lowest mean salinity also occurred in February, and ice was observed to be a local feature, though offshore surface temperatures were >2.0°C. We suggest that ice is formed within the Port Moller complex and that it melts when advected seaward; however, such local formation would not affect mean salinity over the vast region west of Port Moller. Ice formation along the shore of Kuskokwim Bay and the north coast of Bristol Bay may be advected (by wind) to this region of the coastal domain and provide a freshwater flux, but this process would generally occur between late February through March (see Figure 2).

Finally, we note that in the vicinity of Port Heiden, and to a lesser extent west of Port Moller, the mean salinity in a band along the coast was lowest in October. This region is more than 200 km from the Kvichak River, west of the region where river runoff is clearly identifiable in the data. Although there are no gauged rivers on the peninsula, there is substantial rainfall. An estimate of drainage area between Ports Moller and Heiden is about the same as that for the Kvichak River. Thus, the maximum freshwater flux should occur in October and be of a magnitude similar to that of the Kvichak River. We suggest that it was this source that resulted in lower salinities in the coastal domain west of the Kvichak River influence and extending westward to the vicinity of Port Moller.

Stratification: Bottom-surface sigma-t values ($\Delta\sigma_t$) are a measure of stratification that combines the effects of both salinity and temperature. In general, coastal domain waters are well mixed, except in the presence of freshwater addition; middle-shelf waters are two-layered during periods of positive buoyancy input (insolation and ice melt) and well mixed otherwise, and outer shelf domain waters are usually layered (Kinder and Schumacher, 1981a).

Area plots of $\Delta\sigma_t$ are shown in Figure 19 A to D. The strongest $\Delta\sigma_t$ (> 3.5) was observed in August in inner Bristol Bay and was primarily caused by salinity stratification resulting from Kvichak River discharge. Just south of this area, coastal domain waters westward to Port Heiden were mixed ($\Delta\sigma_t$ < 0.1). In the vicinity of Port Moller, a complex distribution of $\Delta\sigma_t$ existed, with values ranging from 0 nearshore to >0.25 over the adjacent portion of the middle shelf. As will be shown later (Section 4.2.6), this distribution was a result of storm mixing and cross-shelf advection. Between Port Moller and Izembek Lagoon, $\Delta\sigma_t$ was generally <0.25, while near the 50-m isobath values were >0.5 and over the outer-shelf domain they exceeded 0.75.

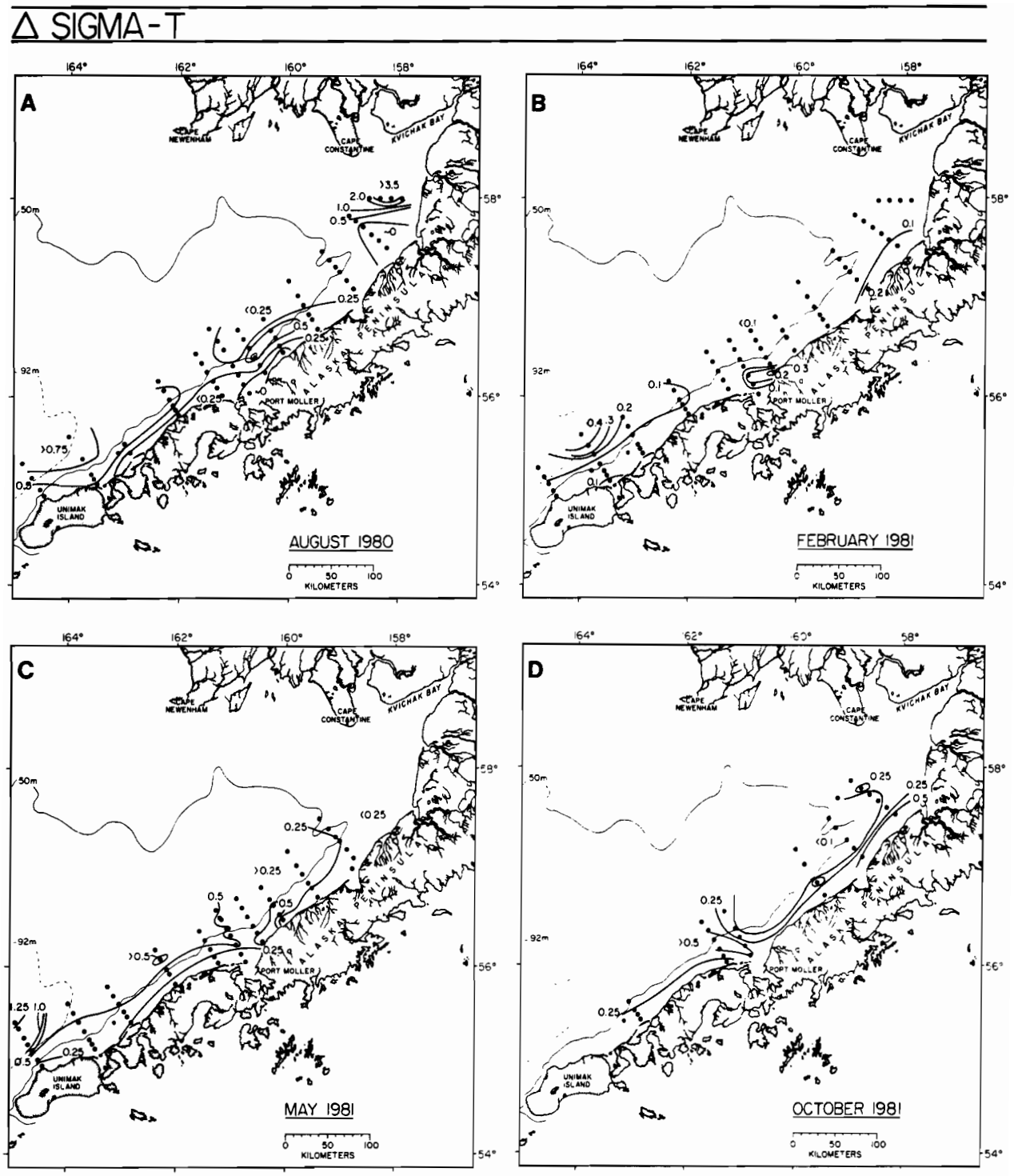


Fig. 19. Bottom minus surface sigma-t contours.

By February, most of the water column from inner Bristol Bay to west of Port Moller was mixed. Exceptions occurred near Ports Heiden and Moller, where $\Delta\sigma_t \sim 0.25$ and again were related mainly to salinity stratification. A likely source of less saline surface water was the melting of local or regional ice. West of Port Moller, the coastal and middle-shelf domains were mixed, while over the outer shelf, moderate stratification (up to 0.4) existed.

The effect of increasing insolation was evident in May; waters over the middle shelf were moderately stratified ($\Delta\sigma_t > 0.25$), although temperatures had increased from February by $\sim 7^{\circ}C$, temperature differences and $\Delta\sigma_t$ were weak in the coastal domain. An exception was near Port Moller where a lens of fresher water had not yet been mixed with more saline bottom water. Over the outer shelf, strong stratification existed as a result of low-salinity surface water well offshore. The presence of a low-salinity band in the vicinity of the middle front is a common feature and has been attributed to the southwest extent of the regional ice field (Kinder and Schumacher, 1981b).

Surface heat loss was evident by October, and that, coupled with weak haline stratification, resulted in a mixed water column over most of the middle-shelf domain. Along the coast east of Port Heiden and just west of Port Moller, $\Delta\sigma_t$'s exceeded 0.5 due to the presence of less saline surface waters. As noted above, this was likely due to freshwater addition not associated with the Kvichak River, but with local freshwater addition.

Dynamic Topography: The combined effect of temperature and salinity on the horizontal pressure field and hence the computed geostrophic flow is shown in Figure 20A to D and 21A to D. While caution is necessary in inferring currents in this manner, particularly to shallow reference levels, good agreement historically between Eulerian and Lagrangian measurement and geostrophic flow exists over this shelf (Schumacher and Kinder, 1983). Both the 0/25- and 0/50-dbar dynamic topography showed that relief of $\geq$1.0 dyn cm was a persistent feature of the baroclinic pressure field across the shelf. Contours typically aligned with the bathymetry and the 0/25-dbar contours paralleled the offshore trend of the 50-m isobath north of Port Heiden. The impact of freshwater addition from the Kvichak River (Figure 20A) and along the peninsula westward to Port Heiden (Figure 20D) was evident in the increased relief. Maximum surface speeds relative to 25 dbar were $\sim$7 cm/s off Port Moller in August and $\sim$11 cm/s in inner Bristol Bay during October. Maximum values (0/50 dbar) also occurred off Port Moller in August. In general, regardless of time of year, the cross-shelf density distribution was such that baroclinic geostrophic surface currents of 2 to 7 cm/s existed with inferred flow into Bristol Bay parallel to isobaths.

### 4.2.2 Short-Period time dependence of hydrographic features

In the previous section we showed that some processes (e.g., runoff, icemelt, change in insolation, etc.) result in changes in hydrographic characteristics on time scales from approximately monthly to seasonal. We present hydrographic, suspended particulate matter (SPM), wind, and

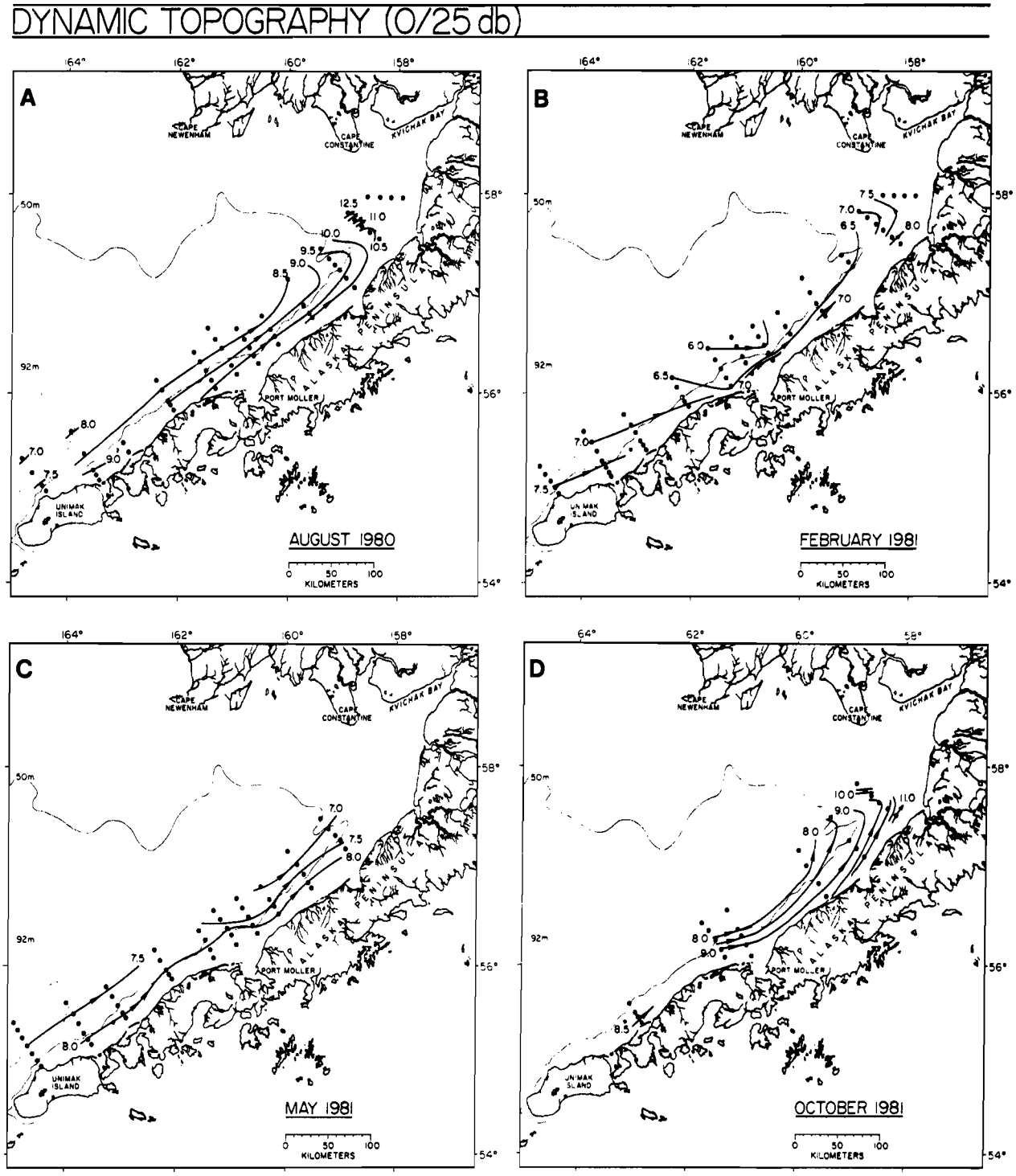


Fig. 20. Dynamic topography (0/25 db).

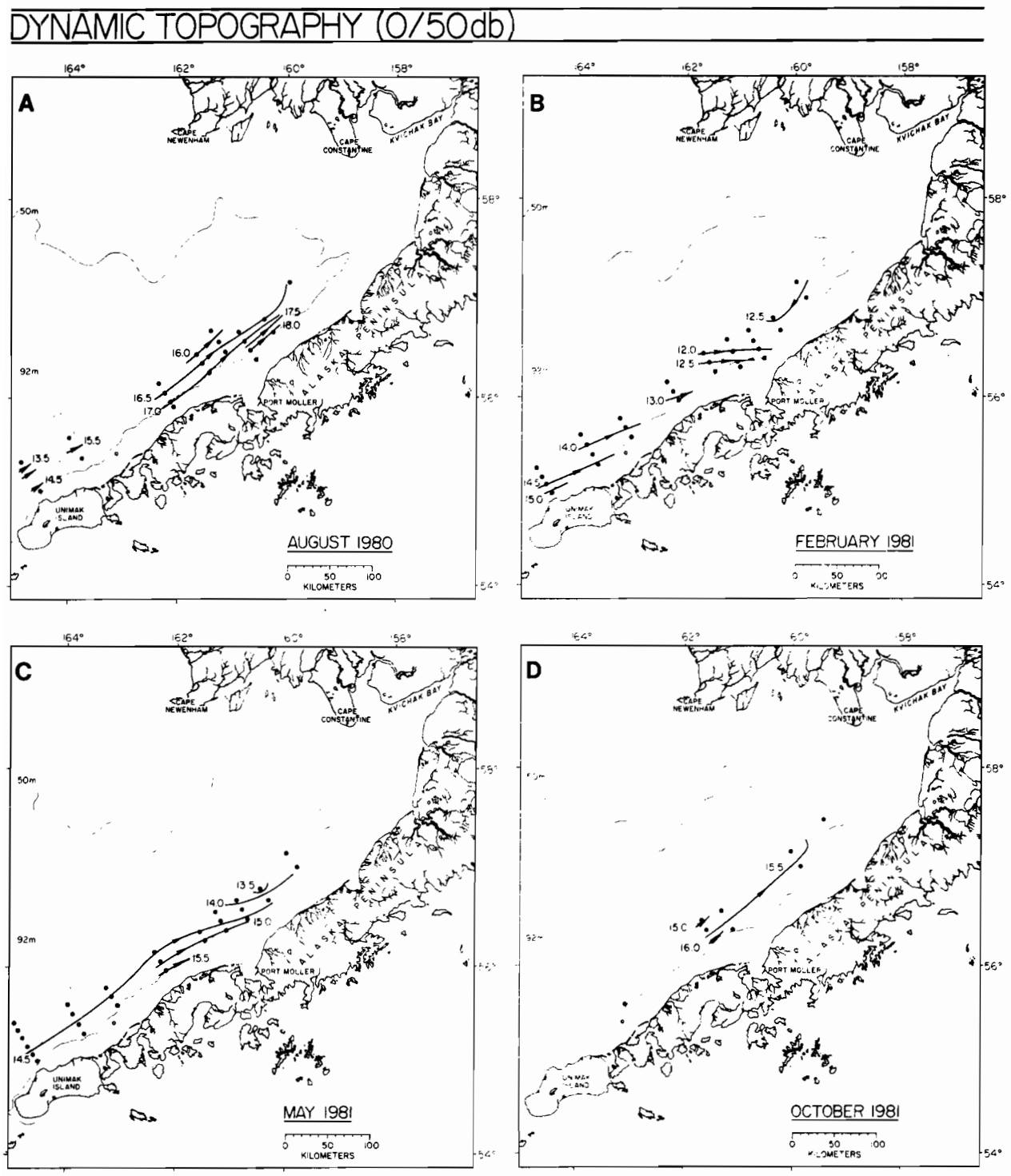


Fig. 21. Dynamic topography (0/50 db).

current data collected along the Alaska Peninsula (Figure 22) during a 14-day period in August 1980. These data show that a storm significantly altered mean hydrographic conditions, vertically mixing middle-shelf domain waters. Further, Ekman fluxes (coastal divergence and convergence) with time scales of 2 to 5 days appeared to play an important role in reestablishment of stratification and, together with enhanced tidal mixing (using the mean of the speed cubed as a measure of mixing energy), resulted in a return to nominal coastal and middle-shelf-domain conditions within 14 days.

Hydrography and Light Attenuation The line of CTD stations normal to the peninsula (Figure 22) was occupied on 19, 24, and 31 August 1980. The time to complete a line was about six hours. About one day prior to running the first section, the remnants of typhoon *Marge* passed eastward through the study area. This storm resulted in winds up to 30 m/s and 6- to 8-m waves. The turbulence associated with this storm mixed the water column at least 50 km seaward of the coast, i.e., into the middle-shelf domain (Figure 23). Suspended particulate matter was also well mixed within 10 km of the shore, and seaward of station 45, isopleths exhibited weak monotonically increasing vertical gradients.

During the second occupation of this section (Figure 24), the entire shelf region was thermally stratified, with surface-minus-bottom-temperature difference ($\Delta T$) from 0.6 to 2.7°C. Colder bottom waters intruded onshore, with a displacement of the 8.5°C isotherm of about 10 km. A similar change from mixed to stratified structure was observed in isohalines with the strongest difference ($\Delta S = 0.13$ g/kg) over the normally mixed coastal domain. Again, the data suggested an onshore flux. For example, at station 42, bottom salinity increased by 0.05 g/kg, while upper-layer salinities decreased. Light attenuation values indicated a 50% reduction in near-shore concentration of SPM, while over the middle-shelf domain a subsurface minimum layer was established.

Hydrographic conditions observed on 31 August (Figure 25) showed a return to more typical stratification; middle-shelf waters were stratified with $\Delta\sigma_t \geqq 0.43$, and coastal domain waters were vertically well mixed. We note that stratification was now stronger than that observed on May 31 (inset, Figure 22) by about a factor of three. SPM profiles also indicated mixed conditions in the coastal domain and a minimum layer was clearly established near or below the pycnocline.

Winds and Currents Alongshore (v positive 60°T, see Figure 22) winds measured from the NOAA ship *Surveyor* are shown in Figure 26. The passage of the storm resulted in maximum alongshore wind speeds of about 25 m/s. About 3.5 days after the storm's peak speeds, a period of relatively steady alongshore winds existed for about 3 days with a mean speed of -5.5 m/s. We note that with the exception of the storm winds and those on 24 August, onshore wind speeds (not shown) were only about 1 m/s.

Currents at 5 and 39 m below the surface at TP3A are shown in the next two panels of Figure 26, where the alongshore axis is the same as for the wind and the onshore axis is u positive 150°T. Near-surface currents reversed from onshore to offshore concomitant with the wind reversal, and this initial offshore pulse lasted for about 3 days. While

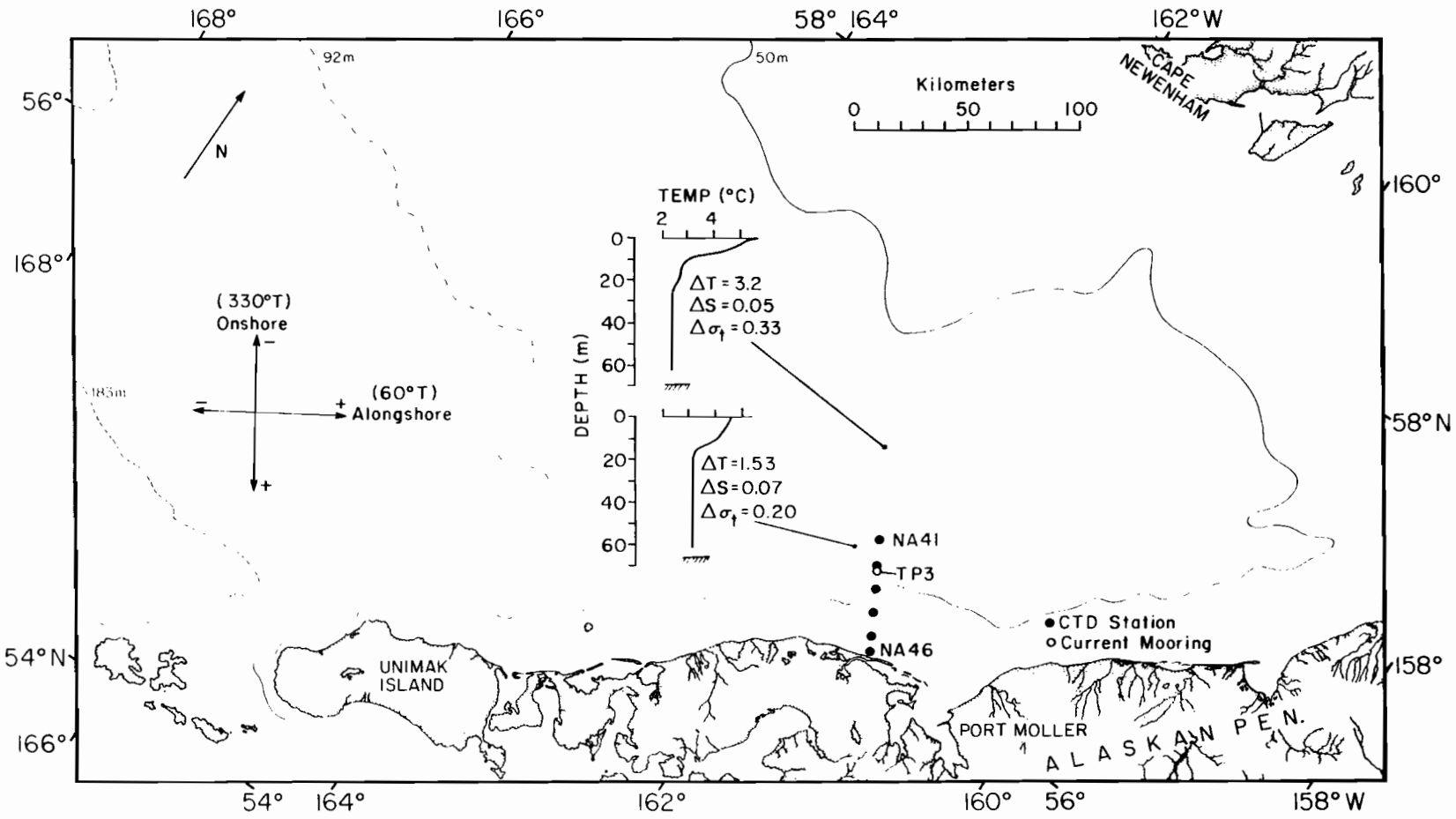


Fig. 22. North Aleutian Shelf study area, showing location of hydrographic data section (NA41 to NA46) and mooring TP3A. Also shown are CTD data from 31 May 1980 and axes used for current and wind data.

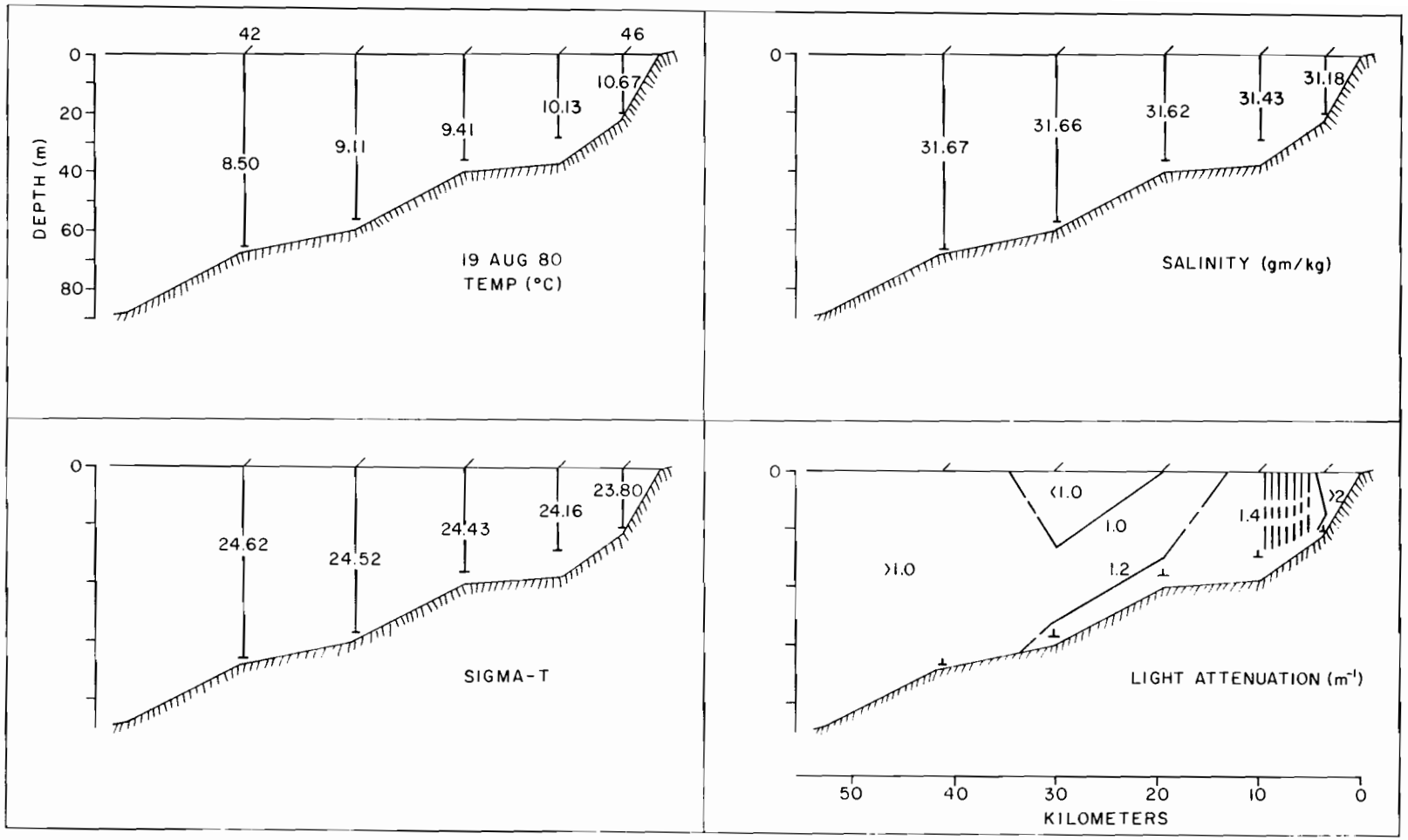


Fig. 23. Hydrographic and light attenuation sections from 19 August 1980. Note the location of the 8.5°C isotherm.

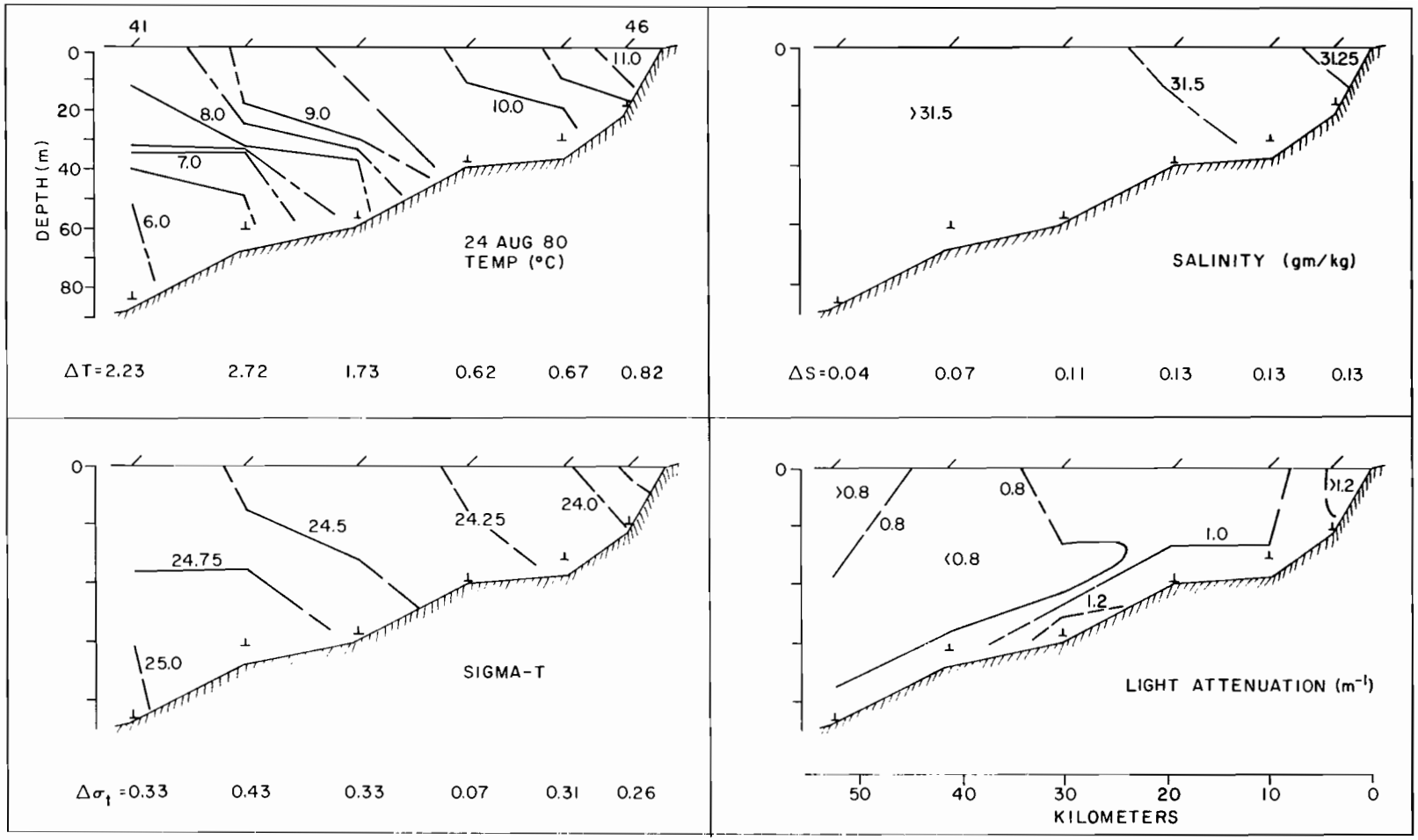


Fig. 24. Hydrographic and light attenuation sections from 24 August 1980. Contour intervals are 0.5°C, 0.25 gm kg $^{-1}$, 0.25 $\sigma_t$ units and 0.2 m $^{-1}$ for light attenuation. Magnitude of upper minus lowest 1 m average parameter is presented under a given station as a Δ. Note, lowest 1 m average salinity at station 42 was 31.71 gm kg $^{-1}$.

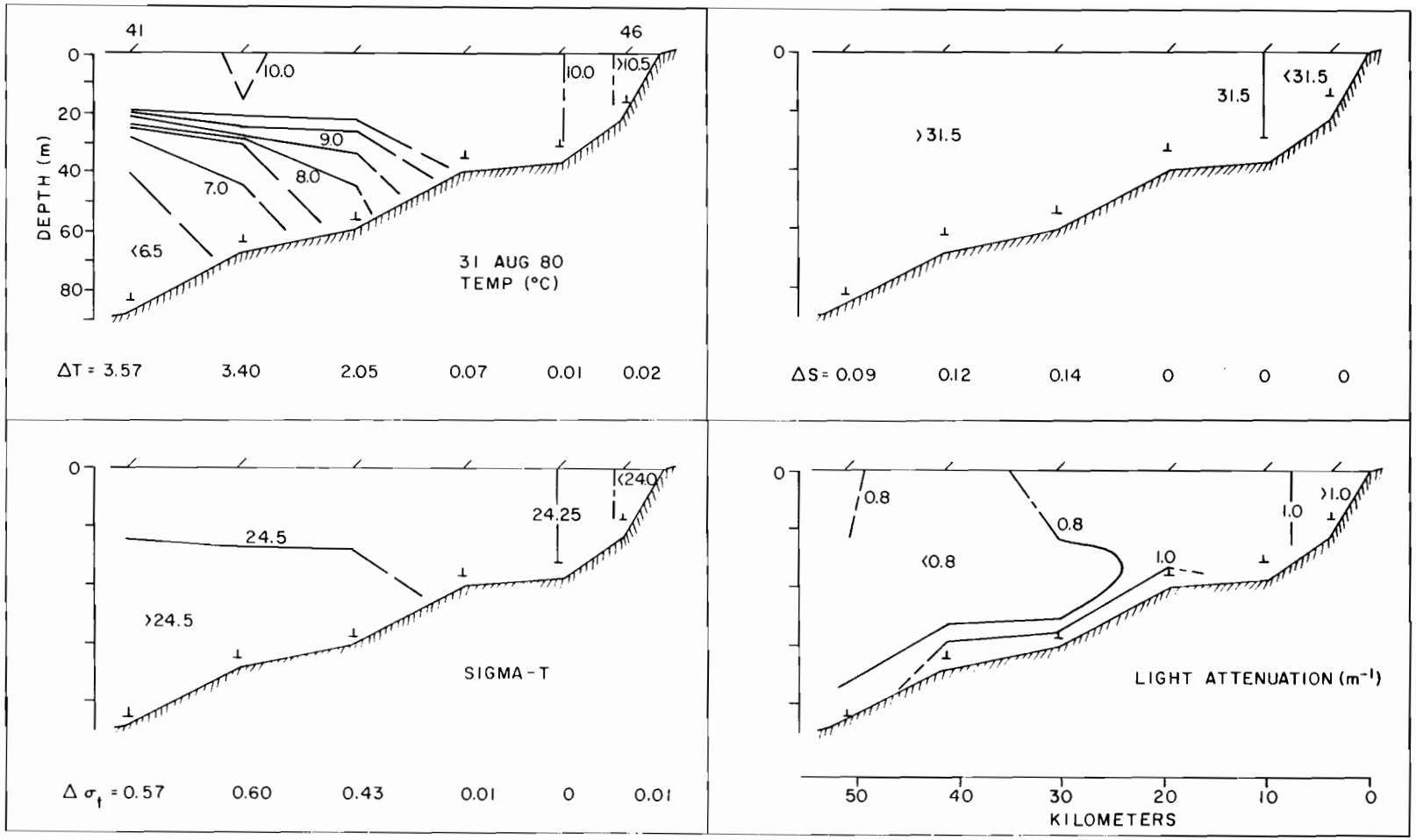


Fig. 25. Hydrographic and light attenuation sections from 31 August 1980.

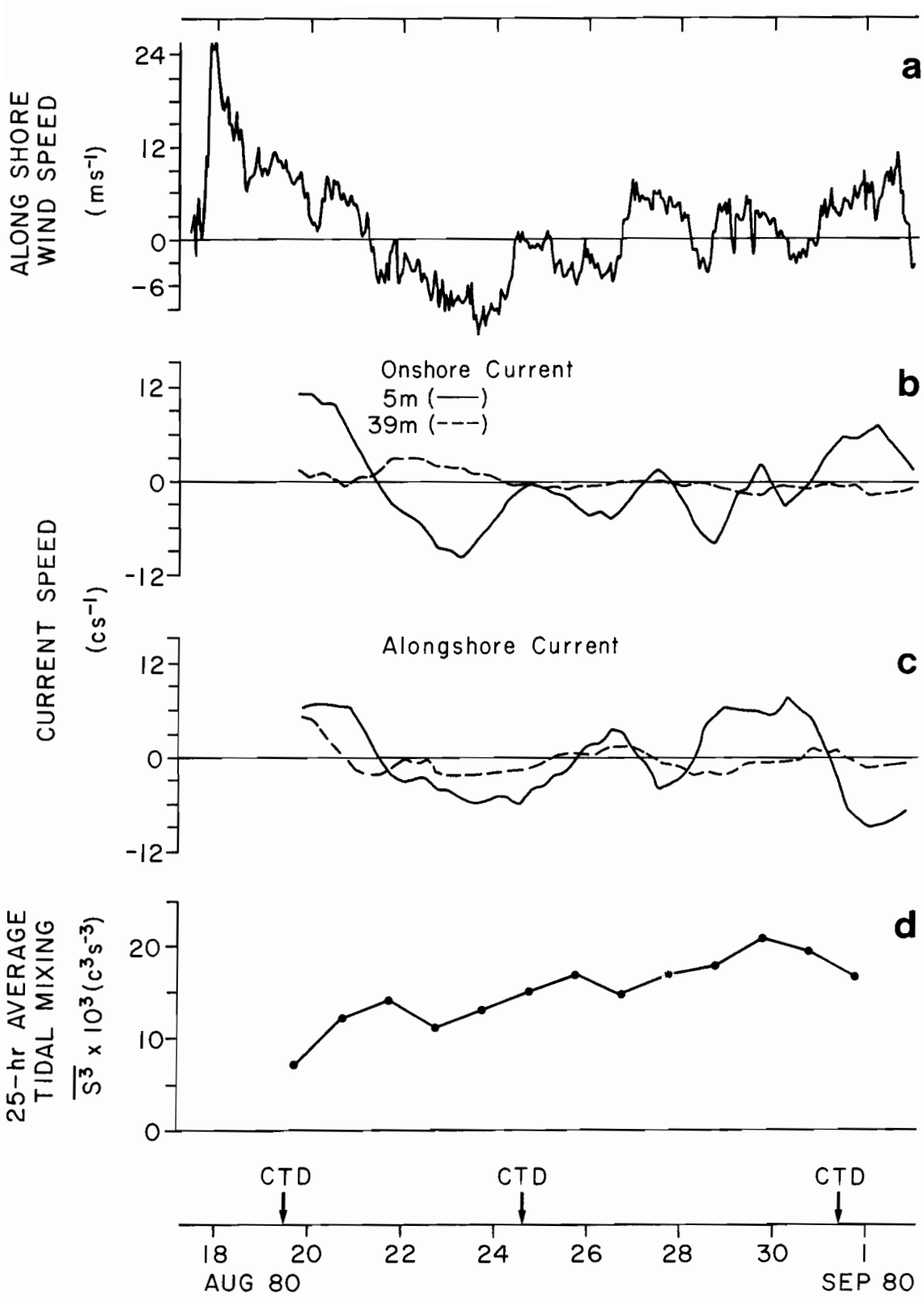


Fig. 26. a) Alongshore windspeed, b) onshore current at 5 and 39 m, c) alongshore current at 5 and 39 m and d) 25-hr average tidal mixing parameter $s^3$ from the 39 m depth current record.

near-surface currents were offshore, those at 39 m were onshore for the same time period. The visual correlation between wind and near-surface current did not extend to currents at 39-m depth. The alongshore current appeared to be similar at the two depths.

In the bottom panel of Figure 26, we present 25-hr-averaged $\bar{s}^3$ values. The flux of turbulent energy generated at the seafloor, $E_t$, was estimated by assuming that the mean rate of work of tidal currents against bottom stress ($\tau=\rho_o C_o u\, u$) is $\bar{\tau}\cdot\bar{u}$, where u is the mean flow velocity near the bottom (Fearnhead, 1975). Here we have used hourly values of current speed from the 39-m-depth current record and have not included either a drag coefficient or density (including these parameters yields dimensions of tidal power, but $\bar{s}^3$ gives a relative measure of this quantity). By the third occupation of the CTD section, tidal mixing power had increased by about a factor of three.

Discussion The destruction and subsequent reestablisment of typical summer middle-shelf and coastal domain hydrographic characteristics were related to winds and tides. The initial vertical mixing of the water column resulted from a combination of wind-wave and current-shear turbulence which destroyed vertical structure to at least 50 km, or twice the usual distance, from the shore. Alongshore winds then reversed and generated an offshore Ekman flux in the near-surface waters and a continuity preserving onshore flux at depth. The offshore flux transported warmer, less saline surface water offshore, while the onshore flux at depth provided colder more saline waters; the net result was stratification across the entire study area. As tidal mixing power increased, coastal domain waters became vertically mixed and middle-shelf domain waters returned to a two-layered configuration.

Near-surface current spectra (not shown) indicated that of the total fluctuating horizontal kinetic energy ($\bar{KE} = \frac{1}{2}[\bar{u}^2+\bar{v}^2]$) per unit mass, subtidal energy was 31.6 $cm^2\ \bar{s}^2$, or about 6%, which is consistent with previous studies (Kinder and Schumacher, 1981b). We note that 50% of the subtidal KE was contained in the 2- to 5-day period bands. The wind spectrum contained little energy (1.3 $m^2\ \bar{s}^2$ or about 10% of the total $\bar{KE}_{\omega}$) at tidal or higher frequencies; however, 25% of the $\bar{KE}_{\omega}$ was contained in 2- to 5-day periods with the remainder at periods ≧7 days.

The visual correlation between alongshore winds and onshore currents, suggesting Ekman dynamics, was substantiated by a linear correlation coefficient between the two low-pass-filtered time series of r = 0.83 at 0 lag. In frequency, the maximum coherence between hourly wind and current components was at a period of 2.9 days with a coherence-squared of 0.995 or about 99% of the variance. A second maximum occurred at 4.8 days with a coherence-squared of 0.91. For both estimates the 95% level of significance was 0.78. Onshore currents and alongshelf winds were correlated to a lesser extent at lower depths, with correlations decreasing (0.57, 0.53, and 0.42) and lags increasing (0, 6, and 60 hours) at 10 m, 15 m, and 29 m, respectively. The current record from 39-m depth had a negative correlation (r = -0.68 at 48 hours) with alongshore winds. These results suggest that alongshore winds generated Ekman fluxes in an upper layer with, at times (e.g., 21 to 24 August), a compensating flow lower in the water column. During this particular event, coastal di-

vergence would result in a barotropic pressure gradient toward shore. If this gradient were geostrophically balanced, then an alongshore current (in this reference frame a negative value) would be generated. The observations indicated such flow during both 21 to 24 August and 30 August to 1 September wind events. An empirical estimate of 5-m onshore current response to alongshore wind was $10^{-2}$ to 1, or a 10 m/s wind generated a 10 cm/s current.

### 4.2.3. Current and Wind Observations

In this section we describe current characteristics from records collected at nine locations along the Alaska Peninsula and wind characteristics from observations near Port Moller (Figure 12). Mooring information and editing procedures are given in Appendix A. In the following analysis, we have used the 35-hr-filtered data unless otherwise noted.

Mean and Low-Frequency Flow:

In Figures 27 and 28 for the first deployment period (August 1980-January 1981) and in Figures 29 and 30 for the second deployment period (January-May 1981), we present the current data as roses (with the direction partitioned into twelve 30° sectors) and vector means with one standard deviation along, and orthogonal to, the principal axis or the axis with the greatest variance). A feature common to all records was that the majority of observations and the principal axes tended to be along the local bathymetry. Vector mean flow, however, did not occur consistently along the bathymetry except seaward of the 50-m isobath. Shoreward of the 50-m isobath and in the vicinity of Port Moller (i.e., TP2A/B, TP7, and TP5), mean flow had a cross-isobath component.

To establish the statistical significance of the vector mean speeds, we employed a method similar to Allen and Kundu (1978). An independent time scale, $\tau$, was defined as the area under the autocorrelation function for a particular record. This time scale was then used to provide a root-mean-squared error estimate, E, given by

$$E = \pm 2\sigma/(t/\tau)^{\frac{1}{2}}$$

where t is the record length and $\sigma$ the standard deviation along a given axis. The results of this technique, together with other record characteristics are given in Table 4. Note that all vectors are resolved into alongshore (positive toward 60°T) and cross-shelf (positive toward 150°T) axes, and that this definition of alongshore is consistent with the orientation of the peninsula, bathymetry, and generally within about 10° of the individual records, principal axis.

The strongest alongshore mean current was observed either seaward of the 50-m isobath (TP4, 6, and 9) or west of Port Moller (TP8), with mean speeds along this component of ~1 to 6 cm/s, where the larger values occurred in the near-surface (12 to 19 m below the surface) records. Statistically significant, but weaker (<1 to 3 cm/s) mean negative alongshore flow existed near shore in the vicinity of Port Moller (TP2A, B, and 7).

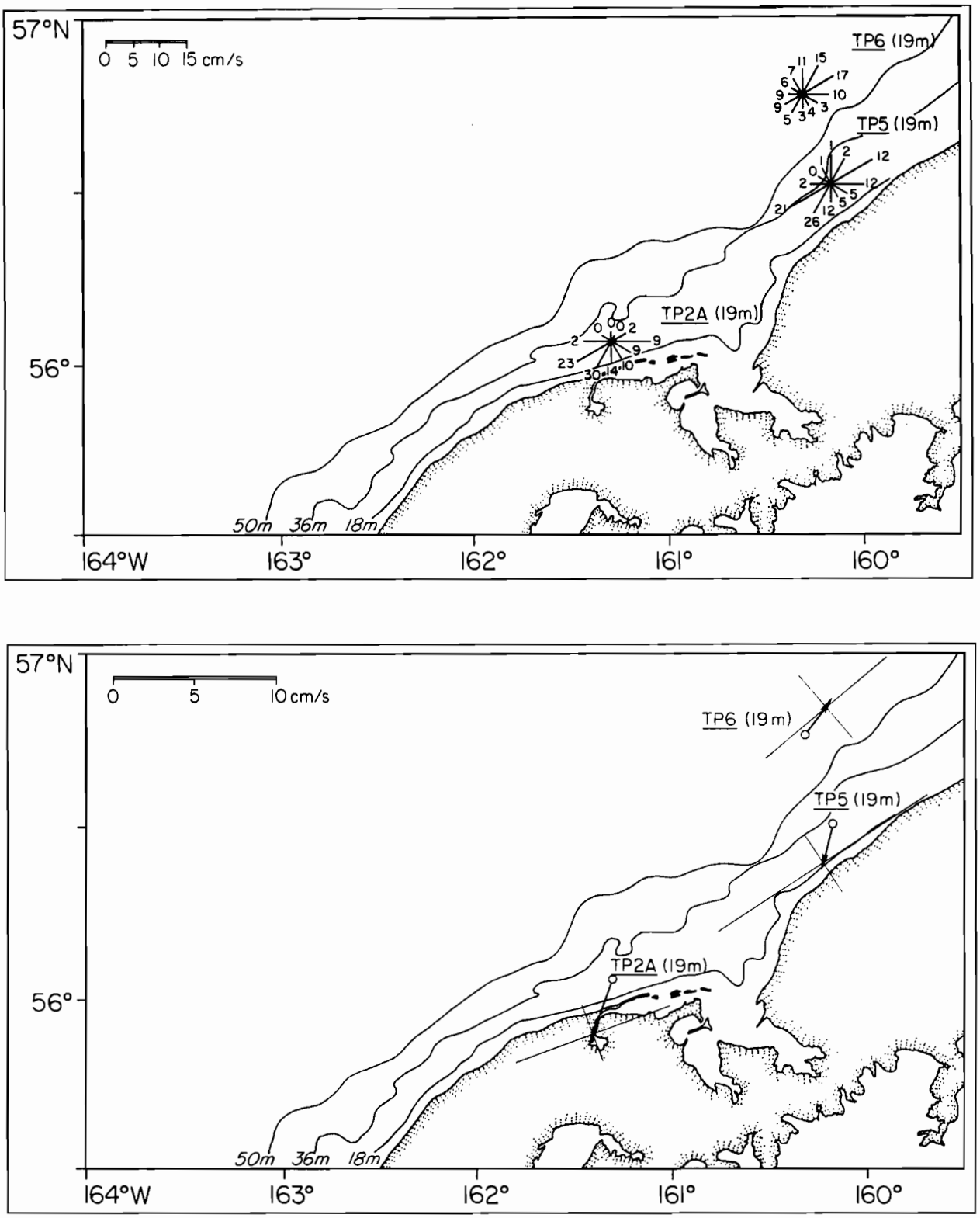


Fig. 27. Current roses and means for near-surface records between August 1980 and January 1981. The cross at the end of the current vector is the standard deviation along and across the principal axis. (Instrument depths are given in parentheses.)

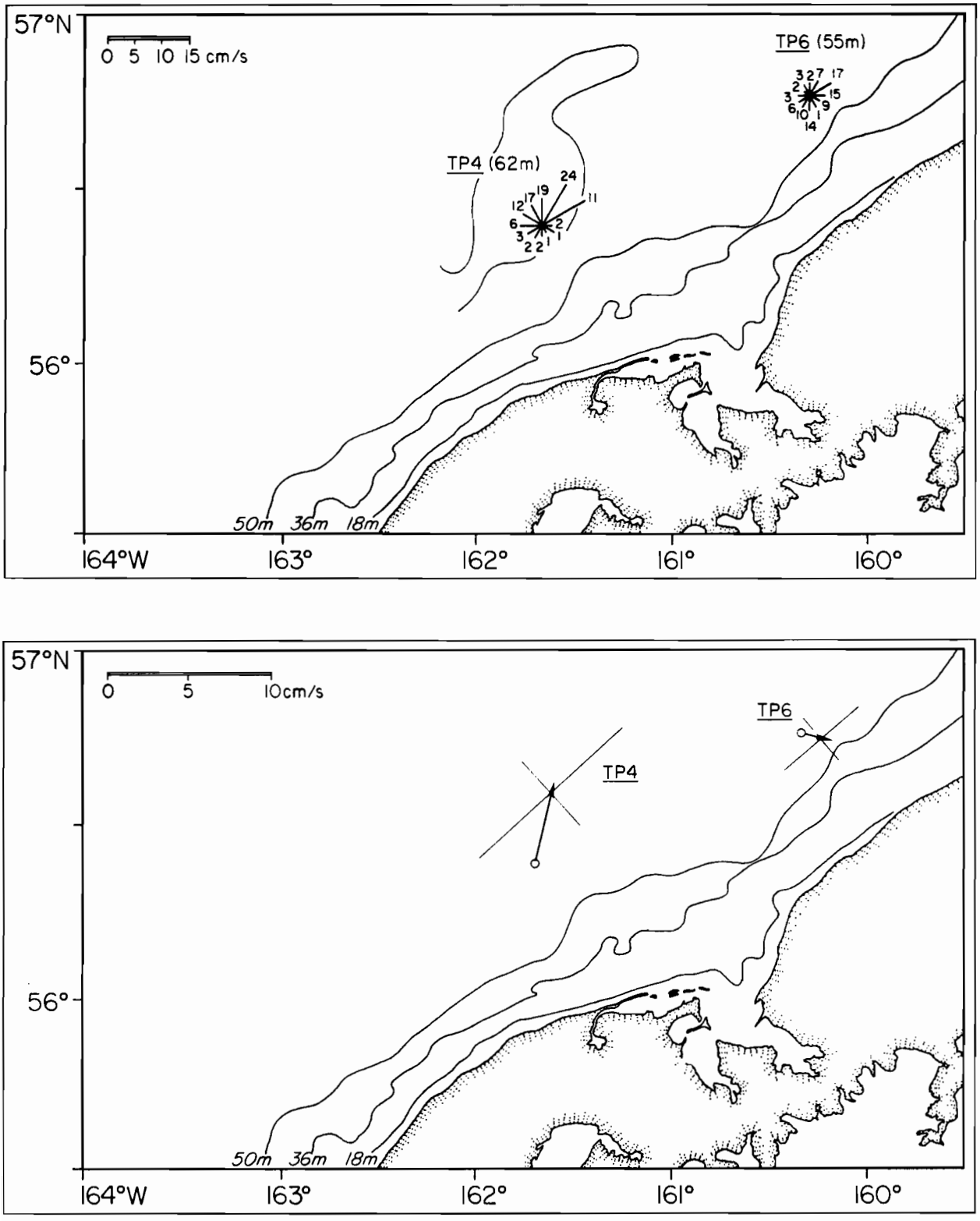


Fig. 28. Current roses and means for near-bottom records between August 1980 and January 1981.

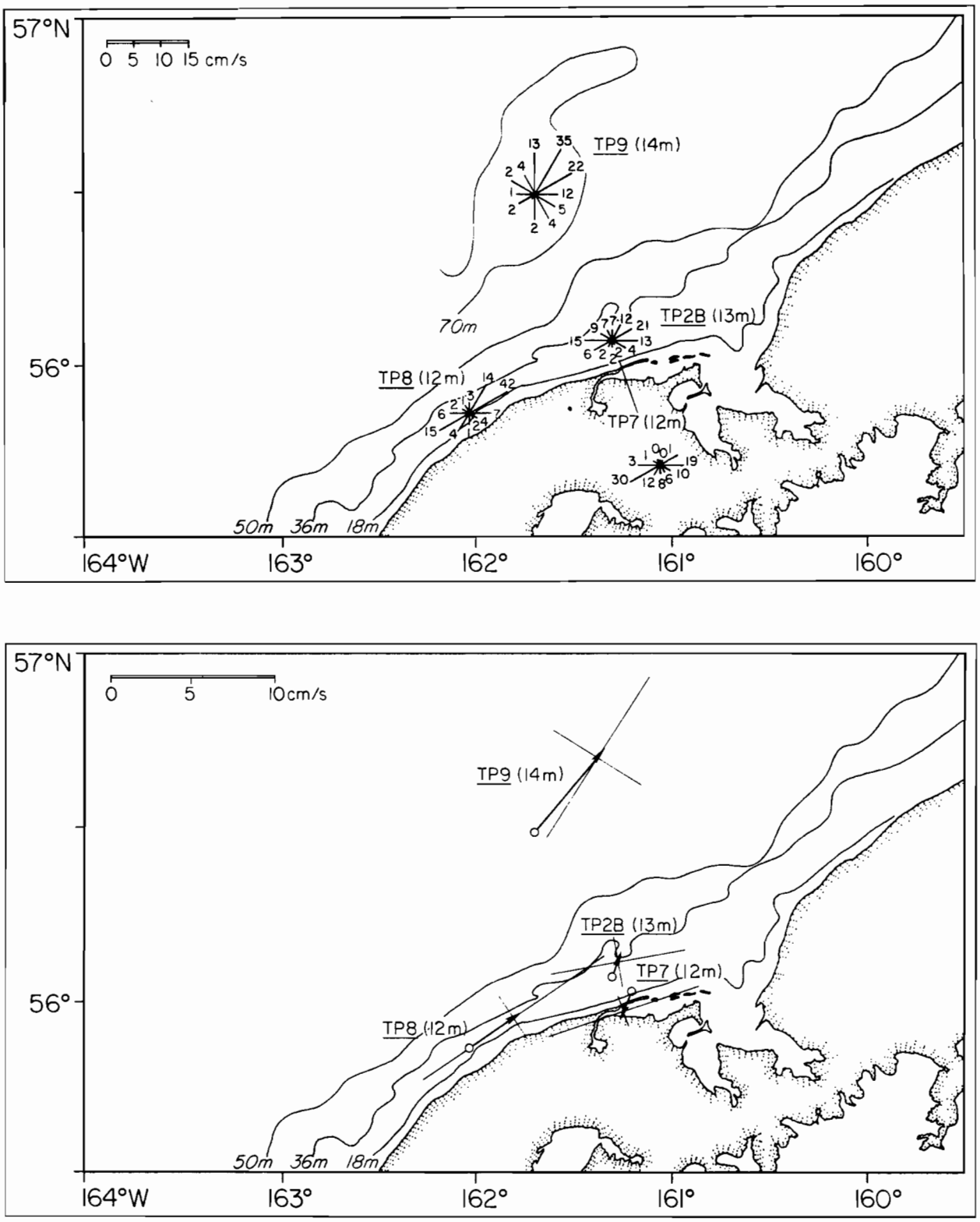


Fig. 29. Current roses and means for near-surface records between January 1981 and May 1981.

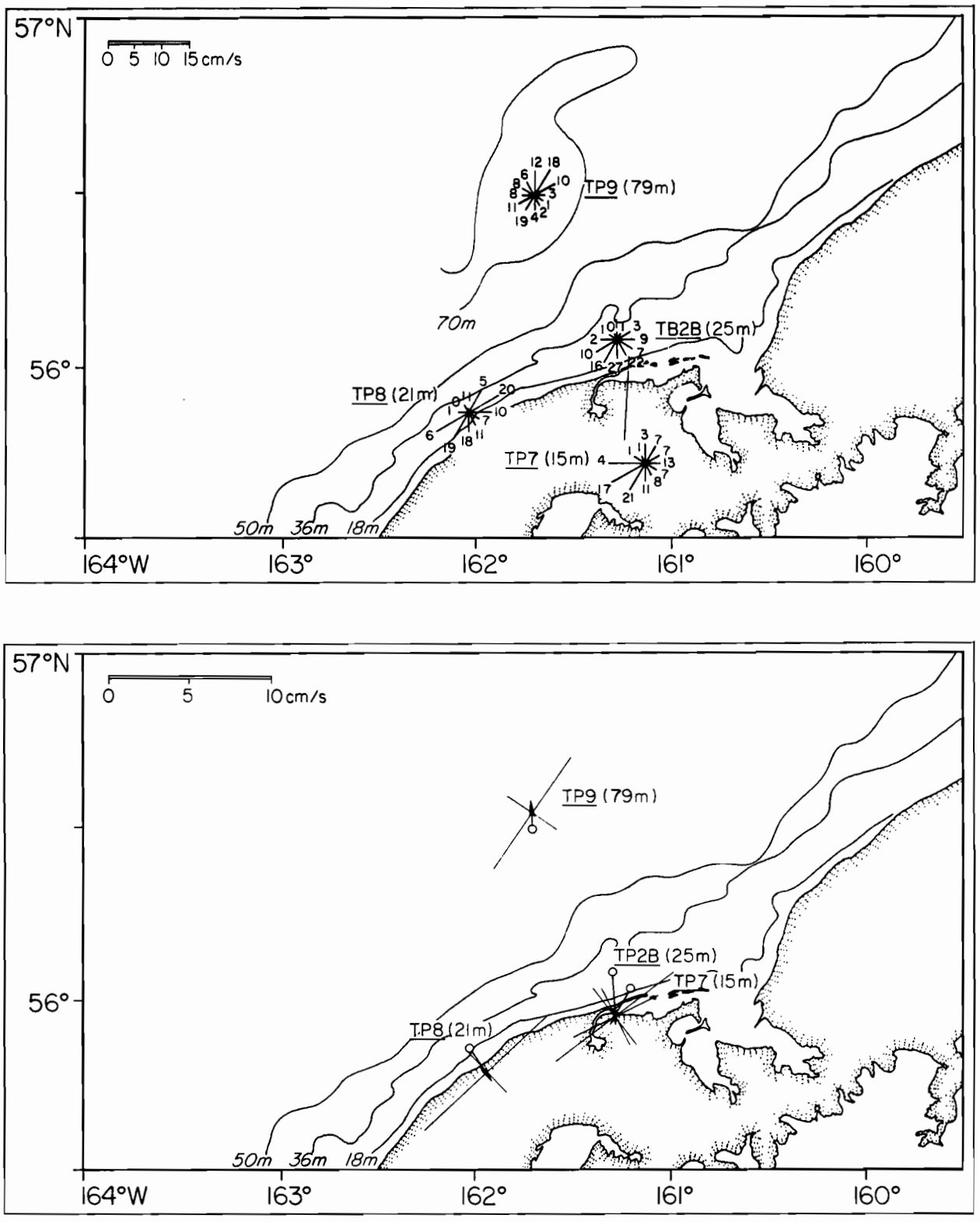


Fig. 30. Current roses and means for near-bottom records between January 1981 and May 1981.

TABLE 4: LOW-FREQUENCY CURRENT CHARACTERISTICS FROM TP MOORINGS

| Mooring Depth (m) | Instru. Depth (m) | Vector Speed (cm/s) | Mean Dir (°T) | Principal Axis & % of Variance | Component Means RMS Alongshore (cm/s) | Component Means RMS Cross-shelf (cm/s) | KE of Components Alongshore ($cm^2\ s^{-2}$) | KE of Components Cross-shelf ($cm^2\ s^{-2}$) |
|---|---|---|---|---|---|---|---|---|
| | | | | AUG 80/JAN 81 | | | | |
| TP2A | 19N | 3.7 | 200 | 70,89 | -2.8±1.4 | 2.4±0.6 | 12.6 | 1.9 |
| (32) | 20 | 3.0 | 211 | 68,69 | -2.6±1.4 | 1.4±0.8 | 13.5 | 5.7 |
| TP5 | 19N | 2.6 | 194 | 57,93 | -1.8±1.8 | 1.9±0.5 | 30.6 | 2.3 |
| (31) | 20 | 3.7 | 180 | 52,83 | -1.8±1.9 | 3.2±0.7 | 26.0 | 6.6 |
| TP6 | 19N | 2.1 | 038 | 50,78 | 2.0±1.0 | -0.8±0.4 | 12.0 | 3.8 |
| (69) | 20 | 1.6 | 058 | 45,68 | 1.6±1.0 | -0.1±0.4 | 10.8 | 5.7 |
| | 55 | 1.2 | 108 | 50,76 | 0.8±0.7 | 0.9±0.2 | 4.5 | 1.6 |
| TP4 | 62N | 4.4 | 013 | 48,84 | 3.0±1.5 | -3.2±0.7 | 18.0 | 4.3 |
| TP2B | 13N | 1.0 | 021 | 80,87 | 0.8±1.4 | -0.6±0.8 | 8.9 | 2.4 |
| (35) | 25 | 2.8 | 176 | 63,68 | -1.2±0.9 | 2.5±0.5 | 4.4 | 1.7 |
| TP7 | 12N | 1.4 | 203 | 71,96 | -1.1±1.4 | 0.8±0.5 | 12.2 | 1.8 |
| (25) | 15 | 2.1 | 210 | 53,81 | -1.8±1.5 | 1.0±0.6 | 9.8 | 2.6 |
| TP8 | 12N | 3.3 | 055 | 55,95 | 3.2±2.4 | -0.3±0.4 | 22.3 | 1.4 |
| (31) | 21 | 1.8 | 145 | 46,90 | 0.2±1.9 | 1.8±0.7 | 13.8 | 2.5 |
| TP9 | 14N | 6.1 | 040 | 32,77 | 5.7±1.5 | -2.1±1.9 | 13.4 | 8.4 |
| (89) | 79 | 1.0 | 357 | 34,83 | 0.5±1.3 | -0.9±0.8 | 8.5 | 3.5 |

Note: All statistics are from 35-hr-data, N represents accoustic current meter, and alongshore and cross-shelf are positive 60° and 150° respectively.

Cross-shelf mean speeds were generally weaker and exhibited the tendency to be offshore in the upper water column and onshore closer to the bottom. This pattern was evident in the records from TP2B, where the cross-shelf component reversed sign over a 12-m vertical separation.

The characteristics of stronger, alongshore mean flow was mirrored in the low-frequency kinetic energy; the alongshore component was always greater than the cross-shelf component, generally by a factor of four. The relation between TP current record characteristics and those collected over the remainder of the southeastern Bering Sea shelf is discussed in Schumacher and Kinder (1983).

Vertical Structure:

In order to provide information illustrating vertical structure of currents over the middle-shelf domain, moorings with surface flotation were deployed in August 1980 (TP3A) and in May 1981 (TP3B). The results are presented in Figures 31 and 32 as 35-hr stick plots and in Figure 33 as 2.9-hr mean speed, component speed, and net current over the observation periods. For TP3A, stratification varied greatly, with the difference in sigma-t between lower and upper current meters ranging from 0 to 0.65, with an average of ~0.5); during TP3B, this index of stratification varied only from 0.25 to 0.44 with an average of ~0.3. The geostrophic wind during the two observation periods was significantly different: during TP3A, winds were towards the south for the first four days and then were weakly northward. During TP3B, by contrast, winds were strongly northward throughout most of the current record. Despite these differences in stratification and wind forcing, the shear in mean speed was similar--2.8 and $1.9 \times 10^{-3}$/s during TP3A and B, respectively. Further, their shear in alongshore speed was nearly identical below 20 m, with the marked difference above this depth likely attributable to stronger and more consistent wind stress during TP3B. The cross-shelf speed profiles were also similar over most of the water column; however, the profile for TP3A indicated onshore flow in the bottom layer.

It is apparent that most of the shear resulted from wind stress (particularly during TP3B) and that estimates of baroclinic shear would account for a 1 to 3 cm/s decrease of alongshore speed between the surface and 25 db. There is also a contribution to the shear from tidal currents, although the majority of this contribution would occur in the bottom boundary layer (about 3 to 15 m thick). Hourly alongshore speeds at four levels are shown in Figure 34. During this period winds were light (3 to 4m/s). Thus, based on a current response of 3% of the wind speed, the wind-induced shear in the upper mixed layer (about 25 m in depth) would be approximately 10 cm/s. Combining this estimate with reasonable values for baroclinic shear would account for most of the shear indicated between 10- and 29-m depth records, but not for the shear of 20 to 25 cm/s shown to exist during floods and ebbs between the 29- and 50-m records. Although some fraction, perhaps up to 50%, may be accounted for by tides and the observation that the lower water column leads the surface (by about 15°) is consistent with the estimate of tidal wave propagation, some of the observed shear is not accounted for by any of these mechanisms.

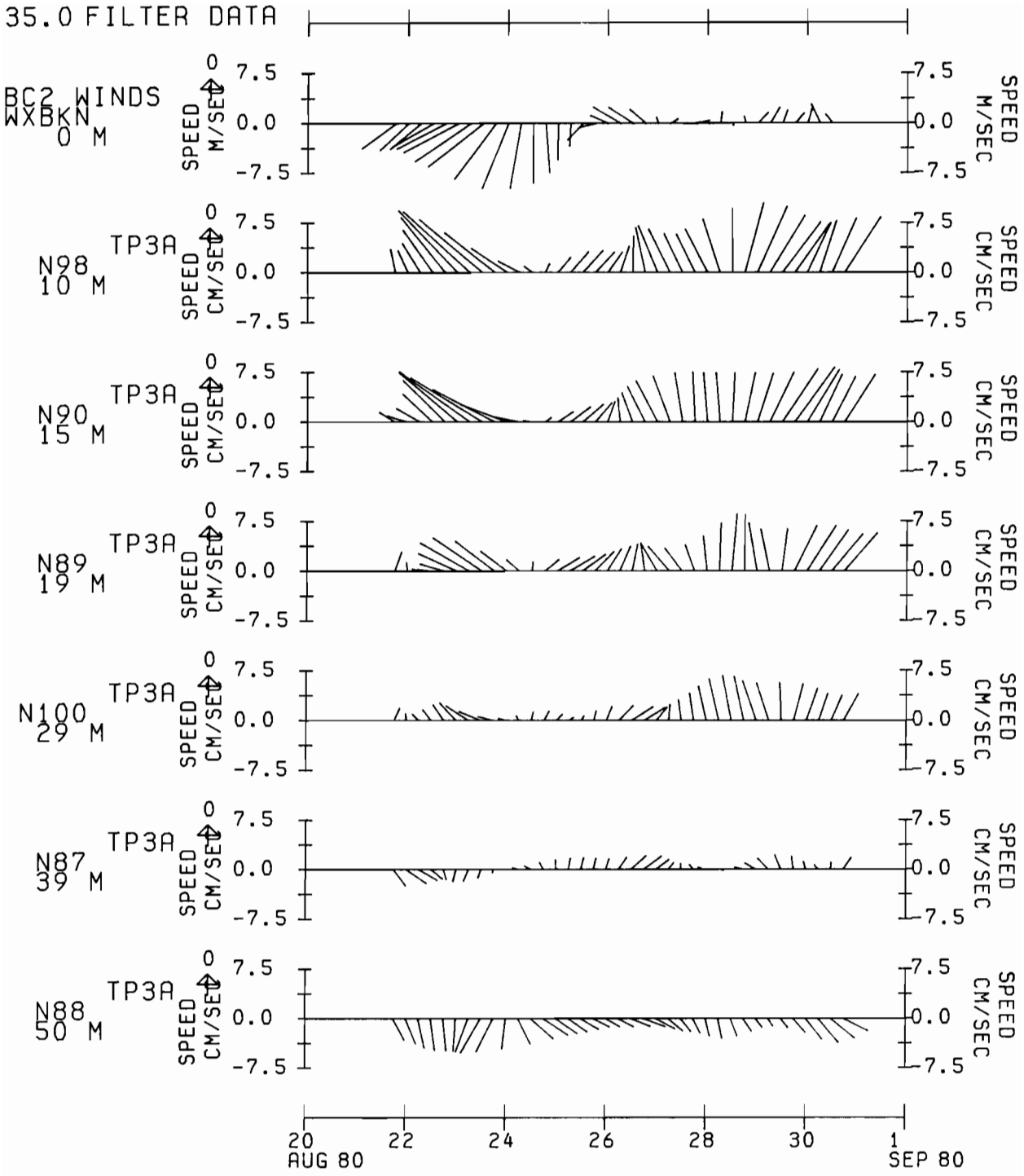


Fig. 31. Current records from TP3A presented as 6-hourly vectors.

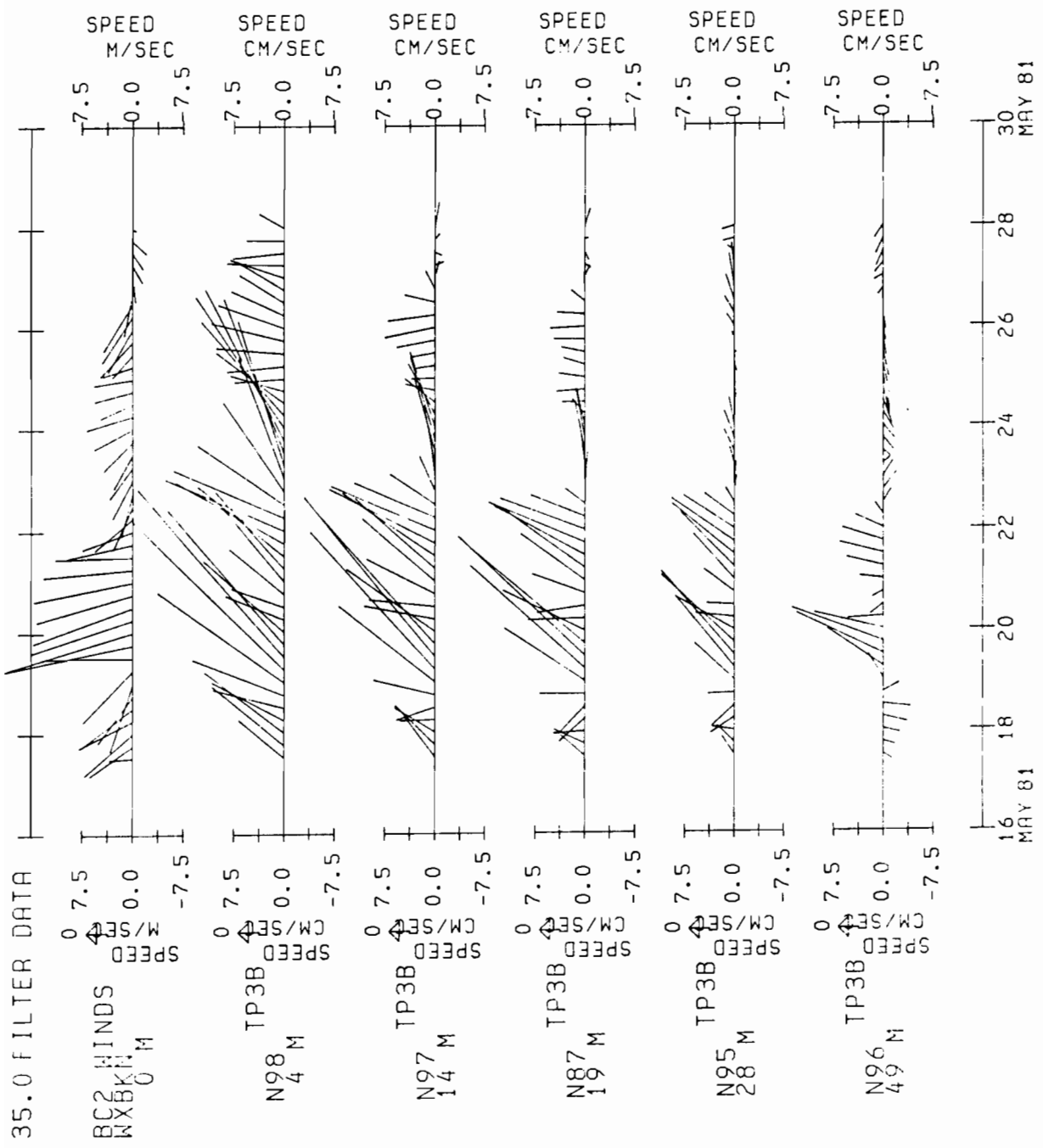


Fig. 32. Current records from TP3B presented as 6-hourly vectors.

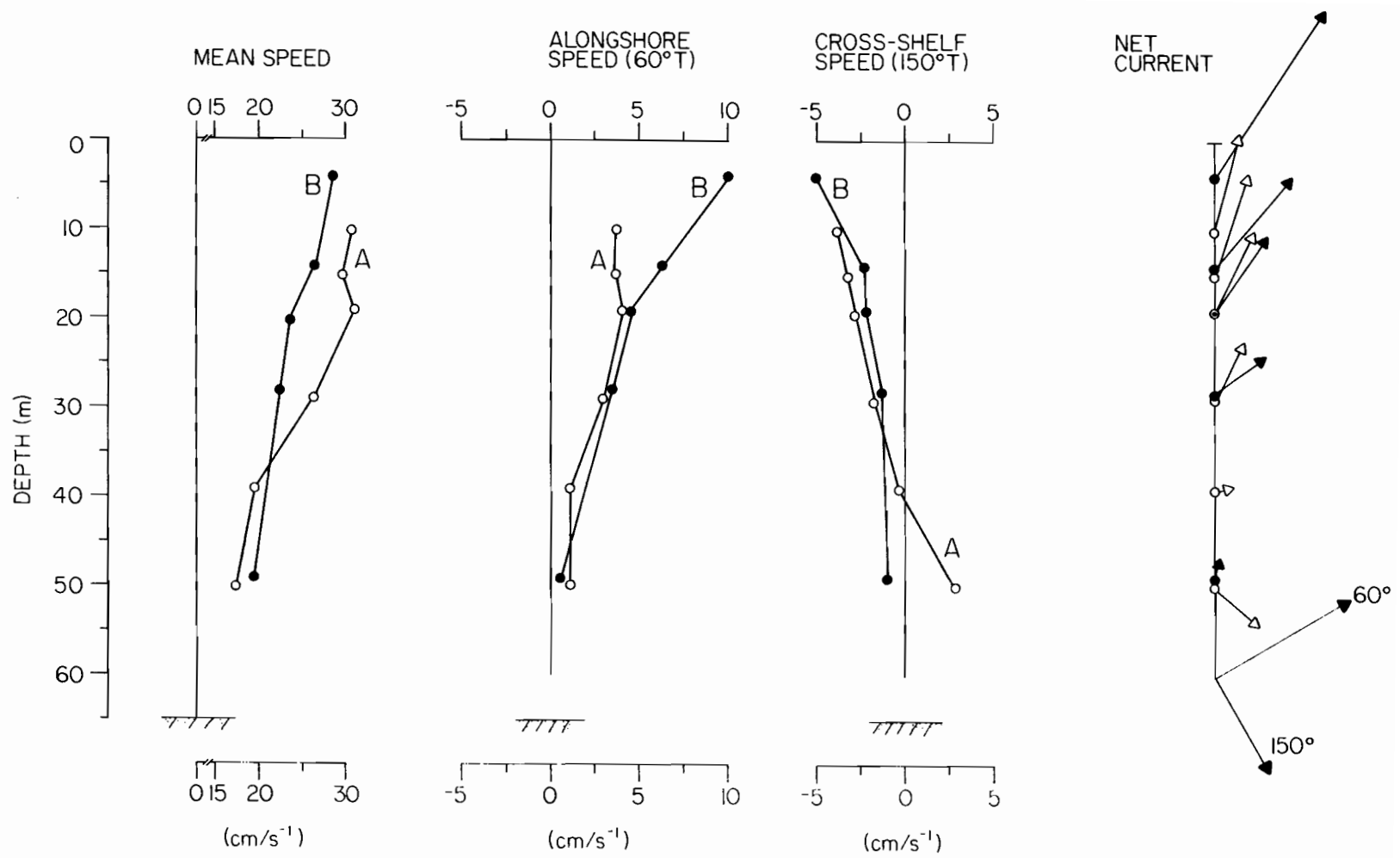


Fig. 33. Profiles of mean, alongshore, and cross-shelf speed and net current from TP3A and B.

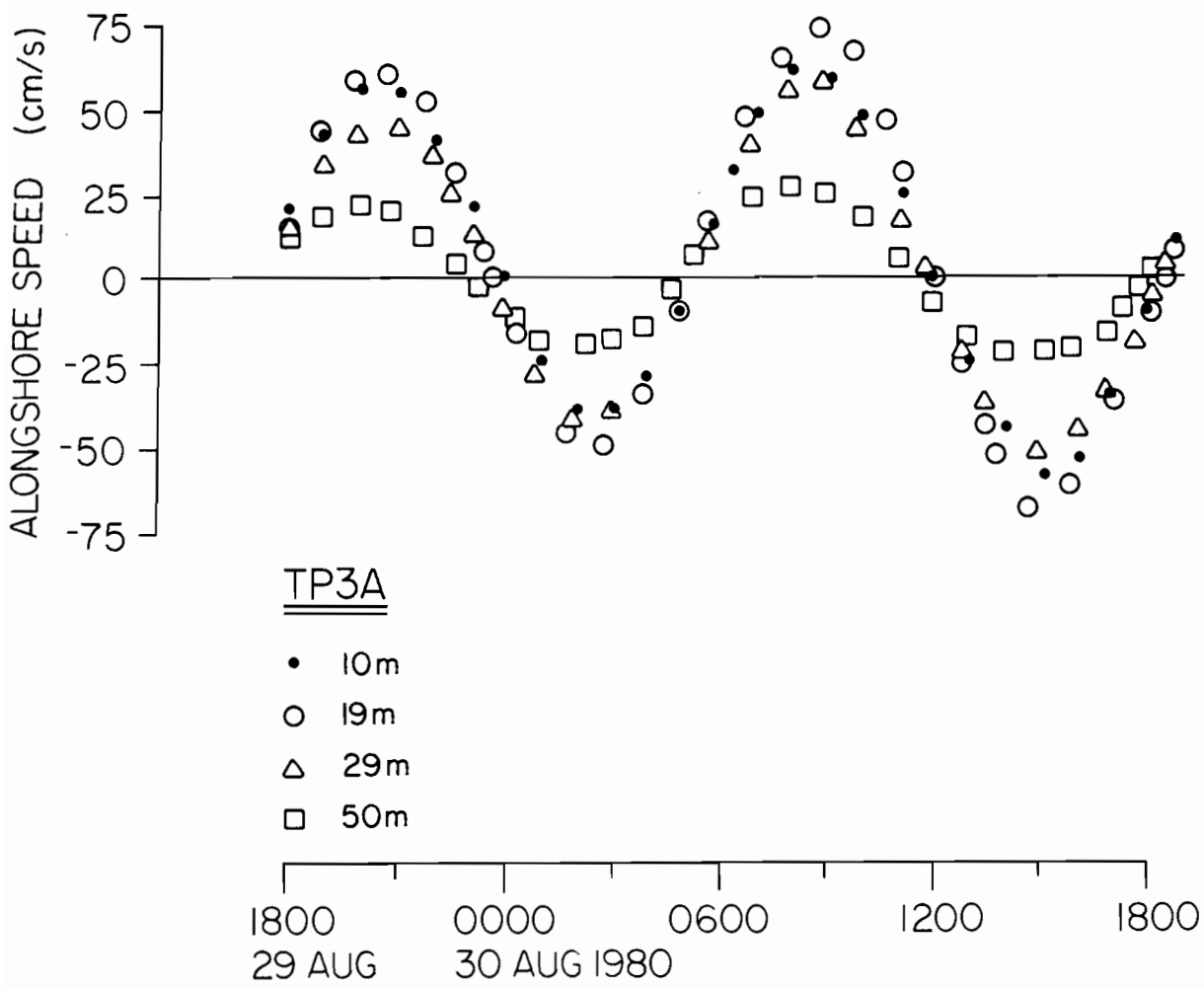


Fig. 34. Current speed at four depths from 2.9 hr data.

Wind: A comparison between alongshore and cross-shelf components of surface winds (herein called BC2 winds) and those measured on Lagoon Point (near Port Moller) is shown in Figure 35. The alongshore components are markedly similar, with BC2 winds indicating somewhat greater speeds (record mean, 2.5 m/s vs 0.3 m/s for TPIA). The cross-shelf winds are also similar, but TPIA winds were generally greater than those computed for BC2 (record mean 1.1 m/s vs ~0 at BC2). Although there were differences in component speeds, the alongshore series were highly coherent ($K^2 \geq 0.6$) at all frequencies (figure 36A). There was, however, significantly less coherence squared at periods between 2.5 and 3.3 days in the cross-shelf series (figure 36B). While some of these differences may be attributed to the method of computing geostrophic winds from surface atmospheric pressure (see Section 3.3), the wind roses generated by the two time series (figure 37) indicated that there was about at 20% difference in the percentage of wind observations in the sectors between 270° and 330°, and between 90° and 150°. Considering the local orography, some portion of the difference was likely due to pressure gradient winds along the orographic axis. In general, this affect may be present wherever there are gaps in the mountain range along the Alaska Peninsula, particularly in the vicinity of Cold Bay where the gap is wide (about 20 km) as well as nearly flat.

### 4.2.4 Salinity Time Series

Moored current meter records provided some further insight regarding temporal changes in salinity (as computed from temperature, conductivity, and pressure). In Figure 38, 15-day averages of salinity are shown, where the individual points were determined by finding the differences between successive 15-day averages and replacing this value at the mid-point of a given averaging interval. The relative change in mean salinity was greatest (~2g/kg) at TP2, but the other series showed a similar trend of decreasing salinity over a period of about one month, and this change was in October. Because the advective transport moves sluggishly and alongshore toward the east, Kvichak River discharge was not a likely source of the less saline water. Instead, the less saline water was probably a result of addition from numerous ungauged streams and ground-water injection. This addition could result in the bands of relatively stratified water shown in Figure 16D.

## 5.0. SUMMARY AND CONCLUSIONS

### 5.1 Currents and Bottom Pressure

The behavior of currents and bottom pressure observed between March and August 1980 has been described for Unimak Pass, Alaska. These data have been interpreted together with atmospheric pressure gradient, geostrophic wind, and CTD data. The following conclusions were reached:

(1) mean flow was from the Gulf of Alaska shelf westward through Unimak Pass, and reversals occurred in 18% of spring and 31% of summer, 35-hr-filtered current observations, with mean flow during spring three times greater than in summer.

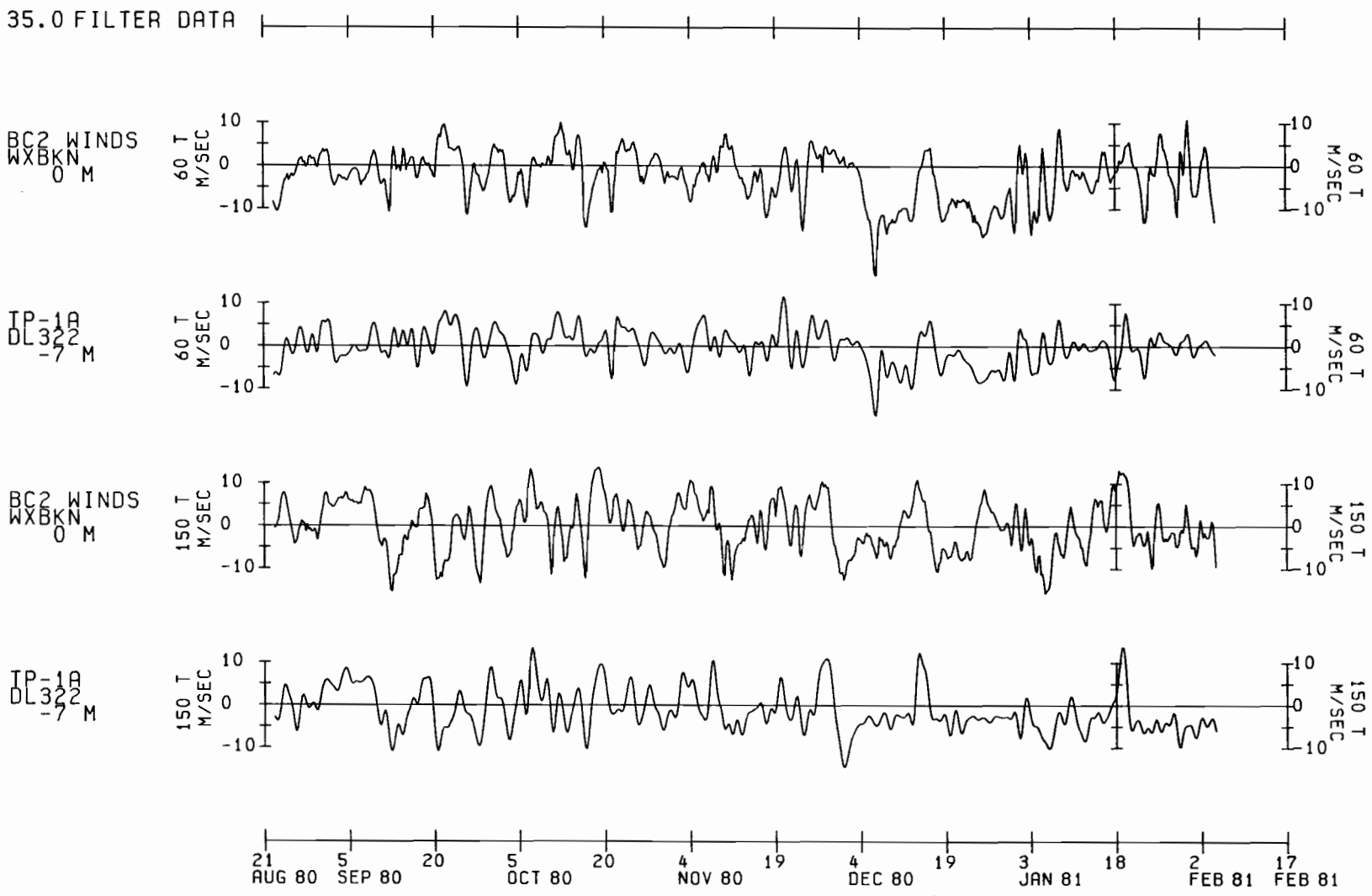


Fig. 35. Comparison of alongshore and cross-shelf components from surface (BC2) and observed (TP1A) wind.

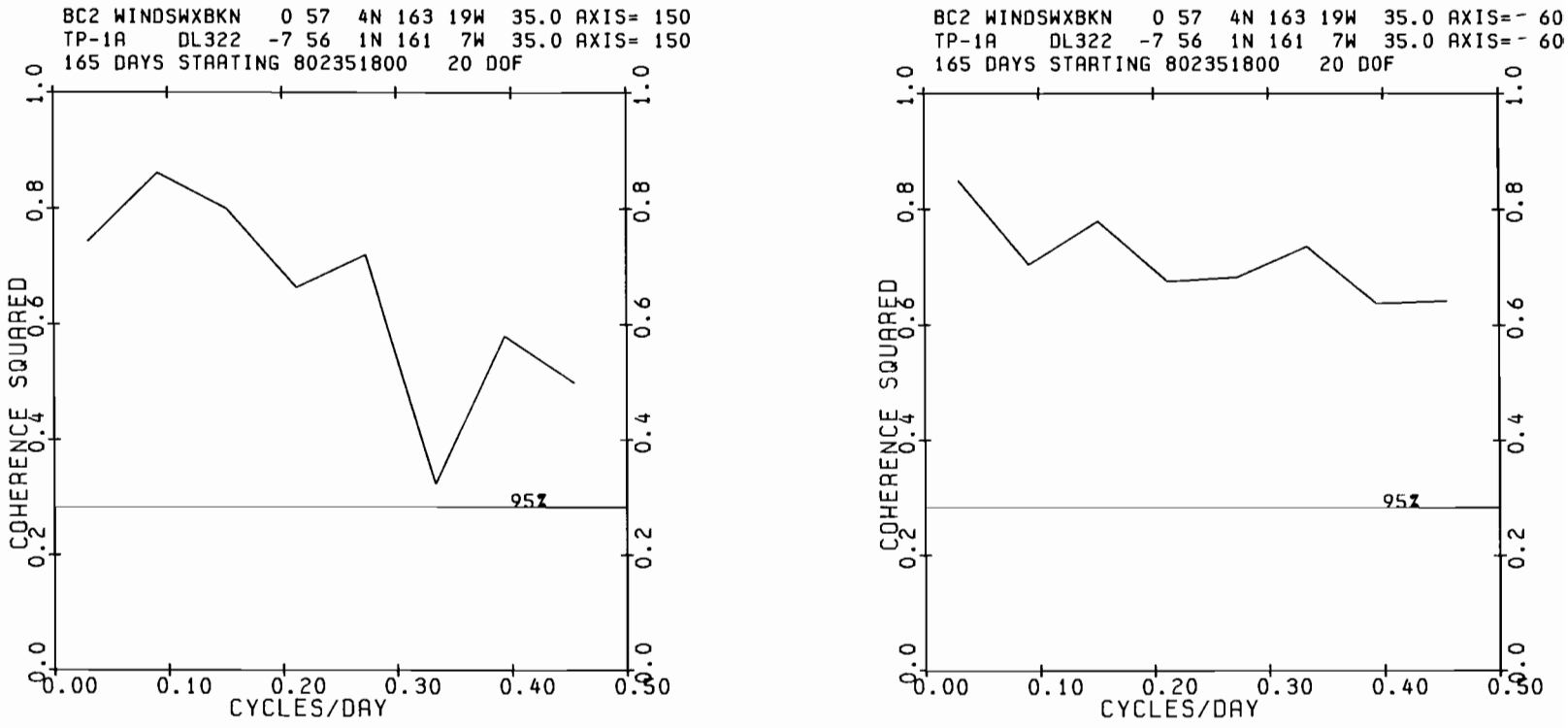


Fig. 36. Coherence squared estimates between surface and observed wind components.

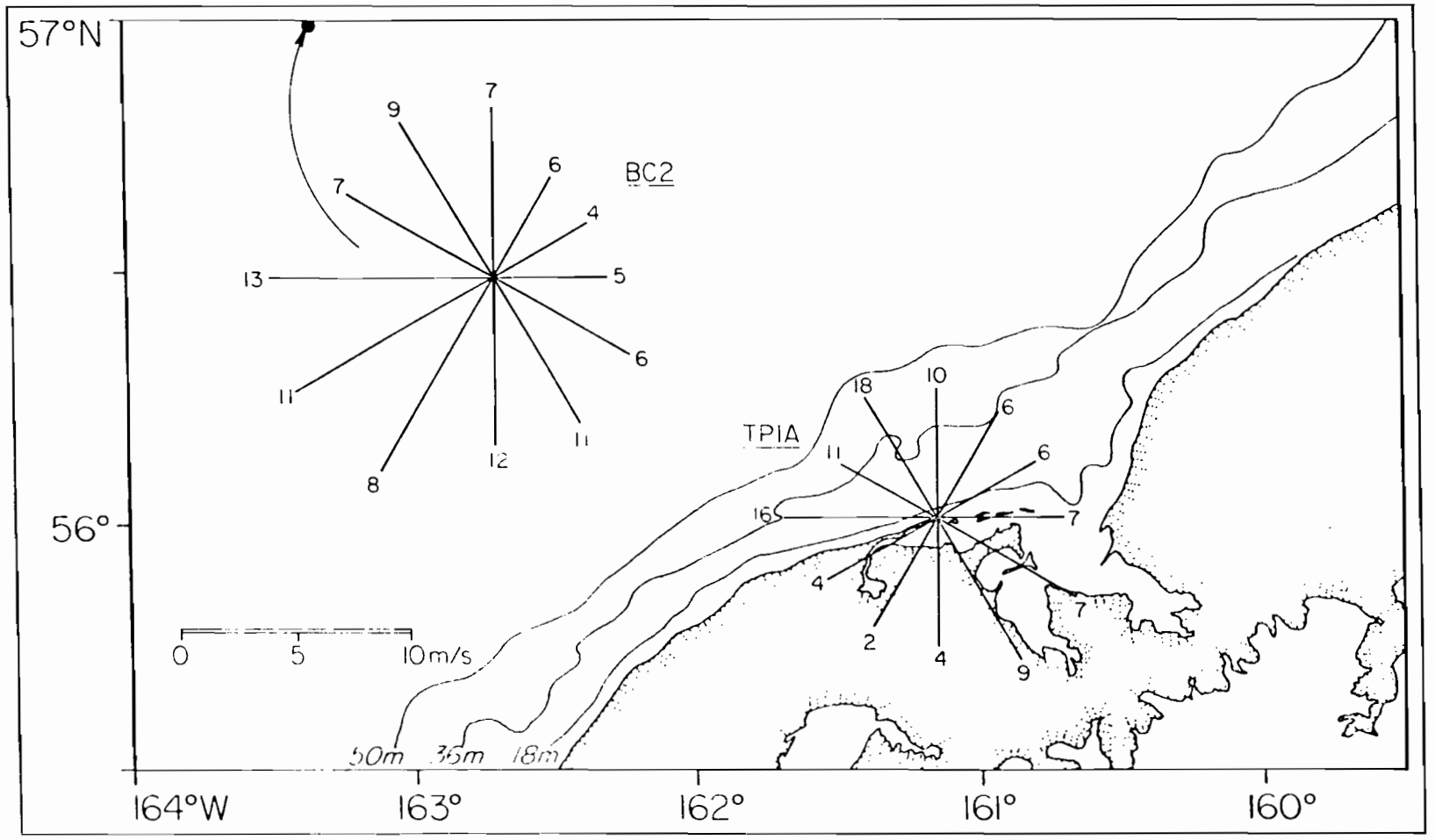


Fig. 37. Wind roses for BC2 and TP1A.

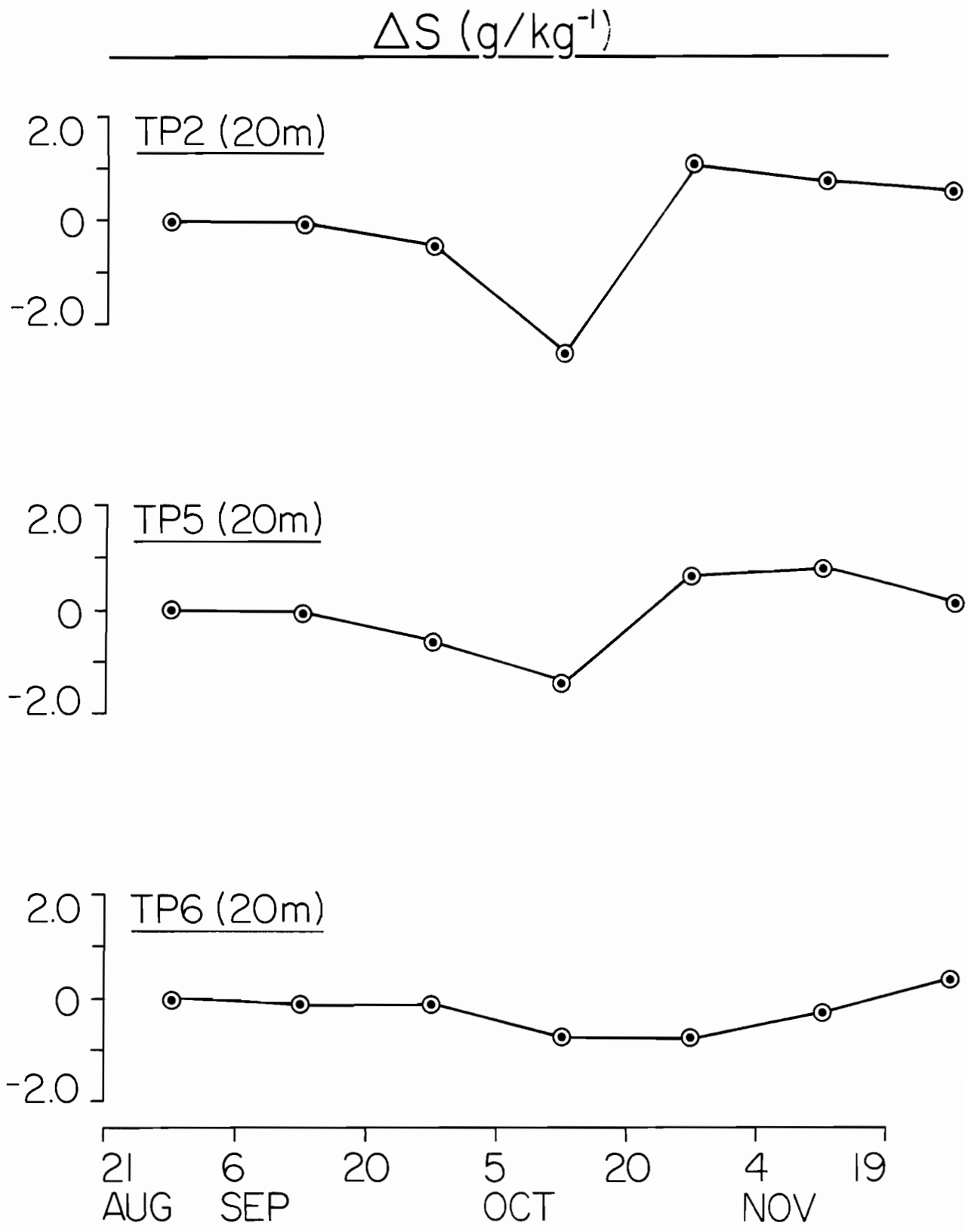


Fig. 38. Salinity time-series (15 day averages) from TP moorings.

(2) currents at periods between 3 and 10 days in Unimak Pass were highly coherent with the bottom pressure difference along the strait, which provided the dominant forcing for fluctuations. At these periods most of the bottom pressure difference was related to alongshore winds, which induced sea level changes along the Gulf of Alaska coast.
(3) Longer period flow and variablity (on the order of months) were accounted for by the presence of a southwestward-flowing coastal current, which appeared to be a westward extension of the Kenai Current.
(4) Flow of fresher coastal water through Unimak Pass resulted in formation of a front in the vicinity of Unimak Pass. This flow also may influence baroclinic flow along the northern side of Alaskan Peninsula and provide some fraction of the northward transport through Bering Strait.

A characterization of hydrographic features and current behavior between August 1980 and October 1981 has also been described for the shelf north of the Alaska Peninsula. These data were interpreted together with wind and river discharge data. The following conclusion were drawn:

1) In general, waters over the continental shelf adjacent to the Alaska Peninsula adhere to the previously defined hydrographic domains (Kinder and Schumacher, 1981a): waters of the outer-shelf domain (the small portion of the study area north of Unimak Island with depths $\geq$ 80m) were always stratified with upper and lower mixed layers and separated by a column of weak stratification. Both temperature and salinity showed small seasonal ranges; middle shelf depths (those greater than 50 m and less than $\sim$80 m) were typically two-layered during summer and well mixed from about October through March. An exception occurs when ice, primarily formed to the northeast, is transported over this domain and melts. Temperature and salinity ranged between $\sim$10°C and $\sim$1.0 g/kg respectively. The coastal domain (less than 50 m) was generally mixed, however, and the addition of freshwater as a "line source" (particularly between Ports Moller and Heiden) and from the Kvichak River, resulted in stratification (up to 3 sigma-t units) even though the water is shallow and tidal-mixing energy strong. There was also a suggestion that melting ice could impact the local buoyancy/tidal-mixing balance. Both temperature and salinity varied greatly, with $\sim$14°C and 8 g/kg changes, respectively, in locations where most of the salinity range was a result of Kvichak River addition.

2) Hydrographic data from February 1981 showed the impact of less saline Kenai current water upon coastal water along the Peninsula. This was most apparent in a reduction of mean salinity between Port Moller and Unimak Island between August 1980 and February 1981. This lends support to a previous hypothesis that the Kenai Current was linked with flow around the perimeter of the southeastern Bering Sea shelf and continued northward toward Bering Strait (Schumacher et al., 1982).

3) Storms radically alter mean hydrographic domain characteristics. The enhanced turbulence can mix middle-shelf water and increase SPM concentrations. These two factors could dominate vertical transport of oil, resulting in greater SPM concentrations on the bottom in a shorter time than detrital rain.

4) Current records support previous results (Kinder and Schumacher, 1981b; Schumacher and Kinder, 1983), which imply a moderate (2 to 6 cm/s) Eulerian mean flow from the vicinity of Unimak Island, counter-clockwise around Bristol Bay, and thence northwest past Nunivak Island. A mechanism for long-term (on the order of months) flow is the persistent cross-shelf density distribution, which resulted in baroclinic speeds of 1 to 5 cm/s, typically concentrated in a 10- to 20-km-wide band in the vicinity of the 50-m isobath. Scaling of Eulerian tidal residual flow suggested a weak contribution, <1.0 cm/s, except were the tidal current was orthogonal to the 50-m isobath off Port Heiden (Schumacher and Kinder, 1983).

5) Although wind energy was evident in alongshore current pulses, mean winds during the current observations were weak and toward the west, in opposition to the observed mean flow. Cross-shelf current pulses were also evident, and the observed tendency was for offshore flow in the upper water column.

6) Comparison between surface and measured winds indicate that these series were highly coherent, particularly in the alongshore component. At short periods (>2.5 to 3.3 days), coherence was weak in the cross-shelf component and the observations showed that measured winds tended to be along the local orographic trend. Such down-pressure-gradient winds have been noted before (Schumacher and Pearson, 1981) and are likely to be more significant at Cold Bay and in Unimak Pass.

7) Substantial vertical shear in currents was observed during two mooring periods. The combination of wind-induced shear and geostrophic baroclinic shear accounted for about one-half the observed values. The number of values attributable to tides requires theoretical examination.

## 6. ACKNOWLEDGEMENTS

We acknowledge the aid of a large number of persons, not only in the preparation of this document but in carrying out the field work and processing which have led to its existence. Of these, special thanks must go to the complement of the research vessels *Discoverer*, *Surveyor*, and *Thompson* (R. B. Tripp, chief scientist) for laboring under less than ideal conditions to carry out field operations. Lynn Long, Sharon Wright, Gini May, and Phyllis Hutchens of NOAA/PMEL are due thanks for their help in processing the data and preparing this document. This study was supported in part by the Bureau of Land Management through interagency agreement with the National Oceanic and Atmospheric Administration, under which a multiyear program responding to needs of petroleum development of the Alaskan continental shelf has been managed by the Outer Continental Shelf Environmental Assessment Program (OCSEAP) Office, Juneau, Alaska, and represents the Final Report for RU549.

## 7. REFERENCES


Allen, J. S. and P.K. Kundu, On the momemtum, vorticity and mass balance on the Oregon shelf, J. Phys. Oceanogr., 8, 13-27, 1978.

Bakun, A., Coastal upwelling indices, west coast of North America, 1946-71. Dept. of Commerce, Tech. Rep. NMFS SSRF-671, NOAA, Monterey, Calif., 1973.

Bowden, K.F., The flow of waters through the Straits of Dover related to wind and differences in sea level, Phil. Trans. R. Soc. London, Ser. A., 248, 517-551, 1956.

Brower, W.A., H.F. Diaz, A.S. Prechtel, H.W. Searby, and J.L. Wise, Climatic Atlas of the Outer Continental Shelf Waters and Coastal Regions of Alaska, vol. 1, Gulf of Alaska, Final Rep. RU-347, U.S. Dept. of Commerce/NOAA/ Alaska Outer Continental Shelf Environmental Assessment Program, Fairbanks, Alaska, 1977.

Chao, S.-Y., and L.J. Pietrafesa, The subtidal response of sea level to atmospheric forcing in the Carolina Capes, J. Phys. Oceanogr., 10, 1246-1255, 1980.

Charnell, R.L., and G.A. Krancus, A processing system for Aanderaa current meter data, Tech. Memo. ERL PMEL-6, NOAA, Boulder, Colo., 1976.

Coachmen, L.K., and K. Aagaard, Reevaluation of water transports in the vicinity of Bering Strait, in The Eastern Bering Sea Shelf: Oceanography and Resources, vol. 1, edited by D.W. Hood and J.A. Calder, pp. 95-110, U.S. Dept. of Commerce/NOAA/OMPA, Washington, D.C., 1981.

Coachmen, L.K., and R.L. Charnell, Finestructure in outer Bristol Bay, Alaska, Deep Sea Res., 24, 809-839, 1977.

Coachmen, L.K., and R.L. Charnell, On lateral water mass interaction: A case study, Bristol Bay, Alaska, J. Phys. Oceanogr., 9, 278-297, 1979.

Coachman, L.K., and J.J. Walsh, A diffusion model of cross-shelf exchange of nutrients in the southeastern Bering Sea, Deep Sea Res., 28, 819-846, 1981.

Coachmen, L.K., K. Aagaard, and R.B. Tripp, Bering Strait, the Regional Oceanography, University of Washington Press, Seattle, 1975.

Coachmen, L.K., T.H. Kinder, J.D. Schumacher, and R.B. Tripp, Frontal systems of the southeastern Bering Sea shelf, in Stratified Flows, edited by T. Carstens and T. McClimans, pp. 917-933, TAPIR, Norway, 1980.

Defant, A., Physical Oceanography, vol. 1, Pergamon, New York, 1961.

Favorite, F., and D.M. Fisk, Drift bottle experiments in the North Pacific Ocean and Bering Sea--1957-60, 1962, 1966, and 1970, Data Rep. 67, NOAA, NMFS, Seattle, Wash., 1971.

Favorite, F., A.J. Dodimead, and K. Nasu, Oceanography of the subarctic Pacific region, 1960-1971, Bull. 33, Int. N. Pacific Fish. Comm., Vancouver, Canada, 1976.

Fearnhead, P.G., On the formation of fronts by tidal mixing around British Isles, Deep Sea Res., 22, 311-322, 1975.

Garrett, C., and B. Petrie, Dynamical aspects of Flow through the Strait of Belle Isle, J. Phys. Oceanogr., 11, 376-393, 1981.

Garrett, C., and B. Toulany, Variability of flow through the Strait of Belle Isle, J. Mar. Res., 39, 163-189, 1981.

Gebhart, B., and J.C. Mollendorf, A new density relation for pure and saline water, Deep Sea Res., 24, 831-848, 1977.

Hattori, A., and J.J. Goering, Nutrient distributions and dynamics in the eastern Bering Sea, in The Eastern Bering Sea Shelf: Oceanography and Resources, vol. II, edited by D.W. Hood and J.A. Calder, pp. 975-992, U.S. Dept of Commerce/NOAA/OMPA, Washington, D.C., 1981.

Hayes, S.P., Variability of current and bottom pressure across the continental shelf in the northeast Gulf of Alaska, J. Phys. Oceanogr., 9, 88-103, 1979.

Hughes, F.W., L.K. Coachman, and K. Aagaard, Circulation, transport and water exchange in the western Bering Sea, in Oceanography of the Bering Sea, edited by D.W. Hood and E.J. Kelley, pp. 59-98, Institute of Marine Science, University of Alaska, Fairbanks, Alaska, 1974.

Iverson, R.L., L.K. Coachman, R.T. Cooney, T.S. English, J.J. Goering, G.L. Hunt, Jr., M.C. Macauley, C.P. McRoy, W.S. Reeburgh, and T.H. Whitledge, Ecological significance of fronts in the southeastern Bering Sea, in Coastal Ecological, edited by R.J. Livingston, pp. 437-468, Plenum, New York, 1980.

Kinder, T.J., and L.K. Coachman, The front overlaying the continental slope in the eastern Bering Sea, J. Geophys. Res., 83, 4551-4559, 1978.

Kinder, T.J., and J.D. Schumacher, Circulation over the continental shelf of the southeastern Bering Sea, in The Eastern Bering Sea Shelf: Oceanography and Resources, vol. 1, edited by D.W. Hood and J.A. Calder, pp. 53-78, U.S. Department of Commerce/NOAA/OMPA, Washington, D.C., 1981a.

Kinder, T.J., and J.D. Schumacher, Hydrography over the continental shelf of the southeastern Bering Sea, in The Eastern Bering Sea Shelf: Oceanograph and Resources, vol. I, edited by D.W. Hood and J.D. Calder, pp. 31-52, U.S. Department of Commerce/NOAA/OMPA, Washington, D.C., 1981b.

Kinder, T.H., J.D. Schumacher, R.B. Tripp, and J.C. Haslett, The evolution of the hydrographic structure over the continental shelf near Bristol Bay, Alaska, during summer 1976, Tech. Rep. Ref: M78-16, Univ. of Washington, Seattle, 1978.

Lagerloef, G., R.D. Muench, and J.D. Schumacher, Low frequency variations in currents near the shelf break: Northeast Gulf of Alaska, J. Phys. Oceaonogr., 11, 627-638, 1981.

Livingstone, D., and T.C. Royer, Observed surface winds at Middleton Island, Gulf of Alaska and their influence on the ocean circulation, J. Phys. Oceanogr., 10, 753-764, 1980.

Muench, R.D., and J.D. Schumacher, Physical oceanographic and meteorological conditions on the northwest Gulf of Alaska, NOAA, Tech. Memo. ERL-PMEL-22, Boulder, Colo., 1980.

Overland, J.E., Marine climatology of the Bering Sea, in The Eastern Bering Sea Sea Shelf: Oceanography and Resources, vol. I, edited by D.W. Hood and J.D. Calder, pp. 15-22, U.S. Dept. of Commerce/NOAA/OMPA, Washington, D.C., 1981.

Overland, J.E., and C.H. Pease, Cycline climatology of the Bering Sea and its relation to sea ice extent, Mo. Wea. Rev., 108, 2015-2023, 1982.

Pearson, C.A., H. Mofjeld, and R.B. Tripp, Tides of the eastern Bering Sea shelf, in The Eastern Bering Sea Shelf: Oceanography and Resources, vol. 1, edited by D.W. Hood and J.A. Calder, pp. 53-85, U.S. Dept of Commerce/NOAA/ OMPA, Washington, D.C., 1981a.

Pearson, C.A., J.D. Schumacher, and R.D. Muench, Effects of wave induced mooring noise on tidal and low frequency current observations, Deep Sea Res., 28A(10), 1223-1229, 1981b.

Pease, C.H., S.A. Schoenberg, and J.E. Overland, A climatology of the Bering Sea and its relation to sea ice extent, NOAA Tech. Report, ERL 419-PMEL 36, 29 pp., 1982.

Quadfasel, D., and F. Schott, Comparison of different methods of current measurements, Deut. Hydrogr. Zeit., 32, 27-28, 1979.

Reed, R.K., Nontidal flow in the Aleutian Island passes, Deep Sea Res., 18, 379-380, 1971.

Reed, R.K., and J.D. Schumacher, Sea level variations in relation to coastal flow around the Gulf of Alaska, J. Geophys. Res., 86, 6543-6546, 1981.

Reed, R.K., J.D. Schumacher, and C. Wright, On coastal flow in the northeast Gulf of Alaska near Yakutat, Atmos. Ocean., 19, 47-53, 1981.

Royer, T.C., Baroclinic transport in the Gulf of Alaska, II, A fresh water driven coastal current, J. Mar. Res., 39, 251-266, 1981.

Royer, T.C., D.V. Hansen, and D.J. Pashinski, Coastal flow in the northern Gulf of Alaska as observed by dynamic topography and satellite-tracked drogued drift buoys, J. Phys. Oceanogr., 9, 785-801, 1979.

Schumacher, J.D., T.H. Kinder, D.J. Pashinski, and R.L. Charnell, A structural front over the continental shelf of the eastern Bering Sea, J. Phys. Oceanogr., 9(1), 79-87, 1979.

Schumacher, J.D., and R.K. Reed, Coastal flow in the northwest Gulf of Alaska: The Kenai Current, J. Geophys. Res., 85, 6680-6688, 1980.

Schumacher, J.D., and C.A. Pearson, Bristol Bay Oceanographic processes, 5th Annual Report, RU549, U.S. Dept. of Commerce/NOAA/Alaska Outer Continental Shelf Environmental Assessment Program, Fairbanks, Alaska, 1980.

Schumacher, J.D., and C.A. Pearson, 6th Annual Report, RU549, U.S. Dept. of Commerce/NOAA/Alaska Outer Continental Shelf Environmental Assessment Program, Fairbanks, Alaska, 1981.

Schumacher, J.D., and T.H. Kinder, Low frequency current regimes over the southeastern Bering Sea shelf, J. Phys. Oceanogr., in press.

Schumacher, J.D., C.A. Pearson, and J.E. Overland, On exchange of water between the Gulf of Alaska and the Bering Sea through Unimak Pass, J. Phys. Oceanogr., 87, 5785-5795, 1982.

Seifert, R., and D. Kane, Effects of seasonability and variability of streamflow on nearshore coastal areas, Final Rep. RU-111, (edited by R.F. Carlson), U.S. Dept. of Commerce/NOAA/Alaska Outer Continental Shelf Environmental Assessment Program, Fairbanks, Alaska, 1977.

Takenouti, A.Y., and K. Ohtani, Currents and water masses in the Bering Sea: A review of Japanese work, in Oceanography of the Bering Sea, edited by D.W. Hood and E. Kelley, pp. 39-75, Occ. Pub. 2, Institute of Marine Science, University of Alaska, Fairbanks, 1974.

Thompson, W.F., and R.V. Van Cleve, Life history of the Pacific Halibut: (2) Distribution and early life history, Rep. Inter. Fish Comm., 9, 1936.

Webster, B.D., Ice edge probabilities for the Eastern Bering Sea, Tech. Memo., NWS, AR-26, NOAA, Anchorage, Alaska, 1979.

Winant, C.D., Coastal circulation and wind-induced currents, Ann. Rev. Fluid Mech., 12, 271-302, 1980.

Wright, C., Observations in the Alaskan Stream during 1980, Tech. Memo. ERL PMEL-23, NOAA, Seattle, Wash., 1981.

# APPENDIX A

## DATA INVENTORY

Data acquisition for RU 549 (North Aleutian Shelf Transport Processes, NAST) began in March, 1980 with the deployment of three moorings in the vicinity of Unimak Pass (Figure 1). This work was conducted under the direction of R. B. Tripp, University of Washington from the ***R.V. Thompson***. The remaining field work for the NAST experiment was accomplished during three cruises in 1980-81. These cruises are listed on the Boulder computer system ($R_2D_2$) by the following cruise identifiers: RP4SU80AL4, Aug-Sept 1980, ship ***Surveyor***, Chief Scientist: Curl; RP4SU81, Jan-Feb 1981, ship ***Surveyor***, Chief Scientist: Schumacher; and RP4DI81A2, May-June 1981, ship ***Discoverer***, Chief Scientist: Pearson. Operations during these cruises included 514 CTD casts (Figures 2-4), and deployment and recovery of 15 moorings and one shore-based meteorological station maintained throughout the current observation period.

Since the completion of field operations for RU 549, two supplemental cruises were conducted in North Aleutian Shelf waters: RP4DI81AL6, Aug-Sept 1981, ship ***Discoverer***, Chief Scientist: Reed; RP40C81AL3, Sept-Oct 1981, Ship ***Oceanographer***, Chief Scientist: Schumacher. A total of 61 CTD casts were conducted during these cruises. The data have been processed and loaded on to $R_2D_2$.

I. Hydrographic Data: Temperature and salinity data were collected during the NAST cruises using Plessey Model 9040 CTD Systems.

The sampling interval was five times per second for simultaneous measurements of conductivity, temperature and depth. Data were recorded during the down cast using a lowering rate of 30 meters per minute. Nansen bottle samples were taken at approximately half of the stations to provide temperature and salinity calibration. The calibration corrections used for each cruise are:

| | | |
|---|---|---|
| NAST 1, temp:-0.01°C | NAST 2, temp:-0.01°C | NAST 3, temp:+0.03°C |
| Salin:-0.04°/$_{oo}$ | salin:-0.05°/$_{oo}$ | salin:+0.09°/$_{oo}$ |

Data from monotonically increasing depth were despiked to eliminate excessive values and were averaged over one-meter intervals to produce temperature and salinity values from which density and geopotential anomaly were computed.

II. Time Series Observations: Time series observations were made using the following equipment:

| | | |
|---|---|---|
| B | - | Neil Brown acoustic current meters |
| RCM | - | Aanderaa RCM-4 current meters |
| RCM/T | - | Aanderaa current meters with transmissometer |
| TG | - | Aanderaa TG2 and TG3A bottom pressure gauges |
| ST | - | Sediment Traps |
| TC | - | Applied Microsystem temperature-conductivity sensors |
| DL | - | Digital data loggers |
| MET | - | Meteorological sensors (wind speed, direction, gust, and atmospheric temperature) |

Taut wire moorings were used with an anchor and acoustic release at the bottom and a 450 kg buoyancy subsurface float about 2 meters above the upper current meter. Pressure gauges were located in a cage which was welded to the anchor. Wind sensors were located on a tower about 7 m above the ground. A compilation of observation period, position and instruments on a particular platform is given in Table 1. Mooring locations are shown in Figure 12.

Current and pressure data were evaluated for quality, including time base accuracy and the presence of zero speeds. Tidal constituents were determined from edited sample interval time series. This is the final stage of our quality control procedures, i.e., the amplitude and phase of the dominant constituents are checked for relative and absolute consistency. The one-hour-interval time series available for use on $R_2D_2$ are produced from the edited data using a Lonczos filter. These series, called 2.9-hr data, are filtered such that over 90% of the amplitude is passed at periods greater than 5 hr, 50% at 2.86 hr, and less than 0.5% at 2 hr.

Table 1: Time Series Observations

| Mooring | Deployed | Recovered | Lat | Long | Depth | Instruments |
|---|---|---|---|---|---|---|
| UP-1 | 22 Mar 1980 | 17 Aug 1980 | 54°33.7'N | 165°23.9'W | 84m | 2 RCM,TG |
| UP-2 | 22 Mar 1980 | 16 Aug 1980 | 54°18.1'N | 164°45.9'W | 80m | 2 RCM,TG |
| UP-3 | 21 Mar 1980 | 16 Aug 1980 | 54°09.6'N | 164°00.4'W | 69.5m | 2 RCM,TG |
| TP-1A | 19 Aug 1980 | 6 Feb 1981 | 56°00.7'N | 161°06.8'W | -7m | MET, DL |
| TP-2A | 19 Aug 1980 | 30 Jan 1981 | 56°07.1'N | 161°17.6'W | 32m | RCM/T,N,TG |
| TP-3A | 18 Aug 1980 | 2 Sep 1980 | 56°24.1'N | 161°39.6'W | 65.4m | MET, 7N |
| TP-4A | 19 Aug 1980 | 31 Jan 1981 | 56°31.2'N | 160°09.3'W | 68.5m | RCM/T,N,TG |
| TP-5A | 22 Aug 1980 | 29 Jan 1981 | 56°31.2'N | 160°18.1'W | 31m | RCM/T,N,TG |
| TP-6A | 22 Aug 1980 | 30 Jan 1981 | 56°46.5'N | 160°18.1'W | 59m | RCM,RCM/T, N,TG |
| TP-1B | 7 Feb 1981 | 29 May 1981 | 56°00.7'N | 161°06.8'W | -7 | MET,DL |
| BBL | 14 May 1981 | 30 May 1981 | 56°18.8'N | 161°33.2'W | 64m | 3 RCM |
| TC | 14 May 1981 | 31 May 1981 | 56°25.8'N | 161°42.8'W | 74m | 12TC,DL |
| TP-2B | 30 Jan 1981 | 29 May 1981 | 56°04.6'N | 161°18.2'W | 35m | N,RCM/T, TG,ST |
| TB-3B | 14 May 1981 | 30 May 1981 | 56°19.1'W | 161°32.5'W | 65m | N,RCM/T TG,ST |
| TP-7 | 31 Jan 1981 | 29 May 1981 | 56°02.0'N | 161°13.1'W | 25m | N,RCM/T, TG,ST |
| TP-8 | 2 Feb 1981 | 30 May 1981 | 55°51.8N | 162°02.4'W | 31m | N,RCM/T, TG,ST |
| TP-9 | 1 Feb 1981 | 30 May 1981 | 56°29.7'N | 161°42.3'W | 89m | N,RCM/T, TG,ST |